U.PORTO

MESTRADO EM ONCOLOGIA

ONCOLOGIA LABORATORIAL

First line drug testing in ovarian cancer cell lines manipulated for Mesothelin expression

Mariana Oliveira Nunes

M

2019

U.PORTO

Mariana Oliveira Nunes. First line drug testing in ovarian cancer cell lines manipulated for Mesothelin expression

First line drug testing in ovarian cancer cell lines manipulated for Mesothelin expression

Mariana Oliveira Nunes

M.ICBAS **2019**

INSTITUTO DE CIÊNCIAS BIOMÉDICAS ABEL SALAZAR

Mariana Oliveira Nunes

FIRST LINE DRUG TESTING IN OVARIAN CANCER CELL LINES MANIPULATED FOR MESOTHELIN EXPRESSION

Dissertação de Candidatura ao grau de Mestre em Oncologia – Especialização em Oncologia Laboratorial, submetida ao Instituto de Ciências Biomédicas Abel Salazar da Universidade do Porto

Orientadora

Doutora Sara Alexandra Vinhas Ricardo
Investigadora – Differentiation and Cancer Group, Instituto de Investigação e Inovação em Saúde/ Instituto de Patologia e Imunologia Molecular da Universidade do Porto (i3S/Ipatimup)
Professora Afiliada – Faculdade de Medicina da Universidade do Porto

Co-orientadora

Professora Maria Leonor Soares David
Professora Catedrática – Faculdade de Medicina da Universidade do Porto
Investigadora – Differentiation and Cancer Group, Instituto de Investigação e Inovação em Saúde/ Instituto de Patologia e Imunologia Molecular da Universidade do Porto (i3S/Ipatimup)

Financial Support

This study was received financial support by Fundação para a Ciência e a Tecnologia (FCT, I.P.) with grant number PTDC/MEC-ONC/29503/2017 – Blocking MUC16-mesothelin interaction to abrogate peritoneal metastization of ovarian cancer" (OVABLOCK). PI: Leonor David. From 15-07-2018 to 15-07-2021.

Acknowledgments

Em primeiro lugar queria agradecer às minhas orientadoras, Doutora Sara Ricardo e Professora Leonor David, pela oportunidade que me deram ao aceitarem que pudesse realizar a minha dissertação de Mestrado em Oncologia integrada no “OVCARTeam”. Agradeço imenso a confiança que desde logo depositaram em mim e no meu trabalho. Obrigada por todos os ensinamentos, pela constante disponibilidade e dedicação, obrigada por tudo! Uma “família” assim torna tudo mais fácil.

Um agradecimento especial à minha orientadora Sara Ricardo, por todo o carinho que sempre teve para comigo, por demonstrar que uma orientadora também pode ser uma amiga. Obrigada por isso e muito mais!

Ao Ricardo Coelho, obrigada por seres um ótimo “orientador” durante esta jornada, pela transmissão de conhecimentos e ensinamentos de grande parte das técnicas utilizadas neste trabalho, pela paciência, dedicação e disponibilidade que sempre tiveste no decorrer da elaboração desta dissertação.

À Professora Doutora Gabriela Almeida pela preciosa ajuda que deu para a concretização deste trabalho.

À Professora Doutora Raquel Almeida por me ter sido aceite no grupo “Differentiation and Cancer”.

A todos aqueles que fazem parte do “Differentiation and Cancer group” por toda a disponibilidade, apoio e amizade.

À Dalila Mexieiro e Ana Rita Silva pelo companheirismo e amizade, por todos os momentos que passamos a rir e por todos os que passamos a chorar, por tudo!

Ao Diogo, por toda a paciência, todo o apoio e incentivo que sempre me deu, por me aturar mesmo quando sou insuportável, sem ti tudo seria mais difícil.

Ao meu irmão Francisco, uma das pessoas mais importantes na minha vida e que sempre me disse “força mana vais conseguir”.

Finalmente agradeço aos meus pais Lucília e José, que sempre tornaram os meus “sonhos” possíveis. Obrigada pela paciência, apoio e amor. Obrigada por acreditarem em mim e por me fazerem acreditar que “voar” é possível!

Table of contents

Abbreviations

Acryl:Bis – Acrylamide/Bis-acrylamide

APS – Ammonium persulfate

ASR – Age-standardized rate

Bad – BCL2-antagonist of cell death

Bax – BCL2-associated X protein

BCA – Bicinchoninic acid

Bcl2 – B-cell lymphoma 2

BER – Base excision repair

BRAF – V-raf murine sarcoma viral oncogene homolog B1

BRCA1/2 – Breast cancer gene 1/2

BRIP1 – BRCA1-interacting protein 1

BSA – Bovine serum albumin

CA125 – Cancer Antigen 125

CAR-T – Chimeric antigen receptor T

Cas9 – CRISPR associated protein 9

CMA – Cell microarray

CCNE1 – Cyclin E1

CO_2 – Carbon dioxide

CT – Computed tomography

CTNNB1 – Catenin beta-1

Cu – Cooper

DAB – Diaminobenzidine

DMSO – Dimethyl sulfoxide

DNA – Deoxyribonucleic acid

E. coli – *Escherichia coli*

ECL – Enhanced chemiluminescence

EDTA – Ethylene-diamino-tetraacetic acid

EGFR – Epidermal growth factor receptor

EMA – European Medicines Agency

EOC – Epithelial ovarian carcinoma

FBS – Fetal bovine serum

FDA – Food and drug administration

FIGO – Federation of Gynecology and Obstetrics

FITC – Fluorescein isothiocyanate

GFP – Green fluorescent protein

GNRH – Gonadotropin releasing hormone

GOG – Gynecologic Oncology Group

GPI – Glycosylphosphatidylinositol

HCl – Hydrochloric acid

HGSOC – High-grade serous ovarian carcinoma

HR – Hazard ratio

HRP – Horseradish peroxidase

H&E – Hematoxylin and Eosin

IC50 – half maximal inhibitory concentration

IgG – Immunoglobulin G

IP – Intraperitoneal

KO – Knockout

KRAS – Kirsten rat viral oncogene homolog

LGSOC – Low-grade serous ovarian carcinoma

MAPK – Mitogen-activated protein kinase

MLH1 – MutL homolog 1

MMR – Mismatch repair

MPF – Megakaryocyte potentiating factor

MRI – Magnetic resonance imaging

MSH2/6 – MutS homolog 2/6

MSLN – Mesothelin

MTT – Methylthiazolyldiphenyl-tetrazolium bromide

MUC16 – Mucin 16

NaCl – Sodium chloride

NAD – Nicotinamide adenine dinucleotide

Na_3VO_4 – Sodium orthovanadate

NP40 – Nonylphenol ethoxylate

ORF_F/_R – Open reading frame forward/reverse

OS – Overall survival

p – Probability value

PARP – Poly (ADP-ribose) polymerase

PB – Preston blue

PBS – Phosphate buffered saline

PCR – Polymerase chain reaction

PD1 – Programmed cell death protein 1

PD-L1/2 – Programmed death-ligand 1/2

PenStrep – Penicillin/Streptomycin

PET – Positron emission tomography

PFS – Progression-free survival

PI – Propidium iodide

PIK3CA – Phosphoinositide-3-kinase-catalytic α

PLA – Proximity ligation assay

PMS2 – Postmeiotic segregation increased-2

PMSF – Phenylmethanesulfonyl fluoride

PS – Phosphatidylserine

PTEN – Prime Time Entertainment Network

r^2 – Determination coefficient

RAD51C/D – RAD51 homolog C/D

RIPA – Radio-immunoprecipitation assay

rpm – Revolutions per minute

RPMI – Roswell Park Memorial Institute

RR – Relative risk

RT – Room temperature

SDS – Sodium dodecyl sulphate

SDS-PAGE – Sodium dodecyl sulphate polyacrylamide gel electrophoresis

SEER – The Surveillance, Epidemiology and End Results

sgRNA – Single guide RNA

SRB – Sulforhodamine B

STIC – Serous tubal intraepithelial carcinoma

STR – Short tandem repeat

TBS – Tris buffered saline

TBS-T – Tris buffered saline with Tween 20

TCA – Trichloroacetic acid

TCGA – The Cancer Genome Atlas

TEMED – Tetramethylethylenediamine

TG – Tris-glycine

TGS – Tris-glycine-SDS

TRAIL – Tumour necrosis factor related apoptosis inducing ligand

Tris – Tris(hydroxymethyl)aminomethane

TP53 – Tumour protein 53

USA – United States of America

VCAM1 – Vascular cell adhesion molecule 1

VEGF – Vascular endothelial growth factor

v/v – Volume/volume

WHO – World health organization

w/v – Weight/volume

Figures Index

Tables Index

Resumo

O cancro do ovário é a neoplasia ginecológica mais letal. A taxa global de sobrevivência a 5 anos para pacientes com cancro do ovário é de 47,6%, e deve-se principalmente ao diagnóstico em estadios avançados, presença de sintomas inespecíficos, falta de bons métodos de rastreio, frequente desenvolvimento de quimioresistência e elevada taxa de recorrência. Apesar dos avanços nos procedimentos cirúrgicos e da implementação de regimes de combinação de drogas quimioterápicas com terapias-alvo, os pacientes continuam a apresentar elevadas taxas de recidivas. A Mesotelina (MSLN) é uma glicoproteína normalmente expressa na superfície das células mesoteliais e sobrexpressa em vários contextos tumorais, incluindo no cancro do ovário. Alguns estudos têm vindo a demostrar que a MSLN tem um papel importante na disseminação peritoneal e na quimioresistência. Assim, a MSLN tem um elevado potencial como alvo terapêutico para prevenir a disseminação peritoneal do carcinoma do ovário.

O objetivo deste trabalho foi avaliar se a expressão de MSLN modula a quimioresistência em linhas celulares de cancro do ovário. Neste sentido, avaliou-se a citotoxicidade de drogas de primeira linha habitualmente utilizadas em pacientes com cancro de ovário (carboplatina e paclitaxel) em linhas celulares parentais e respetivos knockout para a MSLN mediadas pela CRISPR-Cas9. A viabilidade celular foi avaliada pelos ensaios de MTT, SRB e PB, a apoptose por citometria de fluxo e as proteínas associadas às vias apoptóticas (atividade da PARP e PARP clivada) por immunoblot. Adicionalmente, a expressão de MSLN foi avaliada por imunocitoquímica e immunoblot.

OVCAR3 e OVCAR8 *MSLN* KO são significativamente mais sensíveis à carboplatina em comparação com as células parentais correspondentes. A anexina V/PI e a atividade da PARP clivada demonstraram que, para a OVCAR3, a carboplatina induz mais apoptose em células sem expressão de MSLN. Contrariamente, para a OVCAR8, a carboplatina induz mais apoptose em células que expressam MSLN. Estes resultados indicam que para a OVCAR8 a expressão de MSLN não tem efeito sobre a apoptose. Relativamente ao paclitaxel, os resultados indicam que a MSLN não parece modular a quimioresistência. Adicionalmente, para as linhas parentais, os resultados indicaram que após exposição à carboplatina e ao paclitaxel a maioria das células que sobrevivem ao tratamento não expressam MSLN. Assim, podemos concluir que a expressão da MSLN modula a quimioresistência à carboplatina em linhas celulares de cancro do ovário e que, tanto a carboplatina como o paclitaxel interferem com a expressão de MSLN em linhas parentais.

Palavras-chave

Disseminação peritoneal | Mesotelina | Quimioresistência | Carboplatina | Paclitaxel

Summary

Ovarian cancer is the most lethal gynecologic malignancy. The overall 5-year survival rate for ovarian cancer patients is 47.6%, mainly due to advanced disease stage at diagnosis, presence of nonspecific symptoms, lack of effective screening tools, poor treatment responses with development of chemoresistance and high recurrence rate. Despite some improvements in surgical procedures and treatment regimens based on combining chemotherapeutic drugs with targeted therapies were not effective in improving patients´ outcomes. Mesothelin (MSLN) is a glycoprotein normally expressed in the surface of mesothelial cells and overexpressed in many tumour contexts, including ovarian cancer. Some studies demonstrate that MSLN has an important role in peritoneal dissemination and chemoresistance. Therefore, MSLN is an attractive tumour marker for the development of targeted therapy to prevent peritoneal dissemination of ovarian carcinoma.

The purpose of this project is to evaluate if MSLN expression modulates the chemoresistance in ovarian cancer cell lines. For this we assessing the cytotoxicity of first-line chemotherapeutic drugs commonly used in ovarian cancer patients (i.e. carboplatin and paclitaxel) in parental and CRISPR-Cas9 mediated MSLN knockout ovarian cancer cell lines.

Cell viability was evaluated by MTT, SRB and PB assays, apoptosis was assessed by flow cytometry and proteins associated with apoptotic pathways (PARP and cleaved PARP activity) was performed by immunoblot. Additionally, MSLN expression was evaluated by immunocytochemistry and immunoblot.

MSLN KO OVCAR3 and OVCAR8 are significantly more sensitive to carboplatin compared with the corresponding parental cells. Annexin V/PI and cleaved-PARP activity showed that, for OVCAR3 cells, carboplatin induces more apoptosis in cells without MSLN expression. On the other hand, for OVCAR8 cells, carboplatin induces more apoptosis in cells that express MSLN. These results indicate that for OVCAR8, MSLN does not have affect apoptosis. Paclitaxel results indicate that MSLN does not seem to have a regulatory effect in chemoresistance. Additionally, for parental cells exposure to carboplatin and paclitaxel the results showed that the majority of the cells that survive to treatment are MSLN negative. In conclusion, MSLN expression modulates the platinum chemoresistance in ovarian cancer cell lines. Carboplatin and paclitaxel interfere with MSLN expression in parental cell lines.

Key words

Peritoneal dissemination | Mesothelin | Chemoresistance | Carboplatin | Paclitaxel

Chapter 1 | Introduction

1. | Ovarian cancer

1.1. | Epidemiology

Ovarian carcinoma is the 8th type of cancer with highest incidence and the 5th leading cause of cancer-related death among women in Europe (Figure 1) (Ferlay *et al.,* 2018). Therefore, represents the most lethal gynaecologic malignancy (Raja, Chopra & Ledermann, 2012; Weidle *et al.,* 2016; Coelho *et al.,* 2017). The estimated lifetime risk for a woman to develop ovarian cancer is, approximately, 1.3%, and occurs predominantly at postmenopausal ages (47.3% at 55-74 years old) (Crum *et al.,* 2007; Howlader *et al.,* 2018).

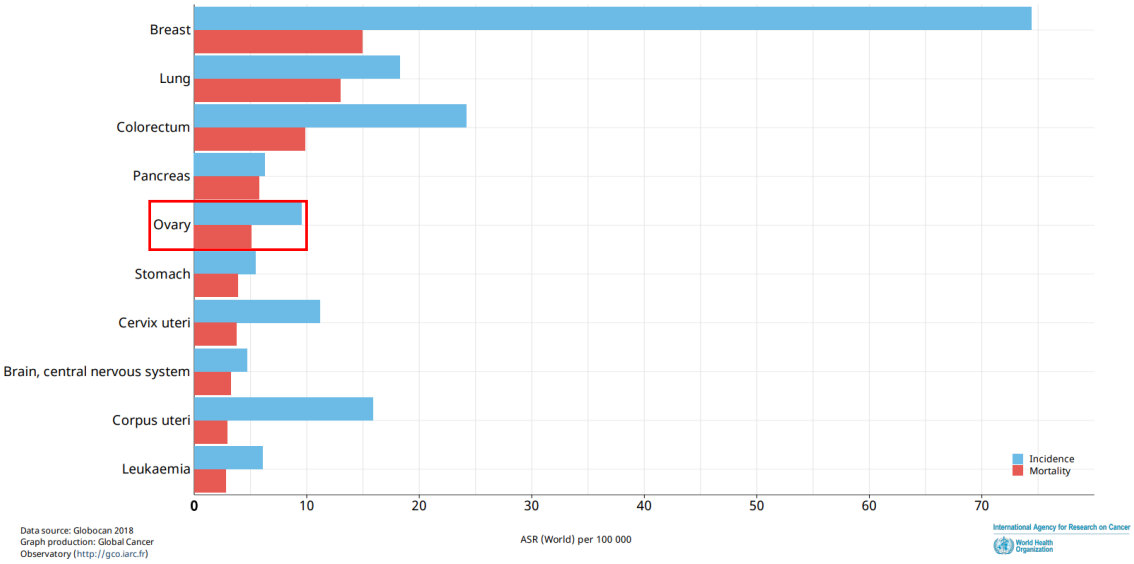

Figure 1 | Estimated age-standardized incidence and mortality rates in Europe for women at all ages. ASR – Age-standardized rate (Globocan 2018 data, order by mortality).

Approximately 75% of the patients diagnosed at advanced stages presenting dissemination of the tumour in the peritoneal cavity (Coelho *et al.,* 2017). This mostly occur due to diverse and nonspecific symptoms and absence of effective screening tools to detect early disease stages (Raja, Chopra & Ledermann, 2012; Jervis *et al.,* 2014). High-grade serous ovarian carcinoma (HGSOC) is the most common and deadliest type of ovarian cancer due to rapid grow and early metastization (Lengyel, 2010; Kurman *et al.,* 2014; Lisio *et al.,* 2019)

The most common ovarian cancer signs and symptoms include pelvic or abdominal pressure, pain and bloating; gastrointestinal disorders, such as loss of appetite, early satiety, indigestion, nausea, vomiting, acid reflux; and constipation or diarrhea (Goff *et al.,* 2004; Kurman *et al.,* 2014**;** Matulonis *et al.,* 2016). Some patients present urinary frequency, back pain or discomfort, fatigue, loss of weight and menstrual irregularities, and in advanced

stages may present respiratory symptoms (Goff *et al.,* 2004: Kurman *et al.,* 2014; Matulonis *et al.,* 2016; Lheureux *et al.,* 2019).

The standard treatment for advanced ovarian cancer is debulking surgery and platinum-taxane-based chemotherapy, however, the majority of patients experience recurrence after developing chemoresistance (González-Martín *et al.,* 2014; Weidle *et al.,* 2016; Testa *et al.,* 2018). According to SEER´s 2009 – 2015 data, the overall 5-year survival rate for ovarian cancer patients is 47.6% the poorest of all gynaecological cancers (Howlader *et al.,* 2018). Around 80% of the patients are diagnosed at advanced stages with regional or distant disease and present a 5-year relative survival rate of 75.2% and 29.2%, respectively (Berek, Crum & Friedlander, 2015; Howlader *et al.,* 2018). On the other hand, women diagnosed at early stages with localized disease present a 5-year relative survival rate of 92.4%, with a better prognosis than women with advanced ovarian cancer (Berek, Crum & Friedlander, 2015; Howlader *et al.,* 2018). Therefore, early detection methods and improved treatment options are needed to decrease the mortality rate of ovarian cancer patients.

1.2. | Risk factors

A first-degree family history of breast and/or ovarian cancer have been implicated as the most significant risk factor for epithelial ovarian cancer (EOC) (relative risk (RR), 1.13 and 1.61, respectively) (Bergfeldt *et al.,* 2002; Jervis *et al.,* 2014; Wentzensen *et al.,* 2016). However, only 10-15% are hereditary breast/ovarian cancer syndromes and are characterized by a family history of multiple relatives with breast and/or ovarian cancer at early ages (Tschernichovsky & Goodman, 2017). This syndrome is mostly associated with germline mutations in BRCA1 or BRCA2 tumour-suppressor genes that can increase the risk from 1.6% to 35-45% (BRCA1) or 15-18% (BRCA2) (Mavaddat *et al.,* 2013; Tschernichovsky & Goodman, 2017). Deletions in BRCA1/2 and other double-strand DNA break repair genes can be also associated with HGSOC susceptibility (Pennington & Swisher, 2012; Lheureux *et al.,* 2019). Women with breast cancer history have two-fold higher risk for ovarian cancer and this is even higher in a background of breast/ovarian cancer family history (Bergfeldt *et al.,* 2002). Women with high genetic risk (BRCA1/2 mutation) with more than 40 years or who have completed maternal age are recommended to perform a prophylactic salpingo-oophorectomy to reduce the risk of BRCA-related gynecologic cancer (Bergfeldt *et al.,* 2002; Berek, Friedlander & Bast, 2017).

Some low penetrance mutations in genes that have an important role in the homologous recombination mediated pathway of DNA repair (BRIP1, RAD51C and RAD51D) confer a high risk to develop ovarian cancer (5.8%, 5.2% and 12%, respectively) (Jervis *et al.,* 2014;

Ramus *et al.,* 2015; Song *et al.,* 2015). Also, Lynch syndrome, characterized by a germline mutation in DNA mismatch repair (MMR) genes (MSH2, MSH6, MLH1 or PMS2), increases the risk for colorectal cancer and a wide range of other malignancies, including ovarian cancer, especially endometrioid or clear cell carcinomas (Lynch *et al.,* 2009; Ketabi *et al.,* 2011; Jervis *et al.,* 2014).

Some hormonal and reproductive factors have a potential role in the pathogenesis of sporadic ovarian cancers, particularly in endometrioid and clear cell carcinomas (Wentzensen *et al.,* 2016). Several epidemiological studies showed that women with more ovulatory cycles present a higher risk for ovarian cancer development (Webb & Jordan, 2017; Testa *et al.,* 2018). During ovulation, the reparation of the surface epithelium amplifies the rate of cellular division which leads to an increased risk of spontaneous somatic mutations in addition to an inflammatory status that favors malignant transformation (Testa *et al.,* 2018). Therefore, factors that reduce or suppress ovulation, such as oral contraceptives, parity, fertility, breastfeeding, late menarche and early menopause have been strongly described as protective factors regarding ovarian cancer development (Cramer & Terrym, 2005; Vessey & Painter, 2006; Jordan *et al.,* 2010; Gong *et al.,* 2013; Luan *et al.,* 2013; Wentzensen *et al.,* 2016; Webb & Jordan, 2017). Recent studies demonstrated that the current use of replacement hormone therapy with oestrogens in menopause increases the risk of ovarian cancer in 40% and the risk remains elevated for at least five years (Collaborative Group on Epidemiological Studies of Ovarian Cancer, 2015). On the other hand, epidemiological studies demonstrate that tubal ligation reduces in 20-30% the risk for invasive ovarian cancer being more evident in endometrioid (RR, 0.60) and clear cell (RR, 0.35) carcinomas (Sieh *et al.,* 2013; Wentzensen *et al.,* 2016). Several studies demonstrated that endometriosis increases the risk of ovarian cancer and has been associated with 5-15% of all EOCs (Sayasneh, Tsivos & Crawford, 2011), mainly endometrioid (RR, 2.32) and clear cell (RR, 2.87) carcinomas (Wentzensen *et al.,* 2016).

Some lifetime factors have been associated to ovarian carcinomas, such as smoking (Wentzensen *et al.,* 2016; Praestegaard *et al.,* 2017) and obesity (Olsen *et al.,* 2013; Nagle *et al.,* 2015) but the direct causality is still rebuttable.

1.3. | Ovarian cancer classification

Ovarian cancer is a heterogeneous disease comprising several types of tumours with diverse origins, pathogenesis, molecular profiles, clinicopathologic features, risk factors and prognosis (Kurman & Shih, 2010; Meinhold-Heerlein & Hauptmann, 2014; Karnezis *et al.,* 2017).

1.3.1. | Histopathological classification

Ovarian carcinoma is classified according to the anatomic structures from which it derives and is commonly subdivided in three main histological types: epithelial, germ cell, and sex-cord stromal tumours (Karnezis *et al.,* 2017).

EOC is the most predominant pathologic type, which accounts 85–90% of all ovarian cancers (Lengyel, 2010; Prat, 2012) and comprises distinct histological subtypes: serous (~70%), endometrioid (~10%), mucinous (~3%), clear cell (~10%) and Brenner tumours (1-5%) (Figure 2) (Gilks & Prat, 2009; Prat, 2012). The serous subtype comprises more than 90% of all ovarian cancer cases (Tavassoli & Devilee, 2003) and is categorized according to their invasiveness and aggressiveness into HGSOC or low-grade serous ovarian carcinoma (LGSOC) (Figure 2) (Kurman & Shih, 2008; Peres, *et al.,* 2018).

Non-EOCs are rare malignancies (10-15% of all ovarian cancers) with germ cell and sex cord-stromal tumours subtypes occurring more frequently (Berek & Bast, 2003; Colombo *et al.,* 2012; Boussios *et al.,* 2016). Germ cell tumours originate from the primordial germ cells of the embryonic gonad (Koulouris & Penson, 2009; Stewart, Ralyea & Lockwood, 2019), are frequently diagnosed at younger ages (< 30 years) and teratoma being the most common subtype (Colombo *et al.,* 2012). Sex cord-stromal tumours originate from ovarian stroma deriving more frequently from granulosa cells (Berek & Bast, 2003; Colombo *et al.,* 2012; Boussios *et al.,* 2016).

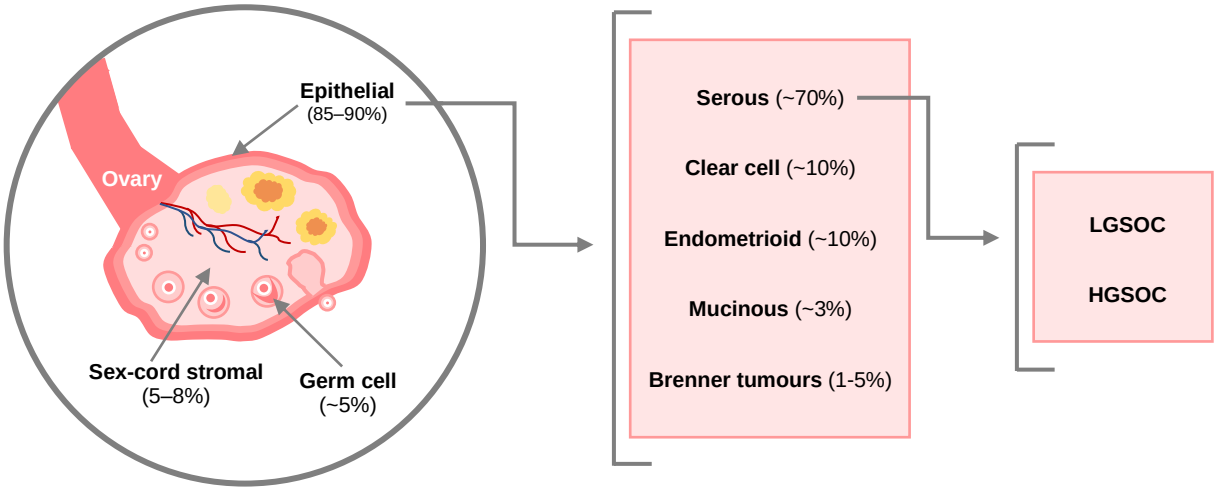

Figure 2 | Histological classification of ovarian tumours. The epithelial subtype comprises 5 subtypes: Serous, Clear Cell, Endometrioid, Mucinous and Brenner tumours. The serous subtype can be further classified based on tumour histology and grade into LGSOC (low-grade serous ovarian carcinoma) and HGSOC (high-grade serous ovarian carcinoma).

Epithelial ovarian tumours can be also classified in benign, borderline and malignant categories that reveal the degree of cell proliferation, nuclear atypia, and the presence or absence of stromal invasion (Prat, 2012). Benign tumours, such as serous cystadenomas (Figure 3), are mostly cystic with thin papillae, a single cell layer (no stratification), no nuclear atypia and absence of stromal invasion. Borderline tumours, such as serous borderline tumours (Figure 3), are an intermediate classification that presents higher proliferation and variable nuclear atypia with absence of stromal invasion. Serous borderline tumours present an exophytic growth, are capable to implant in the peritoneal wall and can progress to LGSOC. Malignant tumours, such as serous adenocarcinomas (Figure 3), are mostly solid, with necrosis, papillary complexity, stratification, nuclear atypia, and stromal invasion (Prat, 2012; Berek, Friedlander & Bast, 2017).

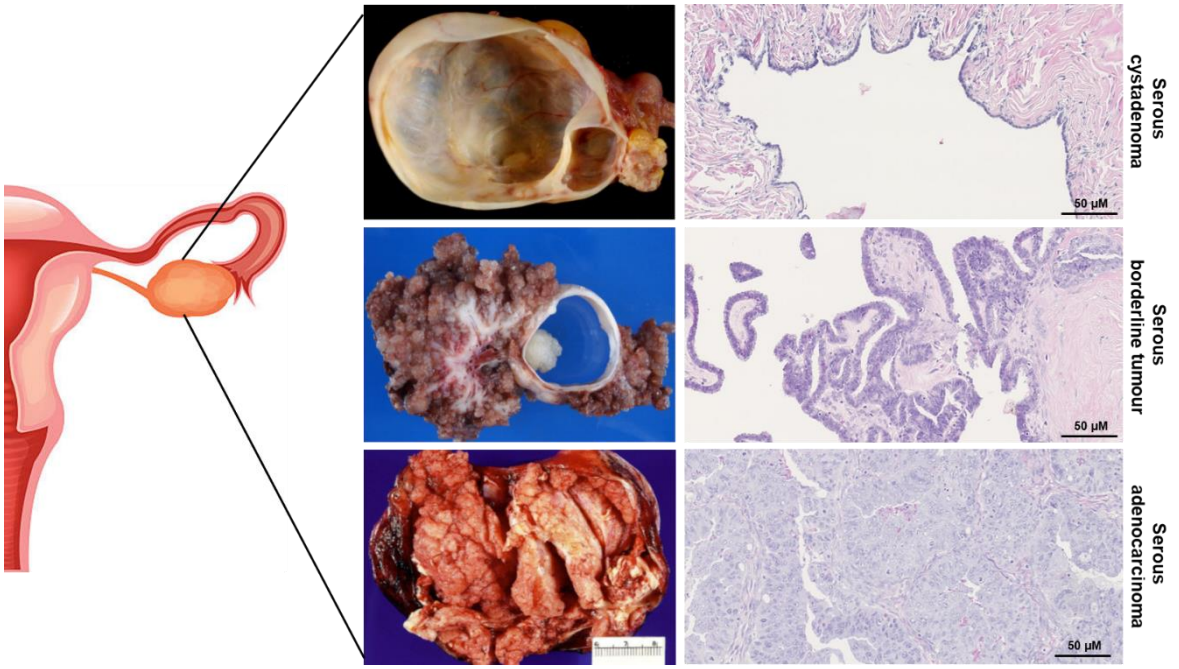

Figure 3 | Epithelial ovarian tumours´ categories. Representative images of serous cystadenoma (benign), serous borderline tumour (borderline) and serous adenocarcinoma (malignant). Microscopic images taken at 100x magnification and scale bar represents 50 µm.

Also, tumour grade, a pathological index that reflects atypical cell and/or architecture of the tumour, is used as supplementary stratification with an important prognosis correlation (GX, G1, G2 and G3) (Berns & Bowtell, 2012; Berek, Crum & Friedlander, 2015; Testa *et al.,* 2018).

1.3.2. | Type I and type II tumours

In 2004, Shih and Kurman proposed a dualistic model of epithelial ovarian carcinogenesis, based on clinicopathologic and molecular-genetic analyses of a large series of epithelial ovarian tumours that categorizes EOC in type I and type II tumours (Shih & Kurman, 2004). In 2014, WHO included this model in the classification guidelines for tumours of the female reproductive organs (Kurman *et al.,* 2014; Meinhold-Heerlein & Hauptmann, 2016). In 2016, Kurman and Shih revised and expanded the original dualistic model of ovarian carcinogenesis to incorporate some important aspects about the origin and molecular pathogenesis of ovarian cancer (Kurman & Shih, 2016). This new model subdivides type I tumours into three subtypes: i) endometriosis-related tumours that comprise endometrioid, clear cell, and seromucinous carcinomas; ii) tubal related tumours that contain LGSOC; and iii) germ cell or transitional cell related tumours that includes mucinous carcinomas and Brenner tumours (Kurman & Shih, 2016). Type II tumours include HGSOC, carcinosarcomas and undifferentiated carcinomas (Kurman & Shih, 2016).

Type I tumours are clinically indolent, progress slowly and present a low stage disease with large masses that are commonly confined to ovary at diagnosis and present a good prognosis (Kurman & Shih, 2011; Berek, Crum & Friedlander, 2015). They are characterized by well-established precursor lesions (i.e. endometriosis, serous cystadenomas or serous borderline tumours) that can undergo malignant transformation (Kurman & Shih, 2016; Lisio *et al.,* 2019). Molecularly, these tumours harbour changes such oncogenic mutations in BRAF, KRAS, PTEN, CTNNB1 and PIK3CA genes (Shih & Kurman, 2004; Kurman & Shih, 2016). Type II tumours are frequently associated with fatal outcomes, are highly aggressive and usually diagnosed in advance stages with rapid progression and metastization resulting in a poor prognosis (Shih & Kurman, 2004; Kurman & Shih, 2008; Kurman & Shih, 2010). These tumours progress from serous intraepithelial tubal carcinoma (STIC) (Kurman & Shih, 2016) and present high levels of genetic instability, caused by widespread DNA copy number or structural aberrations, TP53 mutation, CCNE1 amplification, germline and somatic BRCA1/2 mutation and other anomalies in homologous recombination DNA damage repair pathways (Shih & Kurman, 2004; Ahmed *et al.,* 2010; Cancer Genome Atlas Research Network, 2011; Kurman & Shih, 2016). Clinically, type I tumours have a good prognosis when confined to the ovary but type II tumours, usually diagnosed at advanced stages, have a worse prognosis (Kurman & Shih, 2016).

Table I | Summary of clinicopathological features of type I and type II tumours (adapted from Kurman & Shih, 2016).

	Type I tumours	Type II tumours
Origin	Tubal, endometriosis, germ or transitional cells	Mostly tubal
Precursors	Atypical proliferative (borderline) tumours	Mostly STICs
Risk factors	Endometriosis	Lifetime ovulation cycles BRCA germline mutations
Stage	Early	Advanced
Tumour grade	Low-grade	High-grade
Progression	Slow and indolent	Rapid and aggressive
Overall clinical outcome	Good	Poor
Malignant ascites	Rare	Common

1.3.3. | Molecular subtypes

In 2008, Tothill *et al.,* perform an analysis of differential gene expression profiling in 285 serous and endometrioid invasive ovarian, fallopian tube, and peritoneal cancer samples and identified six distinct molecular subtypes (C1 – C6) that have a significant correlation to clinical outcome (Tothill *et al.,* 2008; Konecny *et al.,* 2014; Lasio *et al.,* 2018; Testa *et al.,* 2019). High-grade serous and endometrioid carcinomas were included in the C1 (high stromal response), C2 (high immune signature), C4 (low stromal response), and C5 (mesenchymal, low immune signature) subtypes and low malignant potential and low-grade tumours were included in C3 (low malignant potential-like invasive tumours) and C6 (low-grade endometrioid) subtypes (Tothill *et al.,* 2008). In 2013, Verhaak *et al.,* described four molecular signatures of HGSOC based on gene expression profile: immunoreactive, differentiated, proliferative and mesenchymal (Verhaak *et al.,* 2013; Kurman & Shih, 2016). However, the clinical applications of these molecular classifications are still debatable.

1.4. | Diagnosis and staging

Cancer antigen 125 (CA125) is a cancer associated antigen that can be detected at high levels in 80-90% of ovarian cancer patients with advanced stages. However, this biomarker can be also found in patients with benign disorders, such as uterine fibroids, ovarian cysts and other situations, such as liver disease and infections (Jacobs & Bast; 1989; Jacobs *et al.,* 1999), therefore, CA125 test alone is not an affective screening tool (Matulonis *et al.,* 2016). Several clinical screening trials using serum CA125 concentrations, transvaginal

ultrasonography and pelvic examination have been tested over the past years, however, they do not present the levels of sensitivity and sensibility needed for a reliable screening tool (Jacobs *et al.,* 2016; Kurman & Shih, 2016).

For ovarian cancer, several clinicopathological factors have prognostic implication that allow to predict outcome and adjust the treatment according to individual risk (Brun *et al.,* 2000; Clark *et al.,* 2001). These factors include age at diagnosis, histological subtype and grade, surgical stage, presence of ascites and extent of residual disease after surgery (Brun *et al.,* 2000; Clark *et al.,* 2001; Engel *et al.,* 2002; Agarwal & Kaye, 2005; Peres *et al.,* 2019; Siegel, Miller & Jemal, 2019).

For the EOC diagnosis, a clinical pelvic, a rectovaginal examination, and a radiographic imaging, such as transvaginal or abdominal ultrasonography, are performed (Matulonis *et al.,* 2016). In some cases, other imaging techniques may provide additional information, such as abdominal or pelvic CT, a pelvic MRI or a PET (Matulonis *et al.,* 2016). In advanced stages extensive peritoneal carcinomatosis and accumulation of ascites are frequently observed (Coelho *et al.,* 2017). So, in clinical evaluation it is important to search for signs of ascites, bowel obstruction, pleural effusion and distended lymph nodes or solid organs (i.e. liver) due to metastasis (Lengyel, 2010; Matulonis *et al.,* 2016). The CA125 can be performed and, in combination with an ultrasonography, might be useful for diagnostic purposes (Matulonis *et al.,* 2016). However, in ovarian cancer, an optimal staging is performed by surgical exploration (Lheureux *et al.,* 2019). Histologic, molecular, and genetic evidence demonstrate that 40-60% of high-grade serous carcinomas of the ovary or peritoneum may have originated in the fimbrial end of the fallopian tube (Crum *et al.,* 2007; Kurman & Shin, 2008). Since 2014, ovarian, fallopian tube, and peritoneal cancer were incorporated in the same staging system by FIGO and the primary tumour site and the histological grade must be specified in the operative and/or final pathology report (Prat & FIGO Committee on Gynecologic Oncology, 2014; Berek, Crum & Friedlander, 2015). The histopathological information confirms the diagnosis and reveals the specific characteristics of the tumour, such as stage, histological type and grade (Lheureux *et al.,* 2019).

In ovarian cancer, peritoneal dissemination is a particular form of malignant progression that precedes hematogenic or lymphatic metastization (Tan, Agarwal & Kaye, 2006; Lengyel, 2010; Coelho *et al.,* 2017). In this type of dissemination, the disease spreads rapidly within the peritoneal cavity and adheres to adjacent organs (i.e. bladder or colon). The spread occurs by detachment of tumour cells from the primary site and spreading by the peritoneal fluid which embeds the cells and acts as a medium to promote dissemination within the peritoneal cavity, allowing cells to attach in the mesothelial layer with consequent

peritoneal carcinomatosis (i.e. peritoneum and omentum) (Lengyel, 2010; Weidle *et al.,* 2016; Coelho *et al.,* 2017). Occasionally some pelvic and/or para-aortic lymph nodes can be involved in ovarian dissemination (Eisenkop & Spirtos, 2001), however, spread outside the peritoneal cavity is unusual (Naora & Montell, 2005). Ovarian cancer cells exhibit a preference for implanting in the omentum (Pradeep *et al.,* 2014). In fact, around 80% of HGSOC metastasis in this organ (Nieman *et al.,* 2011). Sometimes, in advanced stages, metastasis occur in the liver and cells cross the diaphragmatic barrier, enter in pleural spaces, and cause pleural effusions or invade the lung parenchyma (Yeung *et al.,* 2015; Matulonis *et al.,* 2016). Particularly in advanced stages, tumour cells seed in the peritoneal cavity, block the sub peritoneal lymphatic drainage (Tan, Agarwal & Kaye, 2006) and/or secrete vasoactive and angiogenic factors (e.g. VEGF) (Xu *et al.,* 2000) which cause vascular permeability and allow accumulation of ascites (Lengyel, 2010; Kipps, Tan & Kaye, 2013). The malignant ascitic fluid is rich in factors which promote tumour cell growth and invasion (Ahmed & Stenvers, 2013). The accumulation of ascites in abdomen contributes to morbidity by gastrointestinal symptoms and abdominal discomfort, present an adverse impact on prognosis (Berek, Friedlander & Bast, 2017) and play an important role in ovarian cancer dissemination (Yeung *et al.,* 2015).

1.5. | Treatments

Since 1970s, debulking surgery and platinum-taxane based chemotherapy became the standard treatment for ovarian cancer patients (Griffiths & Fuller, 1978; Kim *et al.,* 2012). Radiotherapy is approved only as a palliative care for symptomatic control (Berek, Friedlander & Bast, 2017). Hormone therapy can be also used for palliative care, since it is usually well tolerated by patients without causing a high level of toxicity (Sjoquist *et al.,* 2011).

1.5.1. | Surgery

For women diagnosed with ovarian cancer the primary treatment is debulking surgery also called cytoreduction and allows the resection of visible tumour masses disseminated in the peritoneal cavity (González-Martín *et al.,* 2014; Matulonis *et al.,* 2016; Lisio *et al.,* 2019). The success of cytoreduction surgery is one of the most important prognostic factors, especially for advanced disease with significant differences in the response rate to chemotherapy, progression-free survival (PFS) and overall survival (OS) for patients with optimal cytoreduction in comparison with those with residual disease (Winter *et al.,* 2007; du Bois *et al.,* 2009). The optimal cytoreduction depends on the disease stage and refers

to surgical resection absence (lesion size score: tumours up to 1 cm) of macroscopic residual disease (Stuart *et al.,* 2011; Matuloni*, et al.,* 2016; Lisio *et al.,* 2019). Patients with lower residual disease (tumours <1 cm) have a better prognosis in comparison with high residual disease (tumours >1 cm) (Foley *et al.,* 2013). Depending on the disease stage at diagnosis, the surgical resection of the tumour can be accompanied by abdominal hysterectomy, unilateral or bilateral salpingo-oophorectomy, partial or complete omentectomy, lymphadenectomy and peritoneal washing (Lengyel, 2010; Matulonis *et al.,* 2016; Berek, Friedlander & Bast, 2017). Neoadjuvant chemotherapy with carboplatin and/or paclitaxel can be recommended to reduce the tumour burden and facilitate the debulking surgery (Berek, Friedlander & Bast, 2017).

1.5.2. | Chemotherapy

The platinum-taxane-based chemotherapy remains the standard of care in the frontline therapy of advanced EOC (González-Martín *et al.,* 2014; Berek, Friedlander & Bast, 2017). For patients diagnosed at early stages, the treatment with chemotherapy depends on the histology**,** grade and tumour stage (Matulonis *et al.,* 2016) however, for patients diagnosed with advanced disease, the general recommendation is at least 6 cycles of chemotherapy with a combination of carboplatin and paclitaxel (Lengyel, 2010). Several studies demonstrated a benefit in OS and PFS for combining carboplatin and paclitaxel when compared to a single-agent therapy (McGuire *et al.,* 1996; Piccart *et al.,* 2000). Other drug combinations have been tested to improve efficacy of adjuvant chemotherapy, such as carboplatin or cisplatin and paclitaxel or docetaxel (McGuire *et al.,* 1996; du Bois *et al.,* 2003; Ozols *et al.,* 2003; Vasey *et al.,* 2004; Bookman *et al.,* 2009) with other drugs such as gemcitabine, pegylated liposomal doxorubicin (Pignata *et al.,* 2011) and anti-angiogenic agents, such as bevacizumab (Burger *et al.,* 2011; Perren *et al.,* 2011), pazopanib (du Bois *et al.,* 2014) and nintedanib (du Bois *et al.,* 2016). Despite the initial benefits of combining platinum and taxanes compounds most of the patients acquires drug resistance (Berek, Friedlander & Bast, 2017). Aiming to overcome chemoresistance several randomized trials have been performed and the results showed some improvements using gemcitabine, topotecan, or liposomal doxorubicin (Bookman *et al.,* 2009; Berek, Friedlander & Bast, 2017). However, carboplatin remains the standard treatment for ovarian cancer patients (Bookman *et al.,* 2009; Berek, Friedlander & Bast, 2017).

Ovarian cancer metastasizes in peritoneum and omentum and some studies have been shown that intraperitoneal (IP) administration of chemotherapies allow a more effective treatment of peritoneal metastasis (Berek, Friedlander & Bast, 2017). Despite some

catheter complications, these studies demonstrated that IP chemotherapy is associated with better outcomes in stage IV patients and allow increase the PFS in 5.5 months and OS in 15.9 months in stage III patients with optimal debulking surgery (Armstrong *et al*., 2006; Jaaback & Johnson, 2006; Hess *et al.,* 2007).

1.5.2.1. | Platinum compounds

The platinum-based compounds, i.e. carboplatin and cisplatin, are alkylating agents that inhibit DNA replication and transcription, leading to cellular apoptosis (Figure 4) (Kelland, 2007; Brasseur *et al.,* 2017). Cisplatin is one of the most effective cancer drugs for ovarian cancers, however, is highly toxic to the kidneys and gastrointestinal tract (Kelland, 2007). Carboplatin, as a second-generation analogue of cisplatin, presents a similar mechanism of action, but is less neurotoxic, nephrotoxic and gastrointestinal tract toxic, therefore, became the standard treatment used for ovarian cancer patients (Kelland, 2007). Platinum compounds are activated intracellularly by the aquation of chloride 'leaving' groups, creating reactive platinum complexes that covalently bind to purine DNA bases and form DNA adducts (Kelland, 2007; McWhinney, Goldberg & McLeod, 2009). This mechanism activates several cellular pathways, such as those involved in regulating drug uptake, DNA damage recognition and repair, cell-cycle checkpoints, arrest and death (Wang & Lippard, 2005). DNA adducts caused by platinum compounds trigger cell cycle arrest in G2/M phase, inhibit replication and transcription and launch apoptosis by hyperactivation of PARP (Wang & Lippard, 2005). Most of ovarian cancer patients acquire chemoresistance during cycles of therapy with platinum-based compounds (Kelland, 2007). The mechanisms of platinum resistance include inactivation of platinum by glutathione, metallothionein or other sulphur-containing molecules (Hamilton *et al.,* 1985; Eastman, 1987); changes in cellular uptake and/or efflux that reduce the accumulation of drug (Komatsu *et al.,* 2000; Nakayama *et al.,* 2002); increased DNA repair of adducts formed by platinum agents (Dabholkar *et al.,* 1994; Lai *et al.,* 1988); and increased adduct's tolerance and failure of apoptotic pathways (Mamenta *et al.,* 1994; Eliopoulos *et al.,* 1995).

1.5.2.2. | Taxane compounds

Taxane compounds are antimitotic agents that induce apoptosis by preventing polymerization of microtubules (Brasseur *et al.,* 2017). Microtubules form the mitotic spindle during cell division and are required for the maintenance of cell structure, motility, and cytoplasmic movement within the cell (Kampan *et al.,* 2015). Paclitaxel prevents cell division by binding specifically to the N-terminal region of microtubules β-tubulin (Zhang *et al.,* 2014)

which leads to stabilization of microtubules, prevention of cell division, induction cell cycle arrest in G2/M phase (Schiff & Horwitz 1980; Ganesh *et al.,* 2007) and activation of pro-apoptotic signaling (Figure 4) (Schiff, Fant & Horwitz, 1979; Wang, Wang & Soong, 2000). However, it is uncertain if taxol-induced cell death represents a secondary event subsequent to mitotic arrest or if it comprises another mechanism of action (George, Banik & Ray, 2010), namely by interacting with mitogen-activated protein kinase (MAPK) pathway and act in regulatory proteins that are involved in programmed cell death, such as in dephosphorylation of the proapoptotic protein Bad and Bax (apoptosis promoters) and phosphorylation of Bcl2 (apoptosis suppressor) (Kampan *et al.,* 2015). The effective of paclitaxel is limited because most ovarian cancer patients acquire drug resistance (Kelland, 2007; Chang *et al.,* 2009). Paclitaxel-derived resistance is a complex mechanism that involves multiple steps and multiple genes, and is mainly attributed to changes involving mRNA and protein synthesis, oxidative stress, glycolysis, glutathione metabolism, and leukocyte transendothelial migration pathways (Agarwaland & Kaye, 2003).

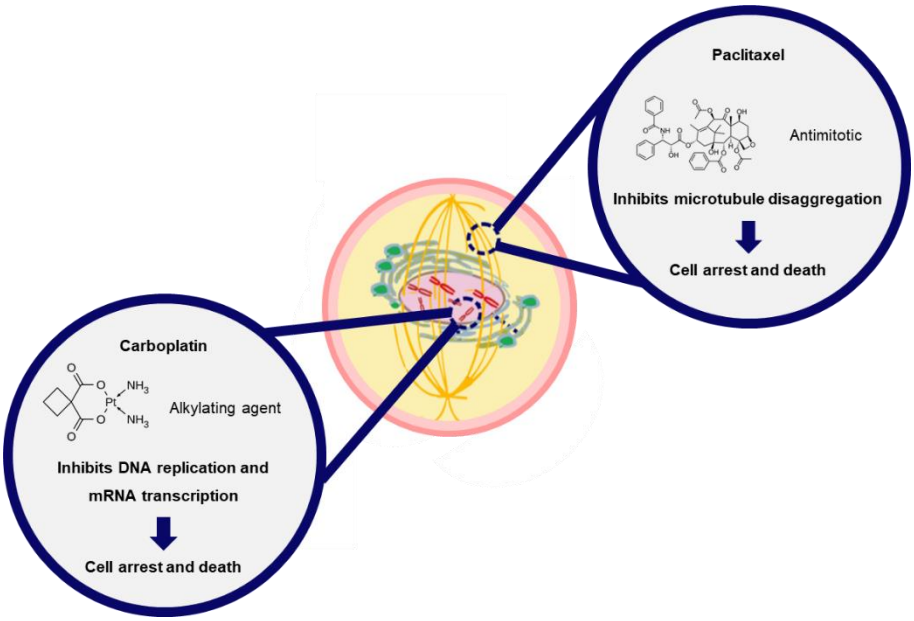

Figure 4 | Mechanism of action of carboplatin and paclitaxel. Carboplatin is an alkylating agent that binds to DNA, inhibits replication and transcription, and induces cell arrest and death. Paclitaxel is an antimitotic that prevents microtubule disaggregation which leads to the inhibition of the depolymerization, prevention of cell division, induction of cell cycle arrest in G2/M phase and cellular apoptosis (Adapted from Starobova & Vetter, 2017).

1.5.3. | Targeted therapy

Targeted therapies inhibit stroma, angiogenesis or cell signaling pathway aberrations in tumour tissues, being more specific and consequently less toxic (Pignata *et al*., 2011). The efficacy of targeted therapies in ovarian cancer has been investigated to be used as single

agent or in combination with cytotoxic drugs (Pignata *et al.,* 2011). The two major molecular targets FDA approved to treat ovarian cancer are bevacizumab (anti-angiogenic antibody) and olaparib (PARP inhibitor) (Kim *et al.,* 2012).

1.5.3.1. | Hormonal therapy

Many gynecological cancers, including ovarian cancer, and specifically low-grade tumours, express high levels of estrogen and androgen receptors (Berek, Friedlander & Bast, 2017). Hormonal therapies block, reduce or interfere with the production or action of hormones and have been used either alone or in combination with cytotoxic drugs in patients with advanced ovarian cancer (Van den Bossche *et al.,* 1994; Sjoquist *et al.,* 2011; Yokoyama & Mizunuma, 2013). In ovarian cancer, hormonal therapy options include antiestrogenic drugs such as tamoxifen; GNRH agonists (Sjoquist *et al.,* 2011; Yokoyama & Mizunuma, 2013); aromatase inhibitors (Van den Bossche *et al.,* 1994) and progestational agents (Yokoyama & Mizunuma, 2013). However, this therapy is often used only for palliative care and its effectiveness is still refutable (Sjoquist *et al.,* 2011).

1.5.3.2. | Angiogenesis inhibitors

Bevacizumab is a recombinant humanized monoclonal antibody that prevents VEGF binding it´s receptor. VEGF is overexpressed in malignant ovarian tumours and has been associated with advanced stage and worse survival rates (Kim *et al.,* 2012). In 2011, two large phase III studies (GOG218 and ICON 7) evaluated the impact of bevacizumab in the first line setting for adjuvant therapy in patients with advanced ovarian cancer (Burger *et al.,* 2011; Perren *et al.,* 2011). These two trials showed an improved survival rate in patients using bevacizumab with carboplatin+paclitaxel compared with patients treated with carboplatin+paclitaxel alone [GOG218 and ICON7 trials demonstrated an increase in PFS of 6 months (hazard ratio (HR), 0.645; p=0.001) and 2 months (HR, 0.81; p=0.004), respectively] (Burger *et al.,* 2011; Perren *et al.,* 2011). The improvements in PFS described in these trials directed the EMA to approve the use of bevacizumab in combination with carboplatin+paclitaxel as maintenance therapy in patients with newly diagnosed cases at advanced stages of ovarian cancer. In 2014, FDA approved bevacizumab in combination with paclitaxel, topotecan or pegylated liposomal doxorubicin to treat patients with platinum-resistant recurrences in fallopian, ovarian and peritoneal carcinomas.

1.5.3.3. | PARP inhibitors

PARPs (poly ADP-ribose polymerases) are a large family of multifunctional enzymes that play an important role in repairing single-strand breaks in DNA, particularly in base excision repair (BER) (Rouleau *et al.,* 2010). PARP inhibitors lead to accumulation of unrepaired single-strand DNA breaks in proliferating cells which cause the collapse of replication forks and subsequently, double-strand DNA breaks (Dedes *et al.,* 2011). Normal cells repair via homologous double stranded DNA pathway, where the essential components are the BRCA/2. In the absence of these tumour suppressor genes, the lesions are not repaired, which results in genetic instability and cell death (Dedes *et al.,* 2011; Berek, Friedlander & Bast, 2017). PARP inhibitors therapy is available for cancer patients and, since 50% of HGSOC harbor dysfunction in the homologous DNA repair pathway, they could benefit from this therapy (Lee, Ledermann, Kohn, 2014). Several studies have shown that olaparib (PARP inhibitor) increased PSF and/or OS among HGSOC patients with platinum-sensitive, platinum-resistant and platinum refractory disease (Mizra *et al.,* 2016; Berek, Friedlander & Bast, 2017). In 2010, Fong *et al.,* demonstrated that patients with BRCA mutations treated with olaparib, presented an OS of 46% (95% CI, 32% to 61%). Also, patients with platinum-sensitive, platinum-resistant and platinum-refractory disease, present an improved response rate to olaparib of 61.5%, 41.7% and 15.4%, respectively (Fong *et al.,* 2010). Lederman *et al.,* demonstrated that women with BRCA mutation present better PFS when treated with olaparib compared with placebo group (11.2 months vs 4.3 months, respectively) (Ledermann *et al.,* 2014). All these results showed that PARP inhibitors play an important role in treatment management of BRCA-mutated ovarian cancer (Berek, Friedlander & Bast, 2017). Olaparib, rucaparib and niraparib are FDA approved drugs for advanced ovarian cancer treatment in patients with BRCA mutation (Cortez *et al.,* 2018).

1.5.3.4. | Immunotherapy

The immunosuppressive tumour microenvironment is one of the major barriers to the successful implementation of immunotherapy in ovarian cancer (Odunsi, 2017). A network of resistance and immunosuppressive mechanisms facilitates tumour progression by actively restricting endogenous anti-tumour immunity presenting an obstacle that must be overcome so that effective immunotherapeutic strategies can be implemented (Odunsi, 2017). Several studies on tumour immunology demonstrated evidences that T cells express inhibitory receptors of immunological checkpoints, such as PD-1, that negatively regulate T cell function as a mechanism of tumour immune evasion (Pardoll, 2012). The blockage of this receptor demonstrated clinical benefits in various types of human cancer, such as

melanoma and lung cancer (Sharma & Allison, 2015). PD-1 is a cell surface receptor expressed in T cells that interacts with two known ligands, PD-L1 and PD-L2, resulting in the inhibition of T cells proliferation and cytokine production (Freeman *et al.*, 2000; Iwai, Terawaki & Honjo, 2005). Several antibodies against PD-1 and PD-L1, such as nivolumab, pembrolizumab and avelumab were administrated in platinum-resistant recurrent ovarian cancer patients and achieved an increase in PFS of 3.5, 1.9 and 10.2 months and OS of 20, 13.1 and 11.2 months, respectively (Hamanishi *et al.,* 2015; Berek, Friedlander & Bast, 2017; Varga *et al.,* 2018; Disis *et al.,* 2019).

In immunotherapeutic fields, a promising approach to treat ovarian cancer patients is target mucin 16 (MUC16) using CAR-T cells (Chekmasova *et al.,* 2010; Koneru *et al.,* 2015). Other strategies based on antibody immunotoxins or antibody drug conjugates that target mesothelin (MSLN) are also being tested in clinical trials (Hassan *et al.,* 2007; Hassan *et al.,* 2010; Tang *et al.,* 2013; Golfier *et al.*, 2014). Amatuximab, a monoclonal antibody that interferes with MUC16-MSLN interaction, is also being tested to inhibit tumour metastasis in patients with mesothelioma and ovarian cancer (Hassan *et al.,* 2010). Other strategies focused on disrupting MUC16-MSLN interaction are being developed such as using TRAIL ligands that are bound to MSLN to target MUC16 expressing cells, single chain monoclonal antibodies and immunoadhesins recognizing MUC16-MSLN binding domains (Xiang *et al.,* 2011; Su *et al.,* 2016; Coelho *et al.,* 2017).

2. | MUC16 and MSLN in ovarian cancer

The peritoneal carcinomatosis is an adverse prognostic factor in ovarian cancer. Therefore, preventing this type of malignant dissemination is crucial to improve ovarian cancer patient's survival (Coelho *et al.,* 2017). The transcoelomic dissemination in ovarian cancer is a multistep process that involves some crucial steps such as dissociation of tumour cells from the primary tumour, development of anoikis resistance, formation of multicellular aggregates, circulation in the peritoneal fluid, implantation in the organs within the peritoneal cavity and growth of tumour cells in distant organs (Naora & Montell, 2005; Weidle *et al.,* 2016). The adhesion of tumour aggregates to the mesothelial layer of the peritoneum, also denominated peritoneal homing, is a crucial step in this type of metastization (Lengyel, 2010). Several adhesion molecules, such as alpha2beta1 integrin (Fishman *et al.,* 1998; Watanabe *et al.,* 2012), VCAM I (Slack-Davis *et al.,* 2009), fibronectin (Rieppi *et al.,* 1999), among others, have been shown to play a role in the peritoneal homing (Lengyel, 2010). Additionally, other proteins and enzymes are involved in other steps of cell invasion (Tan, Agarwal & Kaye, 2006; Yeung *et al.,* 2015; Coelho *et al.,* 2017). MUC16 and MSLN are highly expressed in ovarian carcinomas and MUC16-MSLN interaction has been described to play an important role in cancer cells-mesothelium adhesion and/or invasion (Figure 5) (Rump *et al.,* 2004; Coelho *et al.,* 2017).

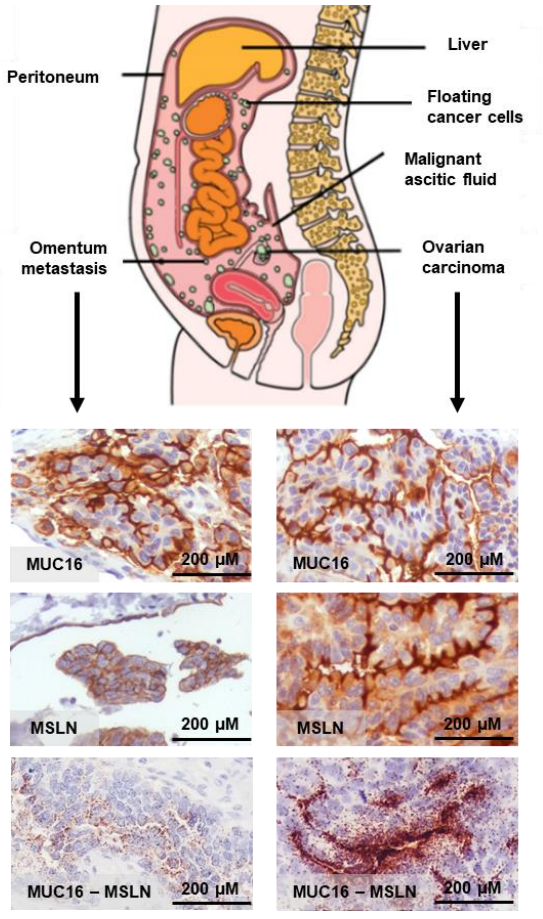

Figure 5 | Illustration of peritoneal dissemination in ovarian cancer and representative images of MUC16 and MSLN expression and MUC16 – MSLN interaction. MUC16 and MSLN expression were assessed by immunohistochemistry and MUC16-MSLN interaction was assessed by PLA in HGSOC with paired samples from primary tumour (ovarian carcinoma) and peritoneal implant (omentum metastasis). Representative brightfield images are shown for MUC16 and MSLN immunochemically staining (brown). Nuclei were stained hematoxylin (blue). Representative PLA images with brown dots representing the interaction between MUC16 and MSLN in tumour and peritoneal implant samples. Microscopic images taken at 100x magnification and scale bar represents 200 μm (Adapted from Coelho *et al.,* 2018).

2.1. | MUC16

In 1981, Bast *et al.,* discovered MUC16, a glycosylated type I transmembrane protein of the tethered mucin's family with a high molecular weight (>2 MDa) that can be detected in the CA125 serum assay (Bast *et al.,* 1981). MUC16 is usually divided in a heavily O-glycosylated N-terminus domain, a tandem repeat region and a carboxy-terminal domain that includes a short cytoplasmic tail with potential phosphorylation sites (O'Brien *et al.,* 2001; O'Brien *et al.,* 2002). This glycoprotein is normally present in the epithelium of fallopian tubes, endometrium, endocervix and mesothelial cells in the pleura, pericardium, and peritoneum (Bast *et al.,* 1981), and stratified corneal and conjunctival epithelia (Argüeso *et al.,* 2003) and have a protective role against several pathogens (Hollingsworth & Swanson, 2004). MUC16 is overexpressed in several inflammatory conditions and in many tumours' contexts such as ovarian, pancreatic and colorectal cancers (Streppel *et al.,* 2012) and peritoneal mesotheliomas (Baratti *et al.,* 2007). In ovarian cancer, MUC16 can be cleaved from tumour cells surface and found in serum (Bast *et al.,* 1981; Theriault *et al.,* 2011). CA125 assay is a screening biomarker that detects MUC16 in circulation and the studies show that 80-90% of the women with advanced stages of HGSOC present high levels of CA125 (Jacobs & Bast, 1989; Pinto *et al.,* 2012; Ricardo *et al.,* 2015; Ricardo *et al.,* 2016). In 2011, two studies demonstrated that MUC16 can modulate EOC cell proliferation, dissemination, invasion and metastasis (Theriault *et al.,* 2011; Das *et la.,* 2015) by inducing epithelial-to-mesenchymal transition and EGFR signalling (Comamala *et al.,* 2011). Recently, Muniyan *et al.,* demonstrated that the downregulation of MUC16 decreases cell growth, tumour and colony formation, migration, and metastasis in an orthotopic xenograft mouse model of pancreatic ductal adenocarcinoma (Muniyan *et al.,* 2016). Other studies also showed that MUC16 expression modulates the sensitivity of ovarian and pancreatic cancer cells to drug response (Boivin *et al.,* 2009; Das *et al.,* 2015).

2.2. | MSLN

In 1992, Chang *et al.,* described MSLN as a GPI (glycosylphosphatidylinositol) – anchored membrane glycoprotein that is synthesized as a precursor protein (~69 kDa) with four potential N-linked glycosylation sites and a hydrophobic tail that is cleaved and substituted by GPI domain (Chang, Pastan & Willingham, 1992). After glycosylation, a furin-like protease cleaves the protein, releasing a soluble N-terminal fragment, the MPF (megakaryocyte potentiating factor) (~31kDa) and the C-terminal fragment-MSLN (~40kDa) that remains anchored to the membrane (Chang, Pastan & Willingham, 1992; Chang & Pastan, 1996). MSLN can be found in normal cells, such as mesothelial cells of the pleura, pericardium and peritoneum (Scholler, 2011), surface of epithelial cells in the ovary, tunica vaginalis, rete testis and tonsillar and fallopian tube epithelial cells (Chang, Pastan & Willingham, 1992; Ordonez, 2003). MSLN is highly expressed and can be detected in cell culture supernatant, serum and malignant effusions from patients with diverse tumours´ contexts (Scholler *et al.,* 1999), such as ovarian (Chang & Pastan, 1996) and pancreatic cancers (Argani *et al.,* 2001) and mesotheliomas (Chang & Pastan, 1996). The role of MSLN in cancer is still unclear but some studies indicate that tumour cells with MSLN overexpression exhibit an increased growth (Zheng *et al.,* 2012) and inhibition of MSLN expression led to a decrease in viability in mesotheliomas, ovarian and pancreatic carcinomas (Wang *et al.,* 2012).

2.3. | MUC16 – MSLN interaction

Rump and collaborators described for the first time the MUC16–MSLN interaction and identified tandem repeat units of MUC16 as the binding domain of MSLN, suggesting that this duet could play an important role in cancer cell adhesion (Rump *et al.,* 2004). MUC16 and MSLN are two molecules overexpressed in ovarian cancer and it has been suggested that they play an important role in peritoneal dissemination. The interaction can be: 1) homotypic (cancer cell – cancer cell) interaction allowing cancer cells aggregation leading to formation of free-floating cancer aggregates (Burleson *et al.,* 2006) and 2) heterotypic (cancer cell – mesothelial cell) interaction that can be important for a successful adhesion of cells aggregates in the peritoneum and mesothelium (Figure 6) (Rump *et al.,* 2004; Coelho *et al.,* 2017).

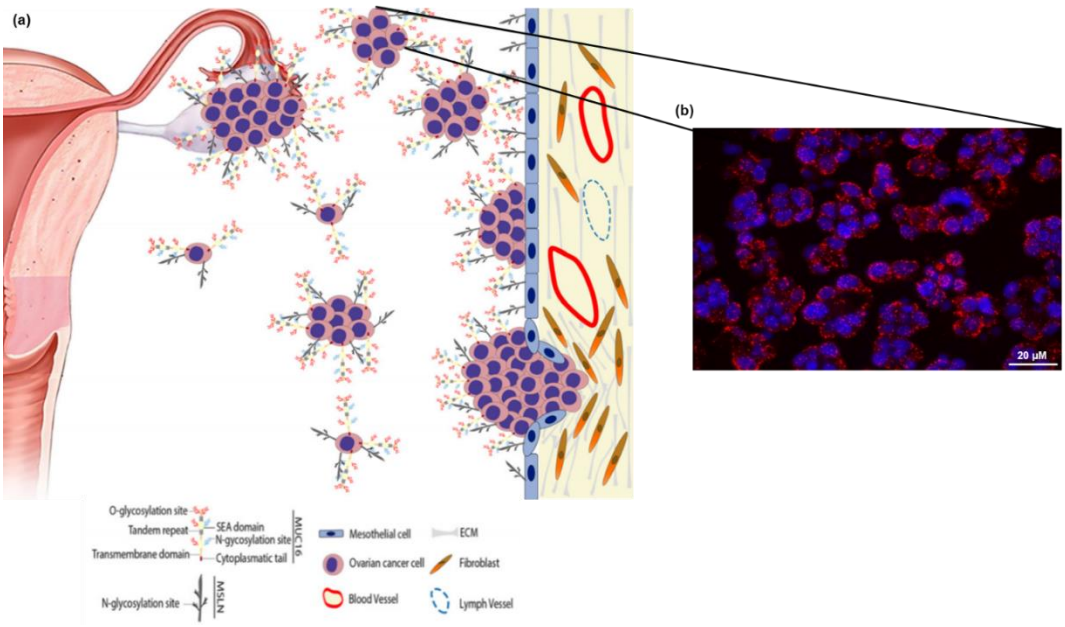

Figure 6 | MUC16-MSLN interaction in peritoneal dissemination of ovarian cancer. (a) Ovarian cancer and mesothelial cell surface express MUC16 and MSLN. These two proteins interact with each other by homotypic (cancer cell – cancer cell) or heterotypic (cancer cell – mesothelial cell) interactions. **(b)** Representative immunofluorescence microscopic image of homotypic interactions (red dots) between OVCAR3 cell aggregates by proximity ligation assay (Adapted from Coelho *et al.,* 2017).

Rump and collaborators also demonstrated that an anti-MSLN antibody was capable to abrogate the interaction between a soluble MSLN and OVCAR3 cells with MUC16 expression, concluding that MUC16-MSLN interaction mediates heterotypic cell adhesion (Rump *et al.,* 2004). In 2006, another study demonstrated that MUC16-MSLN interaction presents high affinity and could be crucial to the initial contact between ovarian cancer cells and mesothelial cells lining the peritoneal surface (Gubbels *et al.,* 2006; Coelho *et al.,* 2017). Additionally, it has been shown that MUC16-MSLN interaction increases motility and invasion in pancreatic cancers (Chen *et al.,* 2013; Coelho *et al.,* 2017). In summary, therapeutic strategies to abrogate this interaction have been used as putative therapeutic strategies to prevent early stages of peritoneal metastization.

Chapter 2 | Hypothesis and Aim

2.1. | Hypothesis

The hypothesis was if MSLN expression can modulate the chemoresistance of ovarian cancer cell lines.

2.2. | Aim

The aim of this project was to evaluate the cytotoxicity of first-line chemotherapeutic drugs commonly used in ovarian cancer patients (i.e. carboplatin and paclitaxel) in parental and CRISPR-Cas9 mediated *MSLN* knockout ovarian cancer cell lines.

Chapter 3 | Material and Methods

3.1. | Cell lines cultures

OVCAR3 cell line was established in 1983 by Hamilton *et al.,* derived from the malignant ascites of a patient with HGSOC after received a combination chemotherapy with adriamycin, cisplatin and cyclophosphamide (Hamilton *et al.,* 1983). OVCAR8 cell line was established in 1990 by *Schild*er *et al.,* derived from the ovarian tumour tissue of a patient with HGSOC after received a high-dose chemotherapy with carboplatin (Schilder *et al.,* 1990). OVCAR3 and OVCAR8 cell lines were kindly provided by Doctor Francis Jacob (Glyco-Oncology, Ovarian Cancer Research, Department of Biomedicine, University Hospital Basel, University of Basel, 4031, Basel, Switzerland).

MSLN knockout (KO) cell lines, *MSLN* KO OVCAR3 and *MSLN* KO OVCAR8, were previously genetically engineered by Ricardo Coelho in the laboratory of Glyco-Oncology – Ovarian Cancer Research in Department of Biomedicine (University Hospital Basel, University of Basel, 4031, Basel, Switzerland). Briefly, a paired sgRNAs (sgRNA1: 5'-ccagggtgcggacac aagctgca-3' and sgRNA2: 5'-cagcctcggtgcgtacttgatgggg-3') approach was used to target the MSLN-encoding gene *locus* following PCR-based identification of *Cas9* activity and homozygous KO clones. Designed and aligned oligos were cloned into pSpCas9 (BB)-2A-GFP (addgene, #PX458) via BsbI restriction site using T4-DNA ligase (Promega, Dübendorf, Switzerland). Constructs were transformed into DH5alpha *E. coli* strains and sequenced for confirmation of the sgRNA inserted into PX458 by Sanger DNA sequencing using Primer human U6. After *Cas9*-activity test in HEK293T cells, CRISPR-*Cas9* plasmids were transiently transfected into OVCAR3 and OVCAR8 cell lines and incubated at 37°C in a 5% CO_2 humidified atmosphere for 72 hours. Single cell sorting was performed in BD FACS Aria™ Cell Sorter (BD Biosciences, California, USA) for GFP^+ cells into 96-well flat-bottom plates with RPMI 1640 – GlutaMAX™ (ThermoFisher Scientific, Massachusetts, USA) supplemented with 10% (v/v) inactivated and filtered fetal bovine serum (FBS) (Biowest, Nuaillé, France) and incubated for 3 weeks at 37°C in a 5% CO_2 humidified atmosphere. Homozygous KO clones were identified based on two genotyping PCR's (Pioneer PCR: CRISPR_F:5'-CCCTACCCCAGGAGGACAAT-3' and CRISPR_R: CCCATGTACCCCGTG ACATC-3'; wild-type specific: ORF_F: 5'CCCTACCCCAGGAGGA CAA T-3' and ORF_R 5'CCCATGTACCC GTGACATC-3'). All homozygous KO clones were further validated by DNA sequencing and western blot.

All the cell lines were authenticated using short tandem repeat (STR) profiling and regularly tested for the absence of mycoplasma.

Ovarian cancer cell lines were maintained as a monolayer, under standard conditions, in complete media [pre-warmed (37ºC) RPMI 1640 supplemented with 10% (v/v) inactivated

and filtered FBS and 1% (v/v) penicillin/streptomycin (PenStrep) (ThermoFisher Scientific)] and incubated at 37°C in a 5% CO_2 humidified atmosphere.

Trypsinization was performed when monolayers achieve approximately 80% confluence. To detach adherent cells from culture flask, culture media was collected and discarded, cells were washed with phosphate buffered saline (PBS) 1x (Grisp Research solutions, Oporto, Portugal), 0.05% trypsin-EDTA (ThermoFisher Scientific) was added and incubated for 5 minutes at 37°C in a 5% CO_2 humidified atmosphere. Following detachment, trypsin-EDTA was neutralized by adding culture media and pelleted by centrifugation at 1200 rpm for 5 minutes at room temperature (RT). Next, culture media was collected and discarded, cell pellets were re-suspended in complete media, transferred into a sterile tissue culture flask and incubated at 37°C in a 5% CO_2 humidified atmosphere.

For cryopreservation of cell lines, cell pellets were re-suspended in FBS containing 10% (v/v) DMSO (dimethyl sulfoxide) (AppliChem, Barcelona, Spain), transferred into a cryovials and incubated overnight at -80°C in a Mr. Frosty™ freezing container (ThermoFisher Scientific) with isopropanol. This system was designed to achieve a freezing rate of, approximately, -1°C per minute, the ideal rate for successful preservation and recovery of cells.

To defrost cryopreserved cell lines, cryovials were taken from -80°C and cells were rapidly re-suspended in pre-warmed (37ºC) complete media and centrifuged at 1200 rpm for 5 minutes at RT. Supernatant was collected and discarded, cell pellets were re-suspended in complete media, transferred into a sterile tissue culture flasks and incubated at 37°C in a 5% CO_2 humidified atmosphere.

To count cells, a Neubauer chamber was used (Marienfeld Superior™ Counting Chamber; Marienfeld, Lauda-Königshofen, Germany). Trypan blue at 0.4% (ThermoFisher Scientific) was used to differentiate viable and non-viable cells. This solution penetrates in cells once the membrane is damaged and when observed under microscope, viable cells exclude dye and dead cells internalize trypan blue. Briefly, cell suspension was diluted 1:5 and mixed with trypan blue solution. Then, 10 µl of cell suspension was placed in a Neubauer chamber and cells were counted in five counting grid squares under a Leica DMi1 inverted phase contrast microscope (Leica Microsystems, Wetzlar, Germany) at 50x magnification.

3.2. | Cytotoxicity assays

3.2.1. | Drugs

Carboplatin and paclitaxel were purchased as powders from Selleckchem (Houston, Texas, USA). Carboplatin stock (10 mM) was diluted in pre-warmed (37ºC) sterile water and paclitaxel stock (10 mM) was diluted in DMSO, aliquoted and stored at -80°C, according to manufacturer's instructions. When necessary, an aliquot was defrosted and diluted in pre-warmed (37ºC) RPMI 1640 medium supplemented with 5% (v/v) FBS at the required concentrations.

3.2.2. | Cell viability assays

Half maximal inhibitory concentration (IC50) is a quantitative measure that represents the concentration of a substance (e.g. drug) that is required for 50% of growth inhibition *in* vitro that can be determined in a dose-response curve (Ayyagari *et al.,* 2017). Dose response curves for OVCAR3 and OVCAR8 cell lines were generated for carboplatin and paclitaxel to determine the IC50. Briefly, $5x10^3$ cells/well for parental/*MSLN* KO OVCAR3 and $2.5x10^3$ cells/well for parental/*MSLN* KO OVCAR8 were seeded into a 96-well plate in complete media and incubated at 37°C in a 5% CO_2 humidified atmosphere and incubated for 48 hours. After 48 hours of seeding, culture media was discarded, cells were treated with increasing concentrations of drugs and incubated at 37°C in a 5% CO_2 humidified atmosphere. Carboplatin was tested at concentration range 1.563 to 200 µM for OVCAR3 and 3.125 to 400 µM for OVCAR8. Paclitaxel was tested at concentrations between 0.781 to 100 nM for all the cell lines. Following 48 hours of treatment, cell viability was measured using Methylthiazolyldiphenyl-tetrazolium bromide (MTT), Presto Blue (PB) and Sulforhodamine B (SRB) assays, according to manufacturer's instructions.

3.2.2.1. | Methylthiazolyldiphenyl-tetrazolium bromide assay

MTT assay was described in 1983 by Mosmann and is based in metabolic capacity of viable cells to reduce MMT, a yellow tetrazolium salt, into a purple formazan crystal product, that accumulates as an insoluble precipitate (Mosmann, 1983; Riss *et al.,* 2004; Ediriweera, Tennekoon & Samarakoon, 2019). When formazan is solubilized produces a colorimetric signal proportional to cell viability (Riss *et al.,* 2004; Ediriweera, Tennekoon & Samarakoon, 2019) (Figure 7).

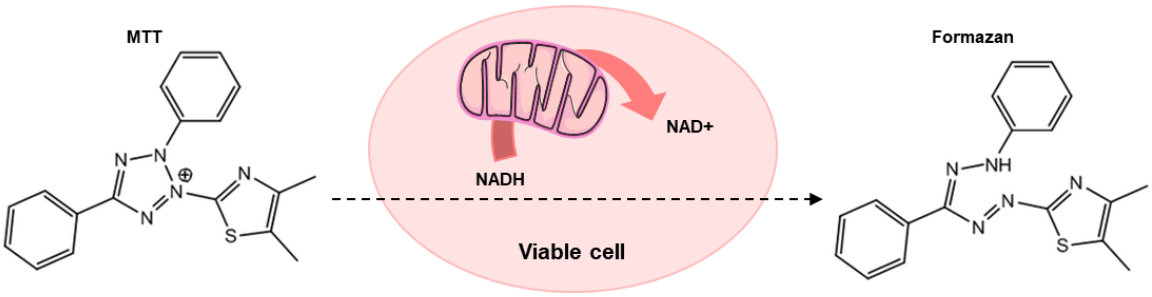

Figure 7 | Principle of cell viability detection by MTT assay. In metabolic active cells, MTT solution (yellow tetrazolium salt) is reduced into a formazan (purple crystal product) that is solubilized producing a colorimetric signal proportional to cell viability.

Briefly, 48 hours after treatment, culture media was discarded and replaced with 500 µg/ml of MTT (Sigma-Aldrich, Missouri, USA) prepared in complete media and incubated for 3 hours at 37°C in a 5% CO_2 humidified atmosphere. After, the supernatant was discarded, and formazan crystals were dissolved in DMSO. Absorbance was measured at 570 nm wavelength using a Bio Tek Synergy™ 2 multi-mode microplate reader (Bio Tek, Vermont, USA).

3.2.2.2. | Presto Blue assay

PB assay (ThermoFisher Scientific) is based in metabolic capacity of viable cells to reduce a substrate. PB reagent is a cell permeable resazurin-based solution and when added to cells, is metabolized by viable cells that convert dark blue oxidized form of dye (resazurin) into a red-fluorescent reduced form (resorufin), becoming highly fluorescent (Figure 8).

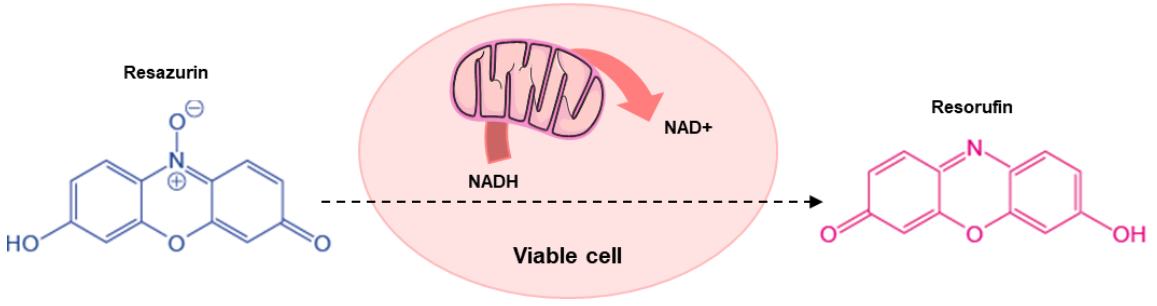

Figure 8 | Principle of cell viability detection by PB assay. In metabolic active cells, PB solution (resazurin, dark blue) is reduced into a resorufin (red fluorescent) producing a highly fluorescent signal proportional to cell viability.

Briefly, 48 hours after treatment, culture media was discarded, adherent cells were washed with PBS 1x, added 50 µl of PrestoBlue™ Cell Viability Reagent 1x (ThermoFisher Scientific) prepared in complete medium and incubated for 45 minutes at 37°C in a 5% CO_2

humidified atmosphere, protected from light. Fluorescence was measured at 560 nm excitation/590 nm emission using a Bio Tek Synergy™ 2 multi-mode microplate reader.

3.2.2.3. | Sulforhodamine B assay

SRB assay was developed in 1990 by Skehan *et al.,* and is based on amount of cellular protein. SRB dye binds to basic amino-acid residues of proteins in cells fixed with trichloroacetic acid (TCA) (Skehan *et al.,* 1990; Vichai & Kirtikara, 2006). In acidic conditions, SRB bind stoichiometrically to target proteins and in basic conditions, can be solubilized for spectrophotometrically measurement to determine relative viability (Skehan & Friedman, 1985). The amount of dye extracted from stained cells is directly proportional to cell mass (Skehan *et al.,* 1990; Vichai & Kirtikara, 2006) (Figure 9).

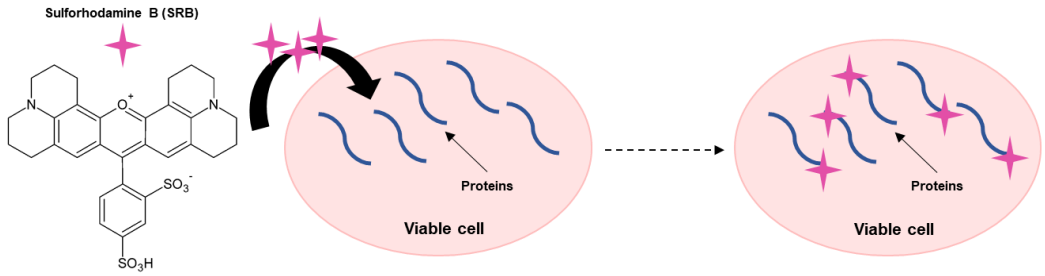

Figure 9 | Principle of cell viability detection by SRB assay. In TCA fixed cells, SRB binds to basic amino-acid proteins residues and, after solubilisation steps, is produced a spectrophotometrically signal proportional to cell mass.

Briefly, after performing PB assay, supernatant was discarded, and adherent cells were fixed with 10% (v/v) TCA (ThermoFisher Scientific) for 1 hour on ice. Following fixation, plates were washed with distillated water, dried at RT and cells were stained in 0.4% (v/v) SRB (Sigma-Aldrich) in 1% (v/v) acetic acid (Sigma-Aldrich) for 30 minutes. Plates were washed three times in 1% (v/v) acetic acid, dried at RT and fixed cells were solubilized in 10 mM Tris (Sigma-Aldrich). Absorbance was measured at 570 nm wavelength using a Bio Tek Synergy™ 2 multi-mode microplate reader.

For all the cytotoxic assays, treated cells were compared with control cells (considered 100% viable) containing 1% (v/v) vehicle (sterile water for carboplatin and DMSO for paclitaxel). All assays were done in triplicate with at least three independent experiments. Data were expressed as mean ± standard deviation, statistical analysis was performed in GraphPad Prism Software Inc. v6 using Student's t-test and a value of $p<0.05$ was considered statistically significant.

3.3. | Cell Microarray construction

Cell Microarray (CMA) are a single paraffin block constructed with several cores from different cell pellets that allow simultaneous analysis of the expression of a specific protein or antigen in a single experiment (Kononen *et al.,* 1998; Rubin *et al.,* 2002; Jensen, 2003). For CMA construction, $4x10^5$ cells/well of parental/*MSLN* KO OVCAR3 and $2x10^5$ cells/well for parental/*MSLN* KO OVCAR8 were seeded into 6-well plates and incubated at 37°C in a 5% CO_2 humidified atmosphere. After 48 hours of seeding, culture media was discarded, cells were treated with increasing concentrations of drugs and incubated at 37°C in a 5% CO_2 humidified atmosphere. Carboplatin was tested at 60 and 120 µM for OVCAR3 and 200 and 400 µM for OVCAR8. Paclitaxel was tested at 6 and 12 nM for OVCAR3 and 7.5 and 15 nM for OVCAR8. After 48 hours of treatment, culture media was removed, adherent cells were washed with cold PBS 1x, scraped from culture dishes and centrifuged at 1200 rpm for 5 minutes at RT. Cell pellets were fixed in 10% (v/v) neutral-buffered formalin (AppliChem) for 1 hour with gently agitation. After fixation, cells were centrifuged at 2800 rpm for 5 minutes at RT, the supernatant was discarded, and cell pellets were re-suspended in liquefied HistoGel™ (ThermoFisher Scientific). After centrifugation (4000 rpm for 1 minute at RT) histogel embedded cells were incubated at 4ºC for 10 minutes and placed in a histological cassette. Before, standard histological processing was performed: dehydration in a crescent series of alcohol concentrations [70% (v/v) – 95% (v/v) – 100% (v/v)], clarification with clear rite (ThermoFisher Scientific) and paraffin impregnation followed by embedded with liquefied paraffin at 60ºC.

To construct CMA block, each condition block (donor blocks) were sectioned at 3 µm thickness and stained with hematoxylin and eosin (H&E; ThermoFisher Scientific) for morphology control. CMA was planned and constructed by adding one core (1.5 mm in diameter) from each donor block to a recipient paraffin block. Control tissue cores (e.g. human ovary tumour, mouse ovary and human liver) were included as positive immunocytochemistry controls and to simplify orientation. After construction, CMA was homogenized overnight at 37ºC, sectioned at 3 µm thickness and adhered to coated glass slides (Superfrost Plus®, ThermoFisher Scientific) (Figure 10).

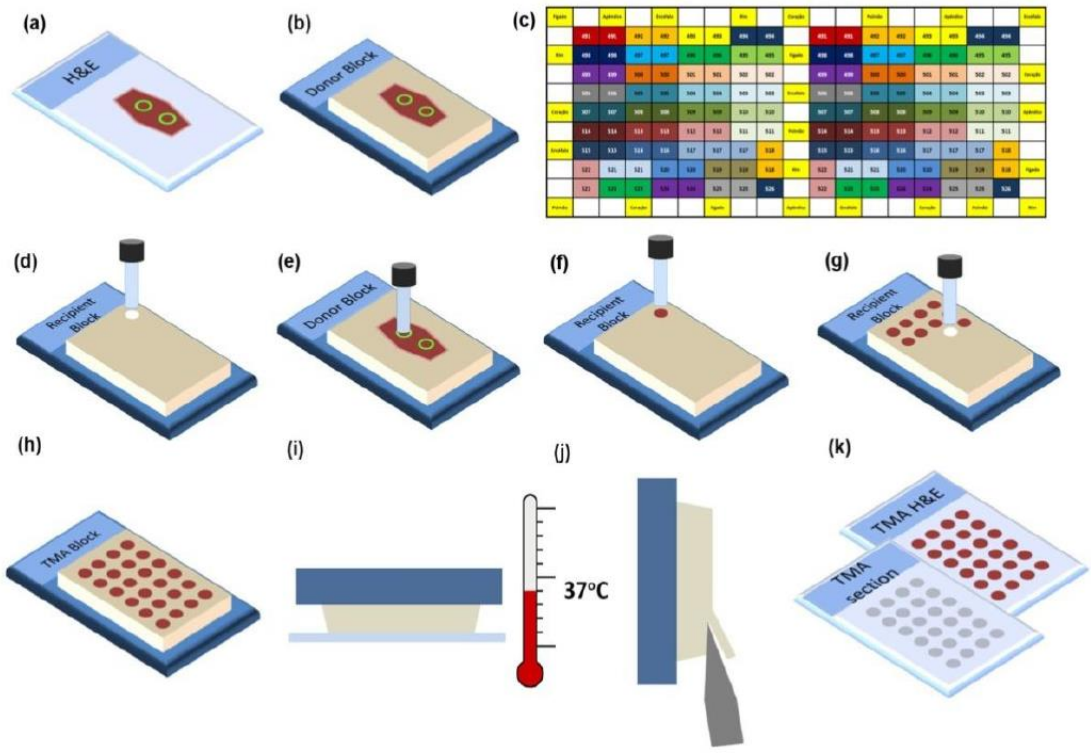

Figure 10 | CMA construction procedure. (a) Cell/tissue areas are selected from H&E sections and **(b)** marked on the correspondent paraffin donor block. **(c)** CMA grid is planned on Excel (Microsoft Office) data sheet. **(d to h)** From recipient block is removed a paraffin core and placed a core of cells obtained from marked areas on donor block. A core of cells was inserted into hole of recipient block. This procedure was repeated to create a complete CMA block. **(i)** Recipient block was slightly melted (37ºC) to bind cores into paraffin block. **(j)** Sequential 3 µm sections were cut **(k)** and adherent to a coated glass slide (Adapted from Ricardo, 2011).

3.4. | Immunocytochemistry

Immunocytochemistry was first reported in 1941 by Coons *et al.,* and allows direct visualization of cellular distribution of an antigen by using labelled antibodies (Coons, Creech & Jones, 1941). Since then, immunocytochemistry has been in constant development to achieve more specific and amplified signals from a single epitope. The indirect target antigen detection method allows more signal amplification since several secondary antibodies binding to a single primary antibody (Burry, 2011). The indirect method using Horseradish peroxidase (HRP) is more frequently used in pathology an in this immunocytochemistry variant, unlabelled primary antibody binds to an epitope in a target antigen, followed by a secondary antibody directed to immunoglobulins of primary antibody species (Burry, 2011). HRP conjugated secondary antibody reacts with a chromogen solution of diaminobenzidine (DAB) that gives a brown color to antigenic epitope in the cell/tissue (Figure 11).

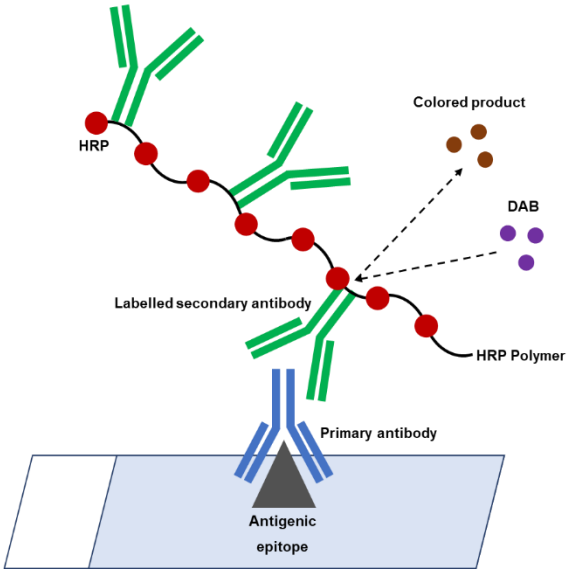

Figure 11 | Schematic representation of indirect immunocytochemistry. Primary antibody binds to the antigenic epitope. Next, labelled secondary antibody binds specifically to immunoglobulins of primary antibody species. The secondary antibody conjugated with HRP polymer is incubated with DAB (substrate) and a brown stain is detected at the antigenic epitope. **DAB –** diaminobenzidine and **HRP –** Horseradish peroxidase.

Immunocytochemistry was performed in CMA slides to access the expression patter of MSLN. Briefly, slides were deparaffinized in xylene (ThermoFisher Scientific), dehydrated in a decreasing series of alcohol concentrations [100% (v/v) – 95% (v/v) – 70% (v/v)] and water. The heat-induced (98ºC) antigen retrieval was performed in a steamer with citrate buffer solution (1:100 at pH 6.0; ThermoFisher Scientific) for 40 minutes. Endogenous peroxidase activity was blocked with hydrogen peroxide solution 3% (v/v) (ThermoFisher Scientific), for 10 minutes at RT in a humidified chamber. After washed with tris buffered saline 1x (TBS; Grisp Research solutions) with 0.05% (v/v) tween 20 (Sigma-Aldrich), slides were incubated with MSLN (1.50; SP74, ThermoFisher Scientific) for 1 hour at RT in a humidified chamber. Then, the slides were washed with TBS-0.05% (v/v) tween 20 and were incubated with a secondary antibody with HRP labelled polymer (Dako REAL™ EnVision™ Detection System Peroxidase/DAB⁺, Rabbit/Mouse) for 30 minutes at RT in a humidified chamber. After incubation, DAB (Dako) was used as chromogen according to manufacturer's instructions. Finally, nuclear staining with hematoxylin was performed and slides were dehydrated in water and a crescent series of alcohol [70% (v/v) – 95% (v/v) – 100% (v/v)], clarified with xylene and coverslip using a permanent mounting medium (Bio mount HM; Bio-Optica, Milan, Italy). For MSLN antibody was included a positive tissue slide. Immunocytochemistry results were evaluated by two independent observers (Mariana Nunes and Sara Ricardo). The percentage of cells stained [<10% (considered negative), ≥10–<25%, ≥25–>50%, ≥50–<75%, and ≥75%] for MSLN expression were assessed.

3.5. | Apoptosis assay

Cell apoptosis was measured by flow cytometry using Annexin V-FITC apoptosis detection kit™ (ThermoFisher Scientific), according to manufacturer's instructions. In normal physiological conditions phosphatidylserine (PS) is placed in internal side of cell membrane and after starting apoptosis, cells translocate these molecules to outside of membrane. Annexin V is a protein that exhibits anti-phospholipase activity and binds to PS on external side of cell membrane. Propidium iodide (PI), a viability dye, can be used to access late-stage of apoptotic and necrotic cells, when cell membrane loses integrity and allowing annexin V to access internal PS (Figure 12).

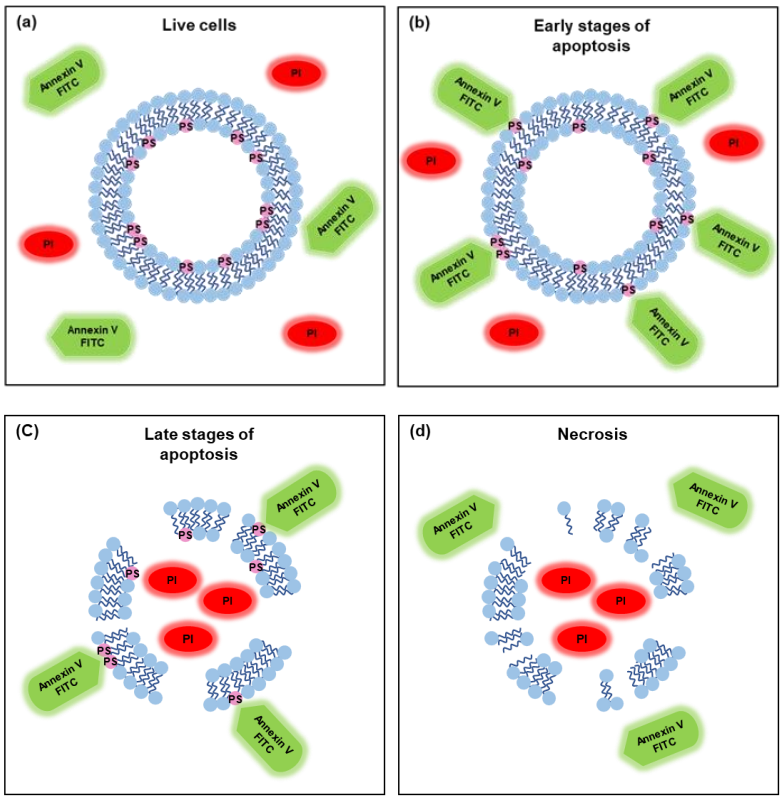

Figure 12 | Schematic representation of Annexin V-FITC apoptosis detection kit™. (a) In viable cells, PS is in the internal part of cell membrane and no signal of annexin V and PI is detected. **(b)** In early stages of apoptosis, loss of cell membrane asymmetry occurs, and PS is exposed to the external part of the membrane and can be detected with annexin V-FITC (green). **(c)** In late stages of apoptosis, cells lose partially integrity of cell membrane and allows PI to enter in the cells (red) and PS (external and internal) can be detected with annexin V-FITC (green). (**d)** In necrotic cells, integrity of cell membrane is extensive lost and allows PI to enter in cells. Also, PS is totally damaged and annexin V-FITC cannot be detected. **FITC** – fluorescein isothiocyante; **PI** – Propidium iodide and **PS** – phosphatidylserine.

To measure cell apoptosis, $4x10^5$ cells/well for parental/*MSLN* KO OVCAR3 and $2x10^5$ cells/well for parental/*MSLN* KO OVCAR8 were seeded into 6-well plates and incubated at

37°C in a 5% CO_2 humidified atmosphere. After 48 hours of seeding, culture media was discarded, cells were treated with increasing concentrations of drugs and incubated at 37°C in a 5% CO_2 humidified atmosphere. Carboplatin was tested at 60 and 120 µM for OVCAR3 and 200 and 400 µM for OVCAR8. Paclitaxel was tested at 6 and 12 nM for OVCAR3 and 7.5 and 15 nM for OVCAR8. After 48 hours of treatment, supernatant was collected, cells were washed with PBS1x. To avoid enzymatic cleavage of cell surface antigens, 1 ml of cell dissociation buffer enzyme-free in PBS (ThermoFisher Scientific) was used to detach cells from culture plates. Cells were collected, re-suspended in complete media and centrifuged at 1200 rpm for 5 minutes at RT. Cell pellets were washed with PBS 1x, centrifuged at 1200 rpm for 5 minutes at RT, re-suspended in 195 µL of binding buffer and filtrated for obtain single cell suspensions. Next, 5 µL of Annexin V-FITC was added and incubated for 10 minutes, protected from light. Then, 10 µL of PI was added for 1 minute, protected from light. Fluorescence was assessed by BD FACS Canto™ II (BD Biosciences) flow cytometer and data was analyzed by FlowJo software v10.0.7 (Oregon, USA). All assays were done in three independent experiments. Data were expressed as mean ± standard deviation and statistical analysis was performed in GraphPad Prism Software Inc. v6 using Student's t-test and a value of $p<0.05$ was considered statistically significant.

3.6. | Immunoblotting

Western blot was first described in 1979 by Towbin *et al.,* and allow protein measurement (qualitative and semi quantitative) using a specificity antibody to detect a antigen (Towbin, Staehelin & Gordon, 1979). Western blot was performed to evaluate expression of key modulators of apoptosis such as PARP and cleaved-PARP. Briefly, $4x10^5$ cells/well for parental/*MSLN* KO OVCAR3 and $2x10^5$ cells/well for parental/*MSLN* KO OVCAR8 were seeded into 6-well plates and incubated at 37°C in a 5% CO_2 humidified atmosphere. After 48 hours of seeding, culture media was discarded, cells were treated with increasing concentrations of drugs and incubated at 37°C in a 5% CO_2 humidified atmosphere. Carboplatin was tested at 60 and 120 µM for OVCAR3 and 200 and 400 µM for OVCAR8. Paclitaxel was tested at 6 and 12 nM for OVCAR3 and 7.5 and 15 nM for OVCAR8. After 48 hours of treatment, supernatant was collected, adherent cells were washed with cold PBS1x, scraped from culture dishes and centrifuged at 1200 rpm for 5 minutes at 4ºC. Then, cell pellets were resuspended in RIPA buffer [50 mM Tris-HCl (Sigma-Aldrich), 1% (v/v) NP40 (Sigma-Aldrich), 150 mM NaCl (Sigma-Aldrich) and 2 mM EDTA (Sigma-Aldrich), at pH 7.5], containing protease (100 mM PMSF; Sigma-Aldrich) and phosphatase (100 nM Na_3VO_4; Sigma-Aldrich) inhibitors and cOmplete™ protease inhibitor cocktail (Sigma-Aldrich) and incubated for 30 minutes on ice. Cell lysates were centrifuged at 14000 rpm

for 15 minutes at 4ºC to pellet insoluble material, and supernatant was collected and stored at -20°C.

Protein quantification was determined using Pierce™ BCA protein assay kit (ThermoFisher Scientific). In an alkaline environment, bicinchoninic acid (BCA) detect the reduction of Cu^{2+} to Cu^{1+} by proteins. First, in biuret reaction occurs chelation of cooper (Cu), peptides containing three or more amino acid residues form a light blue complex with cupric ions. Secondly, BCA interact with reduced cation (Cu^{1+}) resulting in an intense purple-coloured reaction product. Briefly, BSA standards were prepared at concentrations between 25 and 2000 µg/ml and each protein lysate were diluted 5x in distillated water. BCA reagent was prepared in a 1:50 ratio (reagent A to reagent B) and added to either BSA standard or cell lysate and incubated for 30 minutes at 37°C. The absorbance was measured at 562 nm wavelength using a Bio Tek Synergy™ 2 multi-mode microplate reader. From BSA standard A562 nm values, a protein standard calibration curve was obtained and used to calculate protein concentration in each cell lysate. Standard curves were accepted when $r^2 > 0.90$. From each cell lysate, 20 µg protein was added to a loading buffer [Laemmli 4x (1 M Tris-HCl) (Sigma-Aldrich), at pH 6.8, glycerol (Sigma-Aldrich) and SDS (National Diagnosis, Atlanta, Georgia), 5% (v/v) β-mercaptoethanol (Sigma-Aldrich) and 5% (v/v) bromophenol blue (Sigma-Aldrich)], denatured at 95°C for 5 minutes and stored at -20ºC.

SDS-PAGE allows separates proteins according to the mass (Kurien & Scofield, 2009). Briefly, was prepared 12% gel resolving containing [1.5 M Tris at pH 8.8 (Bio-Rad Laboratories, California, USA), 40% Acryl:Bis (29:1; Bio-Rad Laboratories), 10% (v/v) SDS, 10% (v/v) APS (100 mg/ml) (Sigma-Aldrich), 1% (v/v) TEMED (Sigma-Aldrich) and distillated water], added to an electrophorese system and allow gel polymerization at RT. Next, was prepared 4% gel stacking containing [0.5 M Tris at pH 6.8 (Bio-Rad Laboratories), 40% (v/v) Acryl:Bis (29:1), 10% (v/v) SDS, 10% (v/v) APS (100 mg/ml), 1% (v/v) TEMED and distillated water] added to a electrophorese system and allow gel polymerization at RT. Then, was added to the system a running buffer (TGS 1x at pH 8.3; Bio-Rad Laboratories), and protein samples or molecular marker (Precision Plus Protein™ Standards; #161-0374; Bio-Rad Laboratories) were charged into wells. The gel was run at 120 Volts for 1 hour and a half. Following SDS-PAGE, proteins in polyacrylamide gel were subsequently transferred onto Hybond ECL™ nitrocellulose membrane (GE Healthcare, Uppsala, Sweden) with a transfer buffer [TG 1x at pH 8.3 (Bio-Rad Laboratories)], containing 20% (v/v) methanol (ThermoFisher Scientific), at 60 Volts for 1 hour and a half, on ice with agitation. The nitrocellulose membrane was staining with Ponceau S dye (Sigma-Aldrich) to confirm the presence of protein transfer and was washed several times with TBS 1x with 0.1% (v/v) tween 20 (TBS-T).

The nitrocellulose membrane has a high affinity for proteins, therefore is necessary blocking the surface to avoid nonspecific binding of antibodies. So, the membrane was incubated with TBS-T containing 5% (w/v) low fat milk or BSA (Sigma-Aldrich) for 1 hour at RT with gentle agitation. Next, membrane was incubated with a primary antibody (conditions in Table II). In the next day, the membrane was washed three times in TBS-T and incubated with a secondary antibody anti-mouse IgG HRP-linked antibody (A4416, 1:4000; ThermoFisher Scientific) or anti-rabbit IgG HRP-linked antibody (#7074; 1:10000; Cell Signalling Technology) diluted in TBS-T for 1 hour at RT with gentle agitation. After incubation time, membrane was washed three times with TBS-T and protein bands were visualized using GE Healthcare Amersham™ ECL™ Western Blotting Detection Reagents (GE Healthcare) for chemiluminescence detection, according to manufacturer's instructions. Detection was performed in ChemiDoc™ XRS+ system (Bio-Rad Laboratories). Protein bands were assessed using Image Lab Software (Bio-Rad Laboratories) and normalized for β-actin protein levels. All assays were done in at least three independent experiments.

Table II | Primary antibodies and conditions used in immunoblot procedure.

Protein	Clone	Origin	Animal origin	Molecular weight (kDa)	Dilution		Incubation conditions
Cleaved-PARP	D64E10	Cell Signalling Technology	Rabbit	89 (cleaved) 116 (full)	1:1000	Low fat milk 5%	4ºC overnight with gentle shaking
Mesothelin	D4X7M	Cell Signalling Technology	Rabbit	46-48 (cleaved) 70 (precursor)	1:1000		
β-actin	SC-47778 (C4)	Santa Cruz Biotechnology	Mouse	42	1:1000	BSA 5%	

Chapter 4 | Results

4.1. | Carboplatin inhibits cell viability in parental and *MSLN* KO cells

To investigate whether MSLN expression was associated with platinum chemoresistance of ovarian cancer cell lines, three different cell viability assays (MTT, PB and SRB) were performed to determine the necessary concentration of drug to achieve 50% of growth inhibition (IC50). For this, parental/*MSLN* KO OVCAR3 and parental/*MSLN* KO OVCAR8 cells were exposed to carboplatin covering a concentration range from 1.563 to 200 µM and 3.125 to 400 µM, respectively, for 48 hours. As shown in Figure 13, carboplatin inhibited cell viability in both parental and *MSLN* KO ovarian cancer cell lines.

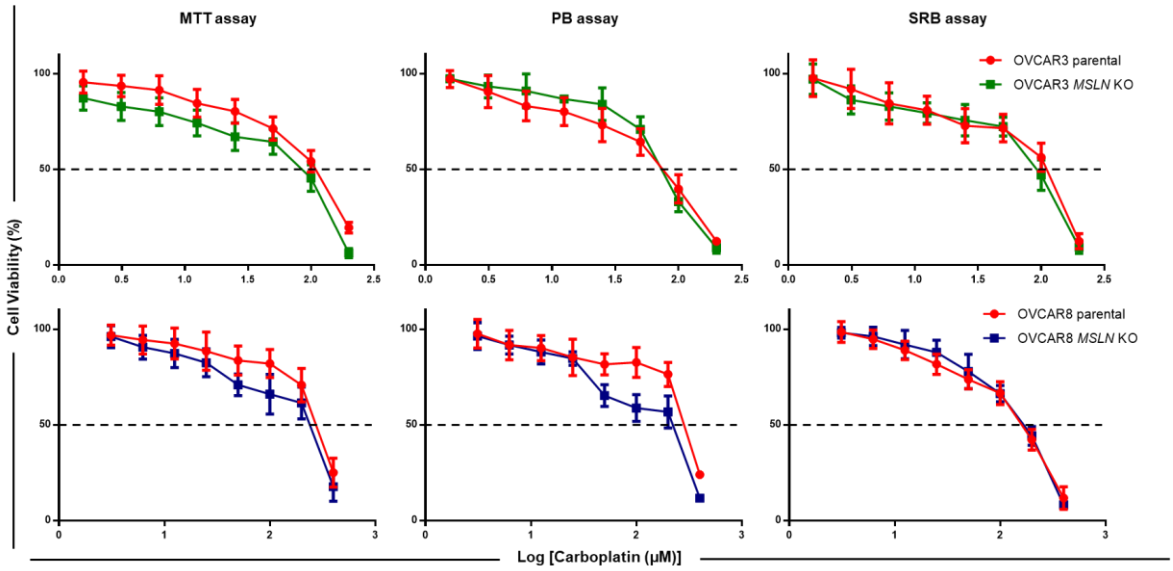

Figure 13 | Carboplatin dose response curves for parental/*MSLN* KO OVCAR3 and OVCAR8 cells. The results were obtained by MTT, PB and SRB assays, after exposure of parental/*MSLN* KO OVCAR3 and OVCAR8 cells to carboplatin covering a concentration range from 1.563 to 200 µM and 3.125 to 400 µM, respectively, for 48 hours. Dotted line corresponds to 50% of growth inhibition. Treated cells were compared with vehicle, considered as 100% viable. All assays were done in triplicate in at least three independent experiments. Data is expressed as mean ± standard deviation and plotted using GraphPad Prism Software Inc. v6.

4.1.1. | *MSLN* KO cells are more sensitive to carboplatin

For parental and *MSLN* KO OVCAR3 cells, carboplatin IC50 values for MTT assay were 111.853 ± 5.412 µM and 87.977 ± 4.529 µM (*p<0.05, n=5); for PB assay were 79.213 ± 3.202 µM and 77.575 ± 1.041 µM (p>0.05, n=3); and for SRB assay were 114.242 ± 6.052 µM and 94.197 ± 3.094 µM (*p<0.05, n=5), respectively (Figure 14). For parental and *MSLN* KO OVCAR8 cells, carboplatin IC50 values for MTT assay were 291.690 ± 11.450 µM and 253.801 ± 24.167 µM (*p<0.05, n=5); for PB assay were 300.717 ± 4.754 µM and 229.822 ± 5.778 µM (*p<0.05, n=3); and for SRB assay were 169.516 ± 11.350 µM and 173.919 ± 7.067 µM (p>0.05, n=5), respectively (Figure 14). The results showed that parental cells are

significantly less sensitive to carboplatin when compared with the corresponding *MSLN* KO cells.

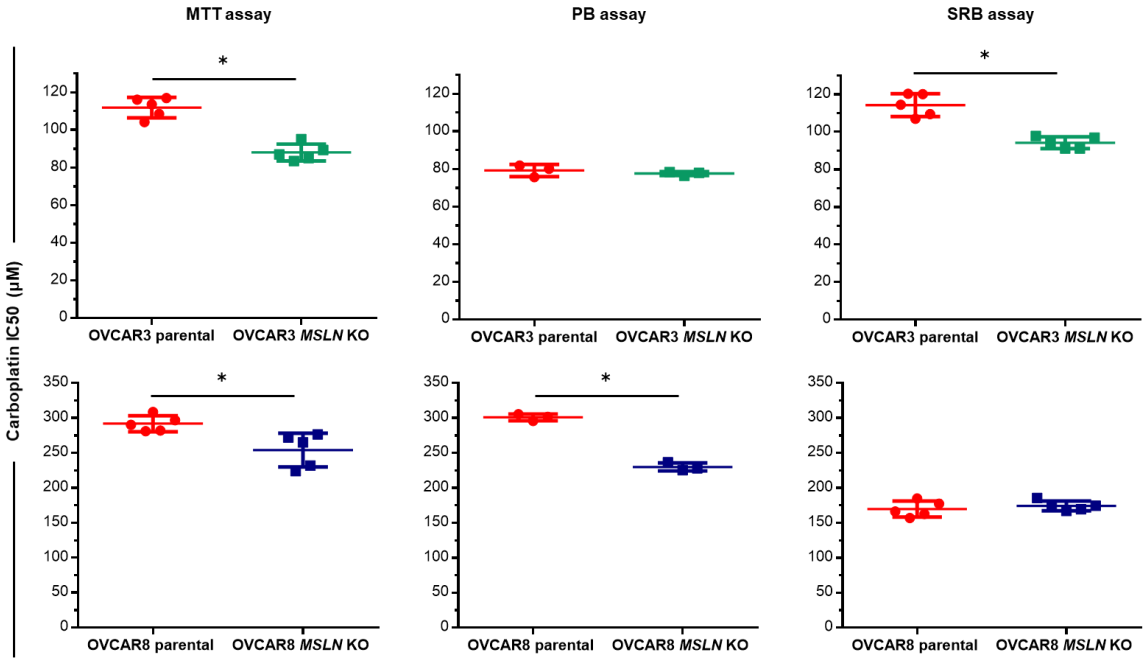

Figure 14 | Carboplatin IC50 for parental/*MSLN* KO OVCAR3 and OVCAR8 cells. IC50 was measured by MTT, PB and SRB assays, after exposure of parental/*MSLN* KO OVCAR3 and OVCAR8 cells to carboplatin covering a concentration range from 1.563 to 200 µM and 3.125 to 400 µM, respectively, for 48 hours. Treated cells were compared with vehicle, considered as 100% viable. All assays were done in triplicate in at least three independent experiments. Data is expressed as mean ± standard deviation and plotted using GraphPad Prism Software Inc. v6. Statistical analysis was performed using Student's t-test and a value of *p<0.05 was considered statistically significant.

4.2. | Carboplatin induces apoptotic cell death

Apoptosis deregulation is often associated with the development of chemoresistance and it has been shown that the molecular mechanisms of platinum resistance involve deregulation of apoptosis (Galluzzi *et al.,* 2012). Carboplatin ability to induce apoptosis was evaluated by flow cytometry through analyzing PS externalization and membrane permeability after Annexin V-FITC/PI labelling. For this, parental/*MSLN* KO OVCAR3 and OVCAR8 cells were exposed to carboplatin at 60 and 120 µM or 200 and 400 µM, respectively, for 48 hours. After exposure of OVCAR3 cells to carboplatin at 60 and 120 µM, the percentage of apoptosis (early and late) for parental cells were 6.695 ± 3.664% and 10.360 ± 4.542% respectively, and for *MSLN* KO cells were 44.540 ± 7.193 % and 44.365 ± 1.811%, respectively. The total percentage of apoptotic cells for parental OVCAR3 after exposure to carboplatin was significantly decreased (*p<0.05, n=3) when compared with

the corresponding *MSLN* KO cells (Figure 15). Therefore, according to previous cell viability results, carboplatin induces more apoptosis in OVCAR3 cells without MSLN expression.

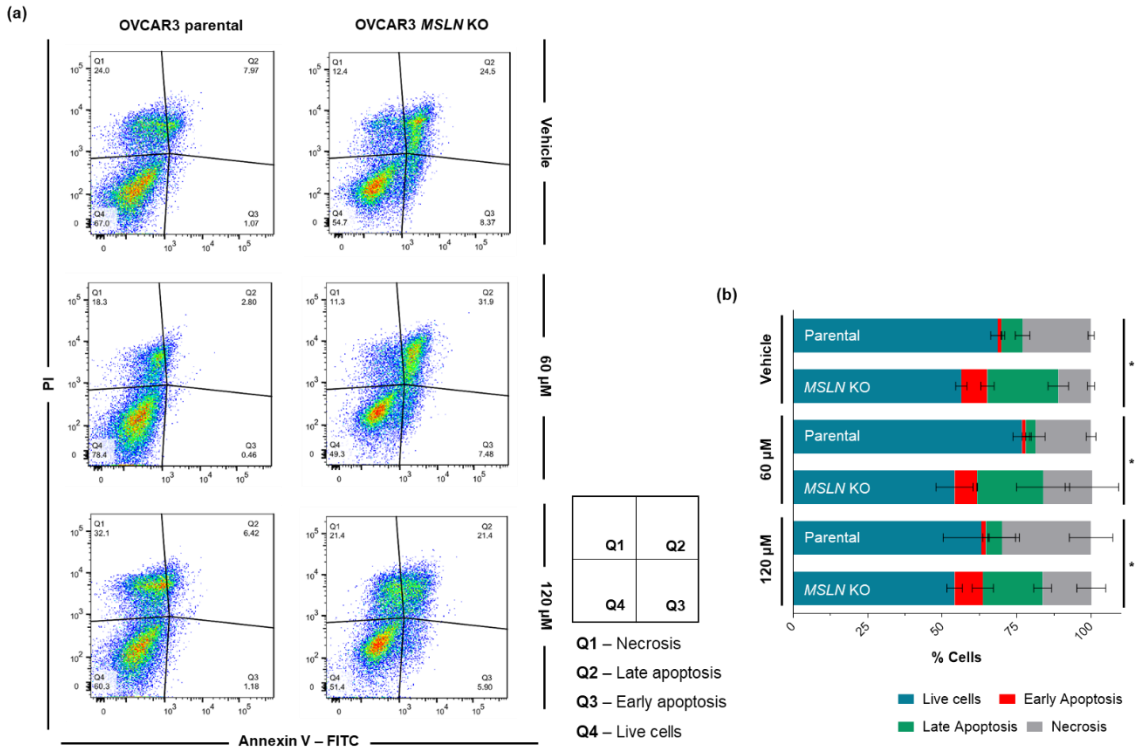

Figure 15 | Carboplatin effect in apoptosis of parental/*MSLN* KO OVCAR3 cells. Apoptotic cells were measured by flow cytometry analysis after Annexin V-FITC and PI labelling in parental and *MSLN* KO OVCAR3 cells exposed to carboplatin at 60 and 120 µM or vehicle, for 48 hours. **(a)** Representative flow cytometry dot plot. **Q1 –** Necrosis; **Q2 –** Late apoptosis; **Q3 –** Early Apoptosis and **Q4 –** Live cells. Fluorescence was assessed by BD FACS Canto™ II (BD Biosciences) flow cytometer and data was analyzed by FlowJo software v10.0.7. All assays were done in three independent experiments. **(b)** Percentage of cell populations (live cells, early apoptosis, late apoptosis and necrosis). Data is expressed as mean ± standard deviation and plotted using GraphPad Prism Software Inc. v6. Statistical analysis was performed using Student's t-test and a value of *p<0.05 was considered statistically significant.

After exposure of OVCAR8 cells to carboplatin at 200 and 400 µM, the percentage of apoptosis (early and late) for parental cells were 7.687 ± 0.848% and 45.200 ± 2.609%, respectively, and for *MSLN* KO cells were 9.080 ± 1.091% and 33.213 ± 4.451%, respectively. The total percentage of apoptotic cells for parental OVCAR8 after exposure to 400 µM carboplatin was significantly increased (*p<0.05, n=3) when compared with the corresponding *MSLN* KO cells (Figure 16). Therefore, contrary to previous cell viability results, carboplatin induces more apoptosis in OVCAR8 cells that express MSLN.

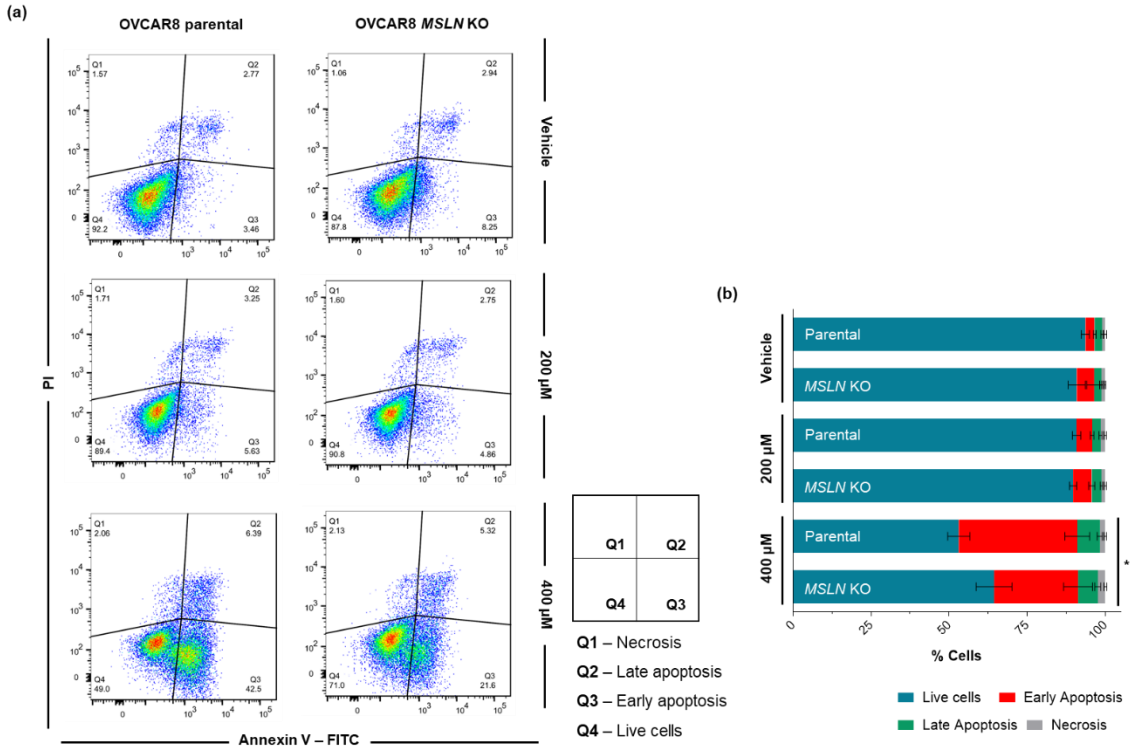

Figure 16 | Carboplatin effect in apoptosis of parental/*MSLN* KO OVCAR8 cells. Apoptotic cells were measured by flow cytometry analysis after Annexin V-FITC and PI labelling in parental and *MSLN* KO OVCAR8 cells exposed to carboplatin at 200 and 400 µM or vehicle, for 48 hours. **(a)** Representative flow cytometry dot plot. **Q1 –** Necrosis; **Q2 –** Late apoptosis; **Q3 –** Early Apoptosis and **Q4 –** Live cells. Fluorescence was assessed by BD FACS Canto™ II (BD Biosciences) flow cytometer and data was analyzed by FlowJo software v10.0.7. All assays were done in three independent experiments. **(b)** Percentage of cell populations (live cells, early apoptosis, late apoptosis and necrosis). Data is expressed as mean ± standard deviation and plotted using GraphPad Prism Software Inc. v6. Statistical analysis was performed using Student's t-test and a value of *p<0.05 was considered statistically significant.

4.3. | Carboplatin enhances cleaved-PARP activity

To explore the role of MSLN expression in carboplatin ability to induce apoptosis, PARP and cleaved-PARP activity were assessed by immunoblot. For this, parental/*MSLN* KO OVCAR3 and OVCAR8 cells were exposed to carboplatin at 60 and 120 µM or 200 and 400 µM, respectively, for 48 hours. As shown in Figure 17, carboplatin induces apoptosis evidenced by decreased PARP and increased cleaved-PARP activity in both parental/*MSLN* KO OVCAR3 and OVCAR8 cells when compared with the corresponding vehicle. Relatively to parental OVCAR3 cells exposed to carboplatin at 120 µM, the amount of cleaved-PARP was decreased when compared with the corresponding *MSLN* KO cells (Figure 17). Consistently to cell viability and Annexin V-PI results, carboplatin induces more apoptosis in OVCAR3 cells without MSLN expression. On the other hand, for parental OVCAR8 cells, exposed to carboplatin at 400 µM, the amount of cleaved-PARP was

increased when compared with the corresponding *MSLN* KO cells (Figure 17). Concordantly to Annexin V-PI results, carboplatin induces more apoptosis in OVCAR8 cells that express MSLN.

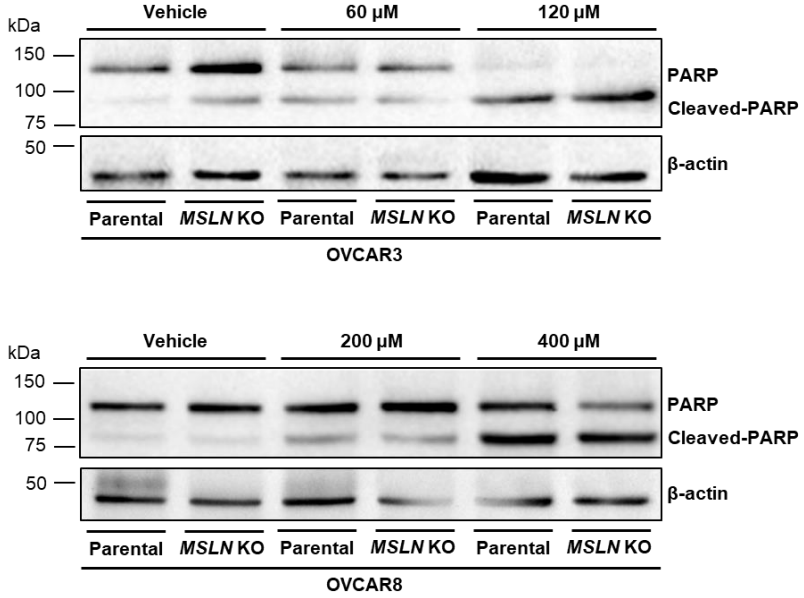

Figure 17 | Carboplatin effect in apoptosis pathway of parental/*MSLN* KO OVCAR3 and OVCAR8 cells. PARP and cleaved-PARP activity were assessed by immunoblot after exposure of parental/*MSLN* KO OVCAR3 cells to carboplatin at 60 and 120 µM or vehicle, and parental/*MSLN* KO OVCAR8 cells to carboplatin at 200 and 400 µM or vehicle, for 48 hours. All assays were done in at least three independent experiments and representative immunoblot are shown. B-actin was used as a loading control.

4.4. | Carboplatin reduces MSLN positive cells

To explore the potential effect of carboplatin in MSLN expression, immunocytochemistry and immunoblot were performed. For this, parental OVCAR3 and OVCAR8 cells were exposed to carboplatin at 60 and 120 µM or 200 and 400 µM, respectively, for 48 hours. As show in Figure 18a, MSLN was mostly expressed in cell membrane (vehicle) and shifts from membrane to cytoplasm when cells were exposed to carboplatin, especially for higher concentrations. Therefore, most of the cells that survive to carboplatin exposure are MSLN negative (Figure 18a and b).

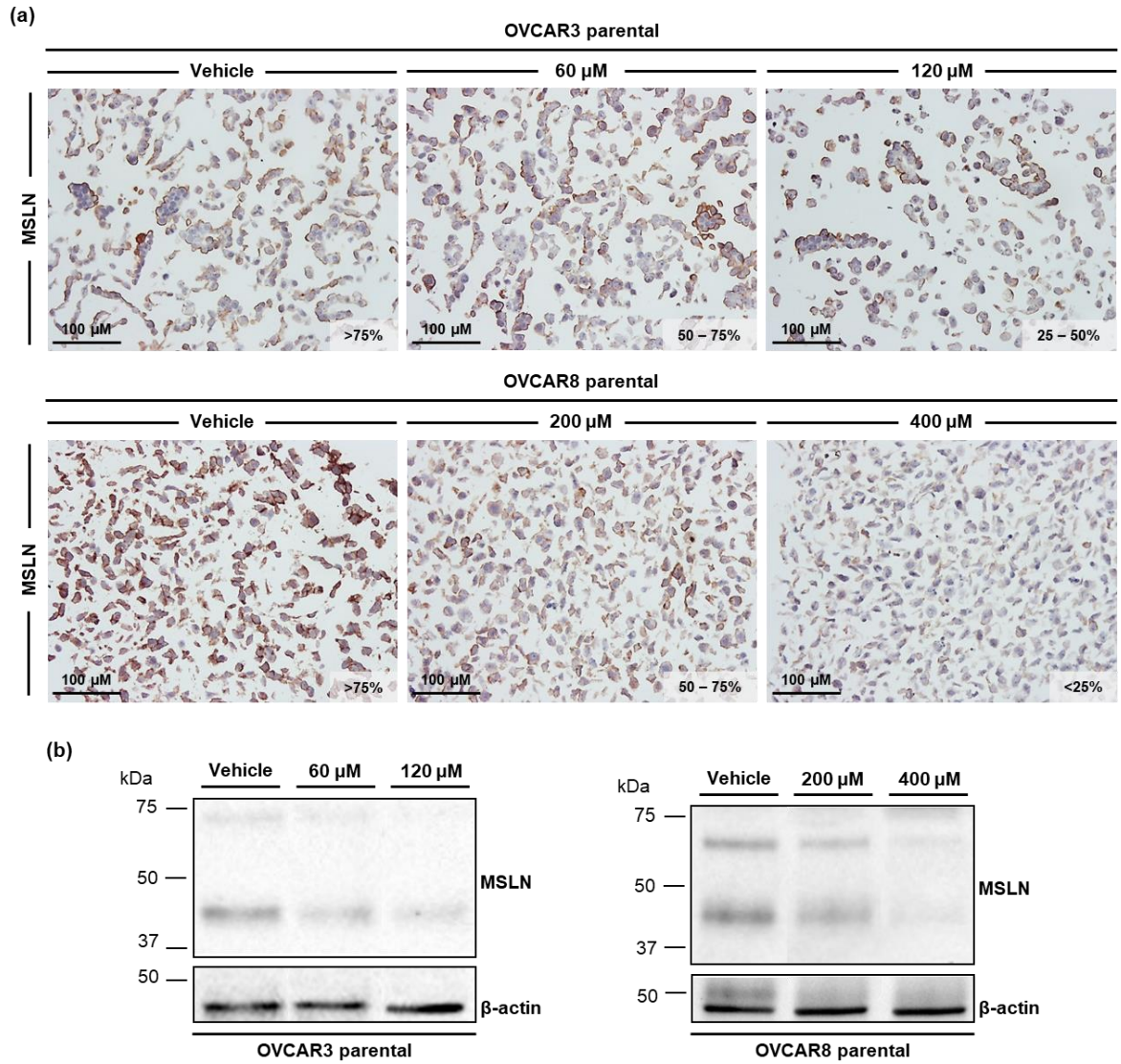

Figure 18 | Carboplatin effect in MSLN expression of parental OVCAR3 and OVCAR8 cells. MSLN expression was assessed by immunocytochemistry **(a)** and immunoblot **(b)** after exposure of parental OVCAR3 cells to carboplatin at 60 and 120 µM or vehicle, and parental OVCAR8 cells to carboplatin at 200 and 400 µM or vehicle, for 48 hours. **(a)** Representative brightfield images are shown for MSLN immunochemically staining (brown). Nuclei were stained hematoxylin (blue). The percentage of MSLN positive cells are represented in images. Microscopic images taken at 200x magnification and scale bar represents 100 µm. **(b)** The assays were done in at least three independent experiments and representative immunoblot are shown. B-actin was used as a loading control.

4.5. | Paclitaxel inhibits cell viability in parental and *MSLN* KO cells

To investigate whether MSLN expression was associated with taxane-based chemoresistance of ovarian cancer cell lines, three different cell viability assays (MTT, PB and SRB) were performed to determine the IC50. For this, parental/*MSLN* KO OVCAR3 and parental/*MSLN* KO OVCAR8 cells were exposed to paclitaxel covering a concentration range from 0.78 to 100 nM, for 48 hours. As shown in Figure 19, paclitaxel inhibited cell viability in both parental and *MSLN* KO ovarian cancer cell lines.

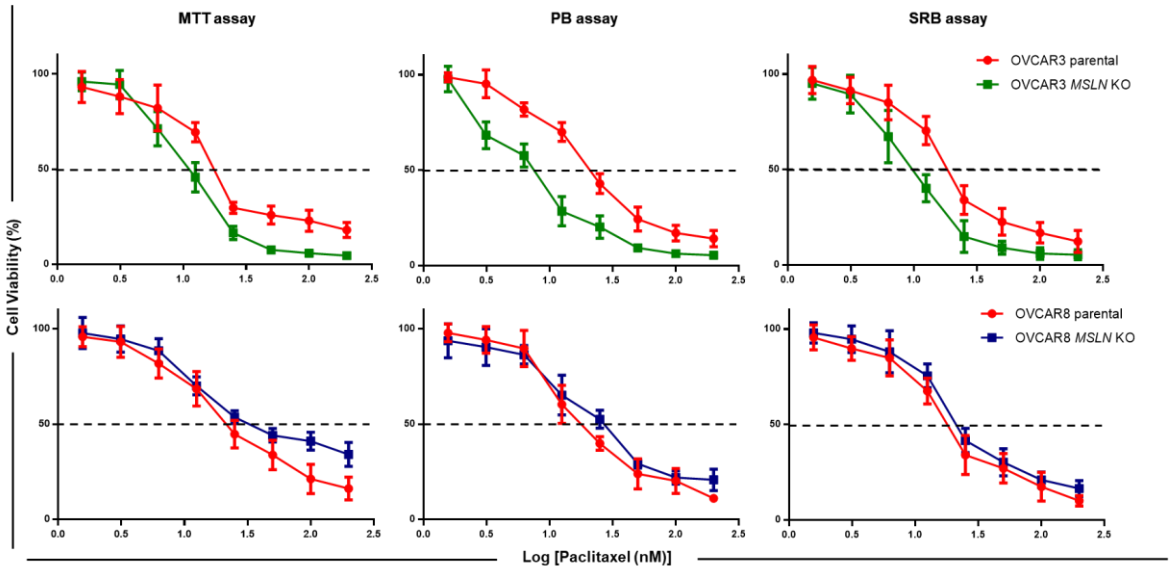

Figure 19 | Paclitaxel dose response curves for parental/*MSLN* KO OVCAR3 and OVCAR8 cells. The results were obtained by MTT, PB and SRB assays, after exposure of parental/*MSLN* KO OVCAR3 and OVCAR8 cells to paclitaxel covering a concentration range from 0.78 to 100 nM, for 48 hours. Dotted line corresponds to 50% of growth inhibition. Treated cells were compared with vehicle, considered as 100% viable. All assays were done in triplicate in at least three independent experiments. Data is expressed as mean ± standard deviation and plotted using GraphPad Prism Software Inc. v6.

4.5.1. | Paclitaxel response is cellular model dependent

For parental and *MSLN* KO OVCAR3 cells, paclitaxel IC50 values for MTT assay were 9.279 ± 0.405 nM and 5.708 ± 0.240 nM (*p<0.05, n=5); for PB assay were 10.871 ± 0.306 nM and 3.943 ± 0.107 nM (*p<0.05, n=3); and for SRB assay were 9.771 ± 0.857 nM and 4.843 ± 0.930 nM (*p<0.05, n=5), respectively (Figure 20). For parental and *MSLN* KO OVCAR8 cells, paclitaxel IC50 values for MTT assay were 11.212 ± 1.086 nM and 17.367 ± 2.165 nM (*p<0.05, n=5); for PB assay were 9.316 ±0.715 nM and 13.844 ± 0.899 nM (*p<0.05, n=3); and for SRB assay were 9.430 ± 1.559 nM and 11.035 ± 0.499 nM (p>0.05, n=5), respectively (Figure 20). The results showed that parental OVCAR3 cells are significantly less sensitive to paclitaxel when compared with the corresponding *MSLN* KO

cells. One the other hand, parental OVCAR8 cells are significantly more sensitive to paclitaxel when compared with the corresponding *MSLN* KO cells.

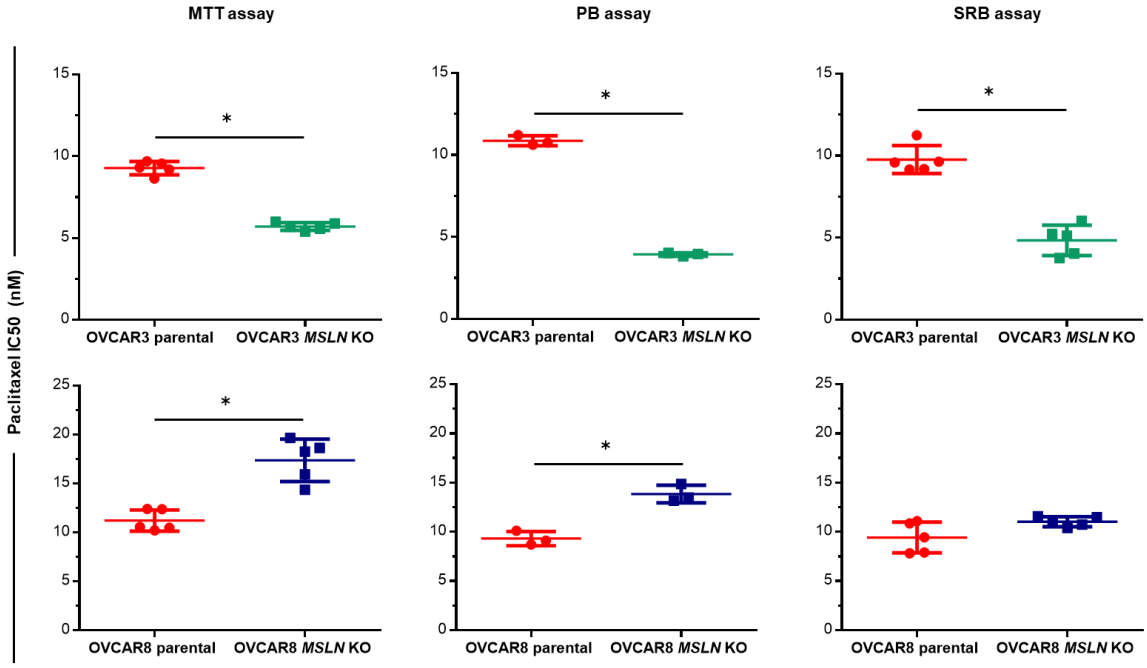

Figure 20 | Paclitaxel IC50 for parental/*MSLN* KO OVCAR3 and OVCAR8 cells. IC50 was measured by MTT, PB and SRB assays, after exposure of parental/*MSLN* KO OVCAR3 and OVCAR8 cells to paclitaxel covering a concentration range from 0.78 to 100 nM, for 48 hours. Treated cells were compared with vehicle, considered as 100% viable. All assays were done in triplicate in at least three independent experiments. Data is expressed as mean ± standard deviation and plotted using GraphPad Prism Software Inc. v6. Statistical analysis was performed using Student's t-test and a value of *p<0.05 was considered statistically significant.

4.6. | Paclitaxel induces apoptotic cell death

Has been shown that the molecular mechanisms of taxane compounds resistance involve deregulation of apoptosis (Cooley, *et al.,* 2015). Paclitaxel ability to induce apoptosis was evaluated by flow cytometry through analyzing PS externalization and membrane permeability after Annexin V-FITC/PI labelling. For this, parental/*MSLN* KO OVCAR3 and OVCAR8 cells were exposed to paclitaxel at 6 and 12 nM, and 7.5 and 15 nM, respectively, for 48 hours. After exposure of OVCAR3 cells to paclitaxel at 6 and 12 nM, the percentage of apoptosis (early and late) for parental cells were 2.105 ± 0.684% and 3.640 ± 0.926%, respectively, and for *MSLN* KO cells were 28.180 ± 4.877% and 35.165 ± 5.774%, respectively. The total percentage of apoptotic cells for parental OVCAR3 after exposure to paclitaxel was significantly decreased (*p<0.05, n=3) compared with the corresponding *MSLN* KO cells (Figure 21). Therefore, similarly to previous cell viability results, paclitaxel induces more apoptosis in OVCAR3 cells without MSLN expression.

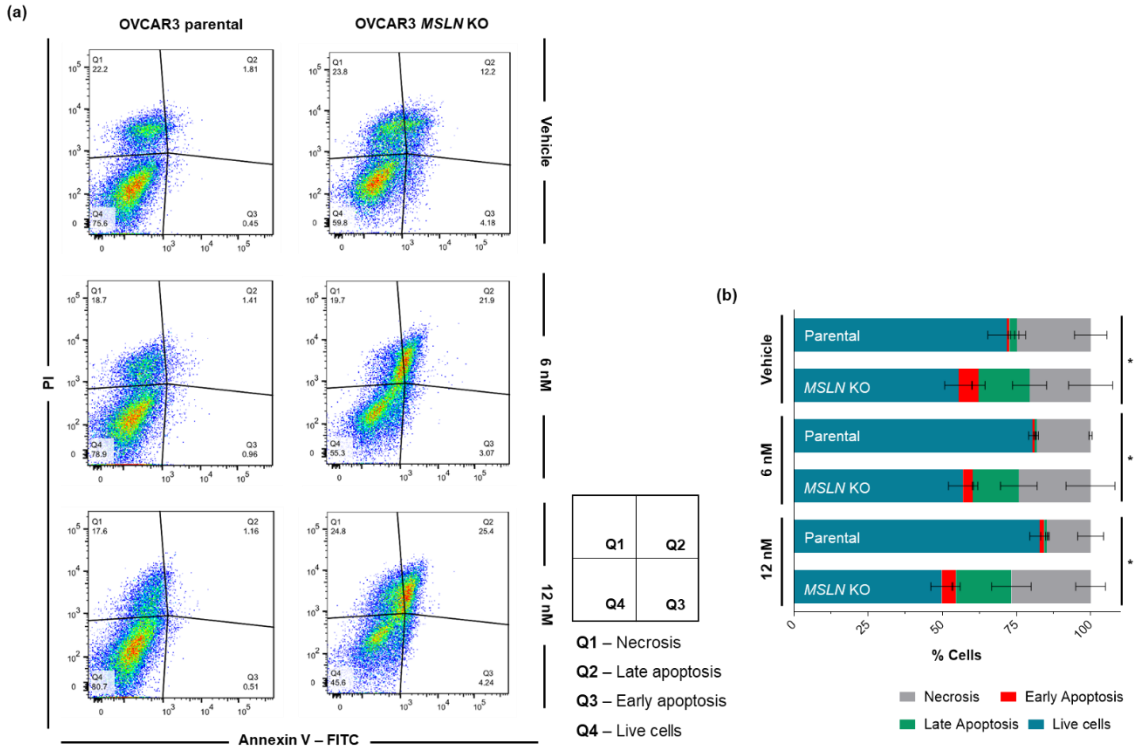

Figure 21 | Paclitaxel effect in apoptosis of parental/*MSLN* KO OVCAR3 cells. Apoptotic cells were measured by flow cytometry analysis after Annexin V-FITC and PI labelling in parental and *MSLN* KO OVCAR3 cells exposed to paclitaxel at 6 and 12 nM or vehicle, for 48 hours. **(a)** Representative flow cytometry dot plot. **Q1 –** Necrosis; **Q2 –** Late apoptosis; **Q3 –** Early Apoptosis and **Q4 –** Live cells. Fluorescence was assessed by BD FACS Canto™ II (BD Biosciences) flow cytometer and data was analyzed by FlowJo software v10.0.7. All assays were done in three independent experiments. **(b)** Percentage of cell populations (live cells, early apoptosis, late apoptosis and necrosis). Data is expressed as mean ± standard deviation and plotted using GraphPad Prism Software Inc. v6. Statistical analysis was performed using Student's t-test and a value of *p<0.05 was considered statistically significant.

After exposure of OVCAR8 cells to paclitaxel at 7.5 and 15 nM, the percentage of apoptosis (early and late) for parental cells were 25.113 ± 2.683% and 46.888 ± 8.446%, respectively, and for *MSLN* KO cells were 13.507 ± 5.748% and 25.653 ± 1.710%, respectively. The total percentage of apoptotic cells for parental OVCAR8 after exposure to paclitaxel at 15 nM was significantly increased (*p<0.05, n=3) when compared with the corresponding *MSLN* KO cells (Figure 22). Therefore, according to previous cell viability results, paclitaxel induces more apoptosis in OVCAR8 cells that express MSLN.

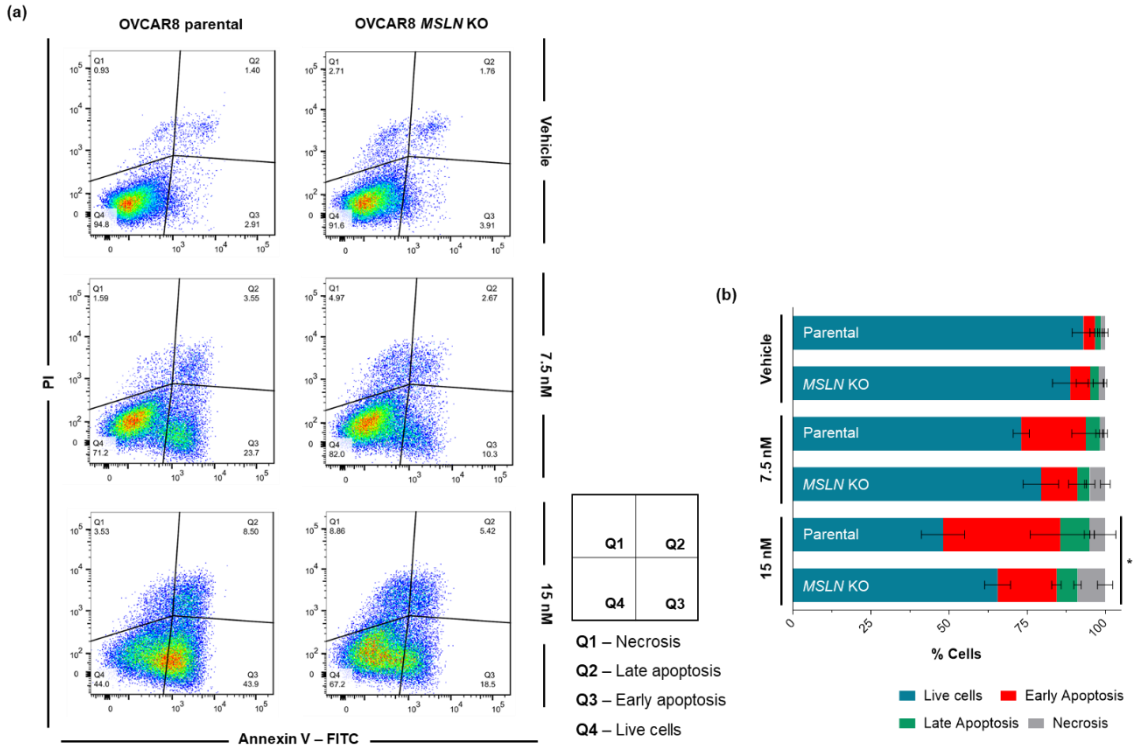

Figure 22 | Paclitaxel effect in apoptosis of parental/*MSLN* KO OVCAR8 cells. Apoptotic cells were measured by flow cytometry analysis after Annexin V-FITC and PI labelling in parental and *MSLN* KO OVCAR8 cells exposed to paclitaxel at 7.5 and 15 nM or vehicle, for 48 hours. **(a)** Representative flow cytometry dot plot. **Q1 –** Necrosis; **Q2 –** Late apoptosis; **Q3 –** Early Apoptosis and **Q4 –** Live cells. Fluorescence was assessed by BD FACS Canto™ II (BD Biosciences) flow cytometer and data was analyzed by FlowJo software v10.0.7. All assays were done in three independent experiments. **(b)** Percentage of cell populations (live cells, early apoptosis, late apoptosis and necrosis). Data is expressed as mean ± standard deviation and plotted using GraphPad Prism Software Inc. v6. Statistical analysis was performed using Student's t-test and a value of *p<0.05 was considered statistically significant.

4.7. | Paclitaxel enhances cleaved-PARP activity

To explore the role of MSLN expression in paclitaxel ability to induce apoptosis, PARP and cleaved-PARP activity were assessed by immunoblot. For this, parental/*MSLN* KO OVCAR3 and OVCAR8 cells were exposed to paclitaxel at 6 and 12 nM, and 7.5 and 15 nM, respectively, for 48 hours. As shown in Figures 23, paclitaxel induces apoptosis evidenced by decreased PARP and increased cleaved-PARP activity in parental/*MSLN* KO OVCAR3 and OVCAR8 cells when compared with the corresponding vehicle. For parental OVCAR3 cells exposure to paclitaxel at 6 nM, the amount of cleaved-PARP was decreased when compared with the corresponding *MSLN* KO cells (Figure 23). Concordantly to cell viability and Annexin V-PI results, paclitaxel induces more apoptosis in OVCAR3 cells without MSLN expression. For parental OVCAR8 cells exposure to paclitaxel at 7.5 nM, the amount of cleaved-PARP was increased when compared with the corresponding *MSLN* KO

cells (Figure 23). Consistently to cell viability and Annexin V-PI results, paclitaxel induces more apoptosis in OVCAR8 cells that express MSLN.

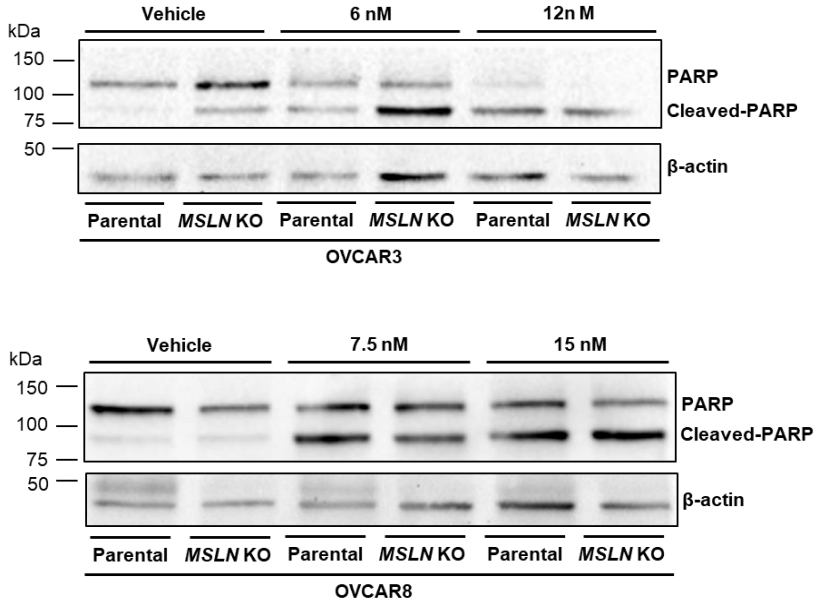

Figure 23 | Paclitaxel effect in apoptosis pathway of parental/*MSLN* KO OVCAR3 and OVCAR8 cells. PARP and cleaved-PARP activity were assessed by immunoblot after exposure of parental/*MSLN* KO OVCAR3 cells to paclitaxel at 6 and 12 nM or vehicle, and parental/*MSLN* KO OVCAR8 cells to paclitaxel at 7.5 and 15 nM or vehicle, for 48 hours. All assays were done in at least three independent experiments and representative immunoblot are shown. B-actin was used as a loading control.

4.8. | Paclitaxel reduces MSLN positive cells

To explore the potential effect of paclitaxel in MSLN expression, immunocytochemistry and immunoblot were performed. For this, parental OVCAR3 and OVCAR8 cells were exposed to paclitaxel at 6 and 12 nM or 7.5 and 15 nM, respectively, for 48 hours. As shown in Figure 24a, MSLN was mostly expressed in cell membrane (vehicle) and shifts from membrane to cytoplasm when the cells were exposed to paclitaxel, especially for higher concentrations. Thus, most of the cells that survive to paclitaxel exposure are MSLN negative (Figure 24a and b).

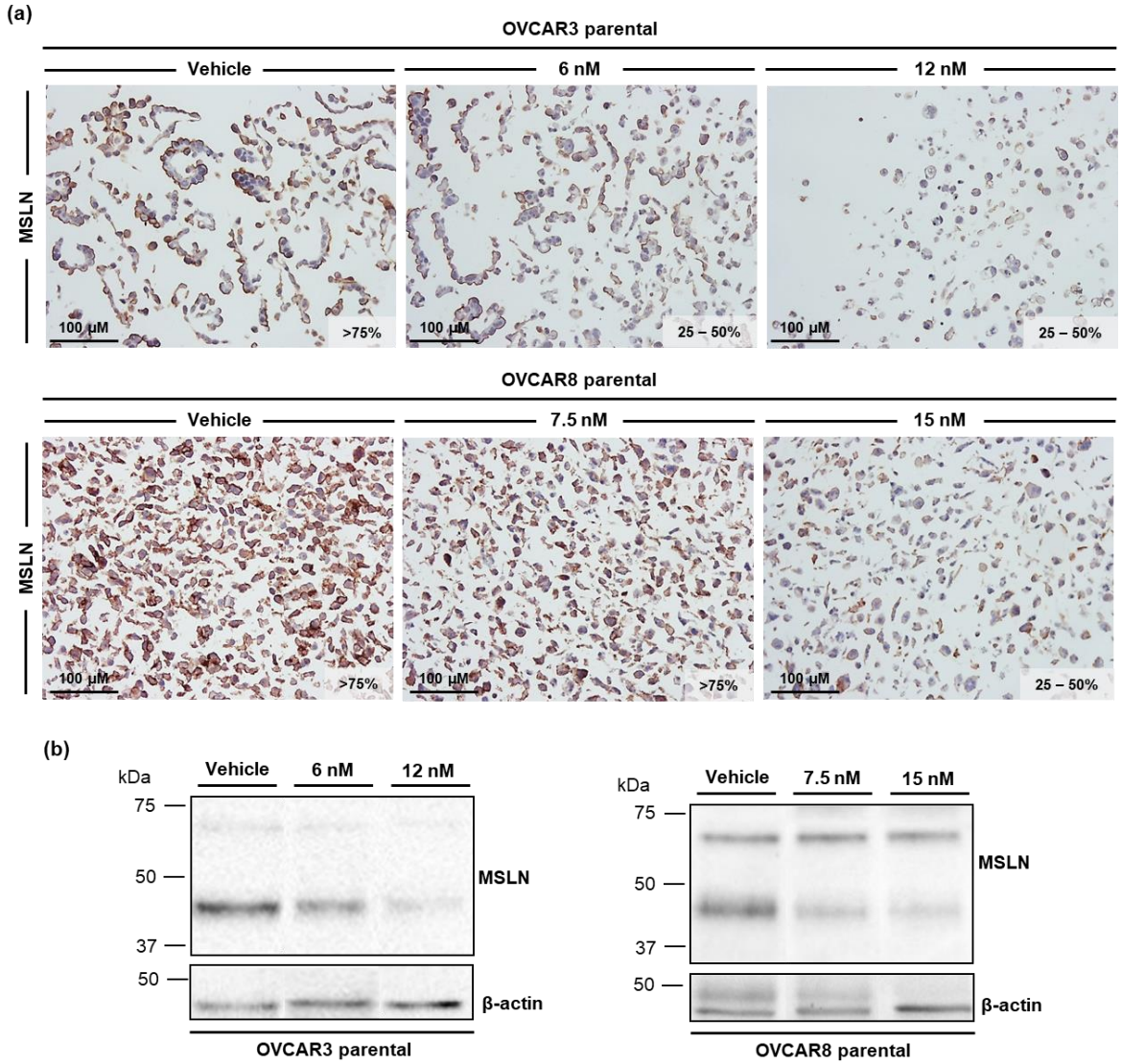

Figure 24 | Paclitaxel effect in MSLN expression of parental OVCAR3 and OVCAR8 cells. MSLN expression were assessed by immunocytochemistry **(a)** and immunoblot **(b)** after exposure of parental OVCAR3 cells to paclitaxel at 6 and 12 nM or vehicle, and parental OVCAR8 cells to paclitaxel at 7.5 and 15 nM or vehicle, for 48 hours. **(a)** Representative brightfield images are shown for MSLN immunochemically staining (brown). Nuclei were stained hematoxylin (blue). The percentage of MSLN positive cells are represented in images. Microscopic images taken at 200x magnification and scale bar represents 100 µm. **(b)** The assays were done in at least three independent experiments and representative immunoblot are shown. B-actin was used as a loading control.

Chapter 5 | Discussion and Conclusion

In ovarian cancer, the overall 5-year survival rate is 47.6%, mainly due to advanced disease stage at diagnosis, presence of nonspecific symptoms, lack of effective screening tools, poor treatment responses with development of chemoresistance and high recurrence rates (Raja, Chopra & Ledermann, 2012; González-Martín *et al.,* 2014; Jervis *et al.,* 2014; Weidle *et al.,* 2016; Howlader *et al.,* 2018). Despite some progresses in surgical procedures and treatment regimens based on combining chemotherapeutic drugs with targeted therapies, no improvements in patients´ outcomes were noted (Cheng *et al.,* 2009). Searching for biomarkers to predict therapeutic responses is essential in the clinical management of ovarian cancer patients (de Graeff *et al.,* 2008; Cheng *et al.,* 2009). MSLN expression is a hallmark of ovarian tumours and seems to have a crucial role in peritoneal metastization, participating in tumour cell adherence, cell survival/proliferation, migration, invasion and tumour progression (Rump *et al.,* 2004; Cheng *et al.,* 2009; Chang *et al.,* 2012; Servais *et al.,* 2012; Coelho *et al.,* 2017). Regardless of previous indications associating high MSLN expression with chemoresistance (Chang *et al*., 2009; Cheng *et al.,* 2009; Bharadwaj *et al.,* 2011), more studies are needed to confirm the role of this glycoprotein as a predictor for chemotherapy response in ovarian cancer. Hence, our aim was to investigate whether MSLN expression modulates chemoresistance in ovarian cancer cell lines.

Several methods are available to assess cell proliferation/viability, such as direct counting of viable cells, measurement of metabolic activity and/or evaluation of the cellular DNA/protein content (Wang, Henning & Heber, 2010). The choice of the cell viability method is crucial, since they can introduce variability in the interpretation of the compound interaction. So, in order to increase the reliability of our results three different cell viability assays, MTT, PB and SRB, were performed to obtain the necessary carboplatin and paclitaxel concentration to induce 50% of growth inhibition (IC50). MTT and PB assays are based on the metabolic capacity of viable cells to convert the substrate into a product, resulting in a colorimetric or fluorescent signal directly proportional to cell viability (Riss *et al.,* 2004; Ediriweera, Tennekoon & Samarakoon, 2019). On the other hand, SRB assay measures the amount of bound dye to protein that is proportional to cell mass (Skehan *et al.,* 1990; Vichai & Kirtikara, 2006). MTT and SRB assays measure metabolic activity and protein content, respectively, thus the results are complementary. PB assay measure metabolic activity and is performed in the same SRB protocol, i.e. the same cells were used for PB and SRB assays, therefore rising consistency of the obtained results. So, we used the IC50 values of these three methods to compare and increase the robustness of the results.

Carboplatin is a first-line chemotherapeutic drug used for ovarian cancer management. After exposure of OVCAR3 cells to carboplatin, cell viability results for MTT and SRB

demonstrated that, parental cells are less sensitive to carboplatin when compared with the corresponding *MSLN* KO cells ($p<0.05$). In the same line, for OVCAR8 cells the MTT and PB results showed that parental cells are less sensitive to carboplatin when compared with the corresponding *MSLN* KO cells ($p<0.05$). Carboplatin IC50 values obtained from MTT, PB and SRB assays revealed the same tendency with minimum differences between parental and *MSLN* KO cells, despite a non-significant statistical value. Our results are in agreement with other studies demonstrating that high MSLN expression levels were positively associated with chemoresistant ovarian cancer cases when compared with chemosensitive ones (2.81 vs 0.43, $p<0.001$) (Cheng *et al.,* 2009; Chang *et al.,* 2012; Wang *et al.,* 2012). Therefore, in agreement to other studies we can conclude that MSLN expression is a key player in carboplatin chemoresistance of ovarian cancer cell lines.

To confirm if MSLN expression modulates the carboplatin ability to induce apoptosis, we performed Annexin V-PI assay by flow cytometry and measured PARP and cleaved-PARP activity by immunoblot. In agreement with cell viability assays, for OVCAR3, the percentage of apoptotic cells and cleaved-PARP activity showed that carboplatin induces more apoptosis in cells without MSLN expression. Besides this, for this cellular model, the loss of MSLN has an effect in cell viability even without treatment, i.e. *MSLN* KO condition confers less viability when compared to parental cells. This effect is supported by our previously results in which was evaluated the effect of MSLN expression in proliferation/viability of OVCAR3 cells and observed a significant decrease in *MSLN* KO compared with the parental cells ($p<0.001$) (unpublished data). Taken together, the results obtained for OVCAR3 allow us to conclude that MSLN affects carboplatin response through apoptosis. Regarding OVCAR8, the percentage of apoptotic cells and cleaved-PARP activity levels showed that carboplatin induces more apoptosis in cells that express MSLN. No differences were observed between parental and *MSLN* KO OVCAR8 cells in vehicle conditions, so *MSLN* KO cells are equally viable when compared with parental cells. These results are consistent with our previously results that evaluate the effect of MSLN expression in proliferation/viability of OVCAR8 cells and no differences between parental and *MSLN* KO cells are show (unpublished data). The results obtained for OVCAR8 led us to conclude that MSLN effect in carboplatin response is not mediated by apoptosis. Taken together, our results suggest that MSLN expression may be related with chemotherapeutic effect in ovarian cancer cell lines. Nevertheless, it is important to keep in mind that carboplatin chemoresistance is a complex biological mechanism and more experiments should be performed to confirm and validate our results.

Additionally, our results for MSLN expression assessed by immunocytochemistry show that after exposure of parental cell lines (OVCAR3 and OVCAR8) to carboplatin, most of the

cells that survive are MSLN negative. Complementarily, the immunoblot revealed that carboplatin reduces MSLN expression. Parental cell lines are heterogeneous models combining positive (~75%) and negative MSLN cells (~25%). After carboplatin exposure we identified a selective pressure to reduce MSLN positive cells. We hypothesize this effect may stem from the lower proliferation and/or increased apoptotic rates of MSLN positive cells. To explore which of these hypotheses is correct, we envisioned a sorting strategy to separate MSLN positive and negative cells in order to evaluate proliferation and apoptosis in the two groups. To this end, we performed a sorting attempt but MSLN antibodies have some limitations in detecting live cells. Moreover, after the separation of MSLN positive from negative cells, the original cellular heterogeneity is restored in culture. We are currently searching for alternative methods to overcome these limitations to increase our insight on the effect of carboplatin in our cell line models.

Paclitaxel is also a frontline anti-neoplastic agent used in treatment of ovarian cancer patients. After exposure of OVCAR3 cells to paclitaxel, cell viability results for MTT, PB and SRB revealed that parental cells are significantly less sensitive compared to the corresponding *MSLN* KO cells ($p<0.05$). On the other hand, for OVCAR8 cells MTT and PB results indicated that parental cells are significantly more sensitive to paclitaxel compared to the corresponding *MSLN* KO cells ($p<0.05$). The results obtained from MTT, PB and SRB assays followed the same tendency with minimum differences between parental and *MSLN* KO cells. Chang and collaborators describe that paclitaxel-resistant patients expressed higher levels of MSLN when comparing with paclitaxel-sensitive group. They suggest that MSLN expression can influence paclitaxel chemotherapeutic sensitivity and can be used as a potential target to reduce paclitaxel. Also, the same group showed that high expression of MSLN confer a proliferative/viable advantage during paclitaxel treatments chemoresistance (Chang *et al*., 2009, Chang *et al.,* 2012). However, our data do not corroborate these findings since OVCAR3 and OVCAR8 showed different results concerning the effect of MSLN expression to paclitaxel. OVCAR3 is derived from a malignant ascites collected from a HGSOC patient post-chemotherapy treatment with adriamycin, cisplatin and cyclophosphamide (Hamilton *et al.,* 1983). On the other hand, OVCAR8 is derived from the ovarian tumour tissue of a HGSOC patient after the administration of a high-dose carboplatin therapy (Schilder *et al.,* 1990). Our group previously described that SOC present high expressing levels of mucins MUC1 and MUC16, and truncated O-glycans (Tn, STn and T) (Ricardo *et al.,* 2015). More recently, we showed that OVCAR3 have also a mucin and O-glycan profile that reflects the characteristic footprint of SOC, in contrast to OVCAR8 that has a different profile rarely expressed by SOC (Coelho *et al,* 2017). Thus, OVCAR3 and OVCAR8 are two distinct cell

lines, with different phenotypes leading to different treatment responses. Concordantly with cell viability assays, the percentage of apoptotic cells and cleaved-PARP activity for OVCAR3 showed that paclitaxel induces more apoptosis in cells without MSLN expression. These results allow us to conclude that MSLN affects paclitaxel response by modifying apoptosis in OVCAR3. Regarding OVCAR8, the percentage of apoptotic cells and cleaved-PARP activity revealed that paclitaxel induces more apoptosis in cells with MSLN expression. Therefore, the results on the effect of MSLN expression in these two cellular models are quite different and can reflect the different nature of these two cell lines but can also suggest that MSLN is not a key player, at least alone, regarding the cellular response to paclitaxel. Similarity to carboplatin, paclitaxel chemoresistance is also a complex biological mechanism that should be further explored.

Our immunocytochemistry results indicate that after exposure of parental cell lines (OVCAR3 and OVCAR8) to paclitaxel, most of the cells that survive are MSLN negative. Complementarily, the immunoblot revealed that paclitaxel exposure reduces MSLN expression. These results are similar to the carboplatin treatment results and can be attributed to drug selective pressure imprinted to the cellular population, as previously described.

Appropriate cell line model systems that closely reproduce the characteristic footprint of SOC are crucial to increase the reliability of the obtained results. OVCAR3 is a good cell line model to study mechanisms of cytotoxic drug resistance in ovarian cancer since it reflects the mucins and O-glycan profile of SOC, an important phenotypic hallmark. In contrast, OVCAR8 does not have the same characteristic footprint (Coelho *et al.,* 2018). Besides that, these two cell line models have different “stories” that may impact on chemoresistance profiles, since they were obtained from patients treated with different regimens (Hamilton *et al.,* 1983; Schilder *et al.,* 1990). Despite all limitations, we could identify MSLN as a key player in carboplatin chemoresistance, but it is important to keep in mind that other markers can be involved in this complex biological process.

Overall our results, summarized in Table III, indicate that MSLN expression modulates carboplatin response, with *MSLN* KO cells being more sensitive to carboplatin treatment. On the other hand, MSLN expression is not a key player regarding paclitaxel response, since our results showed a response to the treatment dependent of the cellular model used. Summing up, MSLN expression seems to be important in the modulation of carboplatin chemoresistance, but not in regulation of response to paclitaxel.

Table III | Summary table of carboplatin and paclitaxel results for parental/*MSLN* KO OVCAR3 and OVCAR8 cells. Less **(-)** and More **(+)**.

		OVCAR3		OVCAR8	
		Parental	***MSLN* KO**	**Parental**	***MSLN* KO**
Carboplatin	IC50 (Sensitive)	-	+	-	+
	Apoptosis	-	+	+	-
	Cleaved-PARP activity	-	+	+	-
Paclitaxel	IC50 (Sensitive)	-	+	+	-
	Apoptosis	-	+	+	-
	Cleaved-PARP activity	-	+	+	-

Chapter 6 | Future Perspectives

This study revealed some limitations concerning validations and additional work should be performed in order to clarify some questions. To provide more evidences to support that MSLN modulates the carboplatin chemoresistance, the same analysis performed in *MSLN* KO should be carried out for others ovarian cancer cell lines, inclusive when naturally not express MSLN, such as, OVCAR4 and BG1, ovarian cancer cell lines without MSLN expression and compare to MSLN overexpression models. Since MUC16 and MSLN form a significant duet, its important performed the same study for *MUC16* KO models. All the cell lines models necessary to perform the previously described analyses, i.e. *MUC16* KO OVCAR3 and MSLN OE OVCAR8 models, was produced by our group and available for these supplementary studies. After confirming our results, a more sensitive and directed study should be performed in order to access the putative role of MSLN (and MUC16) in this process, so, is important to perform cytotoxic tests in primary cultures to validate our hypothesis.

In order to confirm if carboplatin and paclitaxel interfere with MSLN expression more suitable analysis should be performed in other ovarian cancer cell lines and primary cultures. This information could be important to understand the relationship of MSLN expression in the patients´ outcome.

Additionally, was established a paclitaxel-resistant variant from parental OVCAR8 cell line (carboplatin resistant cell line). The purpose was creating a cell line model resistant to the two first-line chemotherapeutic drugs (carboplatin and paclitaxel). In order to validate the establishment of this resistant cell line, we will perform some assays, such as cell growth doubling time, proliferation/viability assays, cell cycle and apoptosis analyses by flow cytometry, phenotypic characterization, inclusive MSLN expression, and other relevant tests. The establishment of a carboplatin and paclitaxel resistant cell line is a powerful toll that will allow future studies on drug-resistance mechanisms in ovarian cancer.

Chapter 7 | References

Agarwal R, Kaye SB. (2003). Ovarian cancer: strategies for overcoming resistance to chemotherapy. Nat Rev Cancer. 3(7):502–516.

Agarwal R, Kaye SB. (2005). Prognostic factors in ovarian cancer: how close are we to a complete picture? Ann Oncol. 16:4-6.

Ahmed AA, Etemadmoghadam D, Temple J, *et al.* (2010). Driver mutations in TP53 are ubiquitous in high grade serous carcinoma of the ovary. J Pathol. 221:49–56.

Ahmed N, Stenvers KL. (2013). Getting to know ovarian cancer ascites: opportunities for targeted therapy-based translational research. Front Oncol. 3:256.

Argani P, Iacobuzio-Donahue C, Ryu B, *et al.* (2001). Mesothelin is overexpressed in the vast majority of ductal adenocarcinomas of the pancreas: identification of a new pancreatic cancer marker by serial analysis of gene expression (SAGE). Clin Cancer Res. 7(12):3862-8.

Argüeso P, Spurr-Michaud S, Russo CL, *et al.* (2003). MUC16 mucin is expressed by the human ocular surface epithelia and carries the H185 carbohydrate epitope. Invest Ophthalmol Vis Sci. 44(6):2487-95.

Armstrong D, Bundy B, Wenzel L, *et al.* (2006). Intraperitoneal cisplatin and paclitaxel in ovarian cancer. N Engl J Med. 354:34–53.

Ayyagari VN, Diaz-Sylvester PL, Hsieh TJ, Brard L. (2017). Evaluation of the cytotoxicity of the Bithionol-paclitaxel combination in a panel of human ovarian cancer cell lines. PLoS One. 12(9):e0185111.

Baratti D, Kusamura S, Martinetti A, *et al.* (2007). Circulating ca125 in patients with peritoneal mesothelioma treated with cytoreductive surgery and intraperitoneal hyperthermic perfusion. Ann Surg Oncol. 14:500–508.

Bast RC Jr, Feeney M, Lazarus H, *et al.* (1981). Reactivity of a monoclonal antibody with human ovarian carcinoma. J Clin Invest. 68(5):1331-7.

Berek JS, Bast RC Jr. (2003). Nonepithelial ovarian cancer. In Kufe DW, Pollock RE, Weichselbaum RR, *et al.,* (Eds). Holland-Frei Cancer Medicine. 6th edition. Hamilton (ON). BC Decker.

Berek JS, Crum C, Friedlander M. (2015). Cancer of the ovary, fallopian tube, and peritoneu. Int J Gynecol Obstet. 131(2):S111-S122.

Berek JS, Friedlander, ML, Bast RC. (2017). Epithelial ovarian, fallopiantube, and peritoneal cancer. Holland-Frei Cancer Medicine. 1-27.

Bergfeldt K, Rydh, B, Granath, F, *et al.* (2002). Risk of ovarian cancer in breast-cancer patients with a family history of breast or ovarian cancer: a population-based cohort study. Lancet. 360(9337):891-4.

Berns EM, Bowtell DD. (2012). The changing view of high-grade serous ovarian cancer. Cancer Res. 72:2701–2704.

Bharadwaj U, Marin-Muller C, Li M, *et al.* (2011). Mesothelin overexpression promotes autocrine IL-6/sIL-6R trans-signaling to stimulate pancreatic cancer cell proliferation. Carcinogenesis. 32(7):1013-24.

Boivin M, Lane D, Piche A, Rancourt C. (2009). CA125 (MUC16) tumour antigen selectively modulates the sensitivity of ovarian cancer cells to genotoxic drug-induced apoptosis. Gynecol Oncol. 115(3):407–13.

Bookman MA, Brady MF, McGuire WP, *et al.* (2009). Evaluation of new platinum-based treatment regimens in advanced-stage ovarian cancer: a phase III Trial of the Gynecologic Cancer Intergroup. J Clin Oncol. 27:1419–1425.

Boussios S, Zarkavelis G, Seraj, E, *et al.* (2016). Non-epithelial ovarian cancer: Elucidating uncommon gynaecological malignancies. AntiCancer Res. 36:5031–5042.

Brasseur K, Gévry N, Asselin E. (2017). Chemoresistance and targeted therapies in ovarian and endometrial cancers. Oncotarget. 8:4008-4042.

Brun JL, Feyler A, Chêne G, *et al.* (2000). Long-term results and prognostic factors in patients with epithelial ovarian cancer. Gynecol Oncol. 78:21–27.

Burger RA, Brady MF, Bookman MA, *et al.* (2011). Gynecologic Oncology Group. Incorporation of bevacizumab in the primary treatment of ovarian cancer. N Engl J Med. 365(26):2473–2483.

Burleson KM, Boente MP, Pambuccian SE, *et al.* (2006). Disaggregation and invasion of ovarian carcinoma ascites spheroids. J Transl Med. 4:6.

Burry RW. (2011). Controls for immunocytochemistry: an update. J Histochem Cytochem. 59(1):6-12.

Cancer Genome Atlas Research Network. (2011). Integrated genomic analyses of ovarian carcinoma. Nature. 474(7353):609-615.

Chang CL, Wu TC, Hung CF. (2007). Control of human mesothelin expressing tumors by DNA vaccines. Gene Therapy. 14:1189–1198.

Chang K, Pastan I, Willingham MC. (1992). Isolation and characterization of a monoclonal antibody, K1, reactive with ovarian cancers and norm al mesothelium. Int J Cancer. 50(3):373-81.

Chang K, Pastan I. (1996). Molecular cloning of mesothelin, a differentiation antigen present on mesothelium, mesotheliomas, and ovarian cancers. Proc Natl Acad Sci USA. 93(1):136-40.

Chang MC, Chen CA, Chen PJ, *et al.* (2012). Mesothelin enhances invasion of ovarian cancer by inducing MMP-7 through MAPK/ERK and JNK pathways. Biochem J. 442(2):293-302.

Chang MC, Chen CA, Hsieh CY, *et al.* (2009). Mesothelin inhibits paclitaxel-induced apoptosis through the PI3K pathway. Biochem J. 424: 449–458.

Chekmasova AA, Rao TD, Nikhamin Y, *et al.* (2010). Successful eradication of established peritoneal ovarian tumours in SCID-Beige mice following adoptive transfer of T cells genetically targeted to the MUC16 antigen. Clin Cancer Res. 16(14):3594-606.

Chen SH, Hung WC, Wang P, *et al.* (2013). Mesothelin binding to CA125/MUC16 promotes pancreatic cancer cell motility and invasion via MMP-7 activation. Sci Rep. 3:1870.

Cheng WF, Huang CY, Chang MC, *et al.* (2009). High mesothelin correlates with chemoresistance and poor survival in epithelial ovarian carcinoma. Br J Cancer. 100(7):1144-53.

Clark TG, Stewart ME, Altman DG, *et al.* (2001). A prognostic model for ovarian cancer. Br J Cancer. 85(7):944–952.

Coelho R, Marcos-Silva L, Ricardo S, *et al.* (2017). Peritoneal dissemination of ovarian cancer: role of MUC16-mesothelin interaction and implications for treatment. Expert Rev Anticancer Ther. 18(2):177-186.

Colombo N, Peiretti M, Garbi A, *et al.* on behalf of the ESMO guidelines working group. (2012). Non-epithelial ovarian cancer: ESMO clinical practice guidelines for diagnosis, treatment and follow-up. Annals of Onc. 23(7):vii20–vii26.

Comamala M, Pinard M, Theriault C, *et al.* (2011). Downregulation of cell surface CA125/MUC16 induces epithelial-to-mesenchymal transition and restores EGFR signalling in NIH: OVCAR3 ovarian carcinoma cells. Br J Cancer. 104(6):989-99.

Cooley M, Fang P, Fang F, Nephew KP. (2015). Molecular determinants of chemotherapy resistance in ovarian cancer. Pharmacogenomics. 16:1763–1767.

Coons AH, Creech HJ, Jones RN. (1941). Immunological properties of an antibody containing a fluorescent group. Proc Society Exp Biol Med. 47(2):200–202.

Cortez AJ, Tudrej P, Kujawa KA, Lisowska KM. (2018). Advances in ovarian cancer therapy. Cancer Chemother Pharmacol. 81(1):17–38.

Cramer DW, Terry KL. (2015). Epidemiology and biostatistics. In: Berek JS, Hacker NF, eds. Berek & Hacker's Gynecol Oncol, 6th edition. Philadelphia. Lippincott Williams&Wilkins. 220–240.

Crum CP, Drapkin R, Miron A, *et al.* (2007). The distal fallopian tube: a new model for pelvic serous carcinogenesis. Curr Opin Obstet Gynecol. 19:3–9.

Dabholkar M, Vionnet J, Bostick-Bruton F, *et al.* (1994). Messenger RNA levels of XPAC and ERCC1 in ovarian cancer tissue correlate with response to platinum-based chemotherapy. J Clin Invest. 94:703–708.

Das S, Rachagani S, Torres-Gonzalez MP, *et al.* (2015). Carboxyl-terminal domain of MUC16 imparts tumourigenic and metastatic functions through nuclear translocation of JAK2 to pancreatic cancer cells. Oncotarget. (8):5772–87.

de Graeff P, Crijns AP, Ten Hoor KA, *et al.* (2008). The ErbB signalling pathway: protein expression and prognostic value in epithelial ovarian cancer. Br J Cancer. 99:341–34.

Dedes KJ, Wilkerson PM, Wetterskog D, *et al.* (2011). Synthetic lethality of PARP inhibition in cancers lacking BRCA1 and BRCA2 mutations. Cell Cycle. 10(8):1192–1199.

Disis ML, Taylor MH, Kelly K, *et al.* (2019). Efficacy and safety of avelumab for patients with recurrent or refractory ovarian cancer: phase 1b results from the JAVELIN solid tumour trial. JAMA Oncol. 5(3):393–401.

du Bois A, Reuss A, Pujade-Lauraine E, *et al.* (2009). Role of surgical outcome as prognostic factor in advanced epithelial ovarian cancer: a combined exploratory analysis of 3 prospectively randomized phase 3 multicenter trials: by the Arbeitsgemeinschaft Gynaekologische Onkologie Studien gruppe Ovarialkarzinom (AGO-OVAR) and the Groupe d'Investigateurs Nationaux Pour les Etudes des Cancers de l'Ovaire (GINECO). Cancer. 115(6):1234–44.

du Bois A, Floquet A, Kim JW, *et al.* (2014). Incorporation of pazopanib in maintenance therapy of ovarian cancer. Clin Oncol. 32:3374–3382.

du Bois A, Kristensen G, Ray-Coquard I, *et al.* (2016). Standard first-line chemotherapy with or without nintedanib for advanced ovarian cancer (AGO-OVAR 12): a randomised, double-blind, placebocontrolled phase 3 trial. Lancet Oncol. 17:78–89.

du Bois A, Lück HJ, Meier W, *et al.* (2003). A randomized clinical trial of cisplatin/paclitaxel versus carboplatin/paclitaxel as first-line treatment of ovarian cancer. J Natl Cancer Inst. 95:1320–1329.

Eastman A. (1987). Crosslinking of glutathione to DNA by cancer chemotherapeutic platinum coordination complexes. Chem. Biol. Interact. 61:241–248.

Ediriweera MK, Tennekoon KH, Samarakoon SR. (2019). In vitro assays and techniques utilized in anticancer drug discovery. J Appl Toxicol. 39(1):38-71.

Eisenkop S, Spirtos NM. (2001). The clinical significance of occult macroscopically positive retroperitoneal nodes in patients with epithelial ovarian cancer. Gynecol Oncol. 82:143–149.

Eliopoulos AG, Kerr DJ, Herod J, Hodgkins L, *et al.* (1995). The control of apoptosis and drug resistance in ovarian cancer: influence of p53 and Bcl-2. Oncogene. 11:1217–1228.

Engel J, Eckel R, Schubert-Fritschle G, *et al.* (2002). Moderate progress for ovarian cancer in the last 20 years: Prolongation of survival, but no improvement in the cure rate. Eur J Cancer. 38(18):2435–2445.

Ferlay J, Ervik M, Lam F, *et al.* (2018). Global Cancer Observatory: Cancer Today. Lyon, France. International Agency for Research on Cancer. Available from: https://gco.iarc.fr/today, accessed [April 2019].

Fishman DA, Kearns A, Chilukuri K, *et al.* (1998). Metastatic dissemination of human ovarian epithelial carcinoma is promoted by alpha2beta1-integrin-mediated interaction with type I collagen. Invasion Metastasis. 18(1):15-26.

Foley OW, Rauh-Hain JA, del Carmen MG. (2013). Recurrent epithelial ovarian cancer: an update on treatment. Oncology. 27(4):288.

Fong PC, Yap TA, Boss DS, *et al.* (2010). Poly (ADP)-ribose polymerase inhibition: frequent durable responses in BRCA carrier ovarian cancer correlating with platinum-free interval. J Clin Oncol. 28(15):2512–2519.

Freeman GJ, Long AJ, Iwai Y, *et al.* (2000). Engagement of the PD-1 immunoinhibitory receptor by a novel B7 family member leads to negative regulation of lymphocyte activation. J Exp Med. 192:1027–1034.

Galluzzi L, Senovilla L, Vitale I, *et al.* (2012). Molecular mechanisms of cisplatin resistance. Oncogene. 31:1869–1883.

Ganesh T, Yang C, Norris A, *et al.* (2007). Evaluation of the tubulin bound paclitaxel conformation: synthesis, biology, and SAR studies of C-4 to C-3¢ bridged paclitaxel analogues. J Med Chem. 50:713–725.

George J, Banik NL, Ray SK. (2012). Survivin knockdown and concurrent 4-HPR treatment controlled human glioblastoma in vitro and in vivo. Neuro Oncol. 12(11):1088–1101.

Gilks CB, Prat J. (2009). Ovarian carcinoma pathology and genetics: recent advances. Hum Pathol. 40:1213–1223.

Goff BA, Mandel LS, Melancon CH, Muntz HG. (2004). Frequency of symptoms of ovarian cancer in women presenting to primary care clinics. JAMA. 291:2705–2712.

Golfier S, Kopitz C, Kahnert A, *et al.* (2014). Anetumab ravtansine: a novel mesothelin targeting antibody-drug conjugate cures tumours with heterogeneous target expression favored by bystander effect. Mol Cancer Ther. 13(6):153748.

Gong TT, Wu QJ, Vogtmann E, *et al.* (2013). Age at menarche and risk of ovarian cancer: A meta-analysis of epidemiological studies. Int J Cancer. 132:2894–2900.

González-Martín A, Sánchez-Lorenzo L, Bratos R, *et al.* (2014). First-Line and maintenance therapy for ovarian cancer: Current status and future directions. Drugs. 74:879.

Griffiths CT, Fuller AF. (1978). Intensive surgical and chemotherapeutic management of advanced ovarian cancer. Surg Clin North A. 58:131–42.

Gubbels JA, Belisle J, Onda M, *et al.* (2006). Mesothelin-MUC16 binding is a high affinity, N-glycan dependent interaction that facilitates peritoneal metastasis of ovarian tumours. Mol Cancer. 5(1):50.

Hamanishi J, Mandai M, Ikeda T, *et al.* (2015). Efficacy and safety of anti-PD-1 antibody (Nivolumab: BMS-936558, ONO-4538) in patients with platinum-resistant ovarian cancer. J Clin Oncol. 33:4015–4022.

Hamilton TC, Winker MA, Louie KG, *et al.* (1985). Augmentation of adriamycin, melphalan, and cisplatin cytotoxicity in drug-resistant and sensitive human ovarian carcinoma cell lines by buthionine sulfoximine mediated glutathione depletion. Biochem Pharmacol. 34:2583–2586.

Hamilton TC, Young RC, McKoy WM, *et al.* (1983). Characterization of a human ovarian carcinoma cell line (NIH: OVCAR-3) with androgen and estrogen receptors. Cancer Res. 43(11):5379-5389.

Hassan R, Bullock S, Premkumar A, *et al.* (2007). Phase I study of SS1P, a recombinant anti-mesothelin immunotoxin given as a bolus I.V. infusion to patients with mesothelin-expressing mesothelioma, ovarian, and pancreatic cancers. Clin Cancer Res. 13(17).

Hassan R, Cohen SJ, Phillips M, *et al.* (2010). Phase I clinical trial of the chimeric antimesothelin monoclonal antibody MORAb-009 in patients with mesothelin expressing cancers. Clin Cancer Res. 16(24):6132-8.

Hess LM, Benham-Hutchins M, Herzog TJ, *et al.* (2007). A meta-analysis of the efficacy of intraperitoneal cisplatin for the front-line treatment of ovarian cancer. Int J Gynecol Cancer. 17(3):561–570.

Hollingsworth MA, Swanson BJ. (2004). Mucins in cancer: protection and control of the cell surface. Nat Rev Cancer. 4(1):45-60.

Howitt BE, Hanamornroongruang S, Lin DI, *et al.* (2015). Evidence for a dualistic model of high-grade serous carcinoma: BRCA mutation status, histology, and tubal intraepithelial carcinoma. Am J Surg Pathol. 39:287e293.

Howlader N, Noone AM, Krapcho M, *et al.* (Eds). SEER Cancer Statistics Review, 1975-2014, National Cancer Institute. Bethesda, MD. Available from: https://seer.cancer.gov/csr/1975_2014/, based on November 2016 SEER data submission, posted to the SEER web site. Accessed [April 2019].

Iwai Y, Terawaki S, Honjo T. (2005). PD-1 blockade inhibits hematogenous spread of poorly immunogenic tumour cells by enhanced recruitment of effector T cells. Int Immunol. 17:133–144.

Jaaback K, Johnson N. (2006). Intraperitoneal chemotherapy for the initial management of primary epithelial ovarian cancer. Cochrane Database Syst Rev. 9(11):CD005340.

Jacobs I, Bast RC Jr. (1989). CA125 tumour-associated antigen: a review of the literature. Hum Reprod. 4:12.

Jacobs IJ, Menon U, Ryan A, *et al.* (2016). Ovarian cancer screening and mortality in the UK Collaborative Trial of Ovarian Cancer Screening (UKCTOCS): a randomised controlled trial. Lancet. 387:945e956.

Jacobs IJ, Skates SJ, MacDonald N, *et al.* (1999). Screening for ovarian cancer: a pilot randomised controlled trial. Lancet. 353:1207–1210.

Jensen TA. (2003). Tissue microarray: advanced techniques. J Histotechnol. 26:101–4.

Jervis S, Song H, Lee A, *et al.* (2014). Ovarian cancer familial relative risks by tumour subtypes and by known ovarian cancer genetic susceptibility variants. J Med Genet. 51:108-113.

Jordan SJ, Siskind VC, Green A, *et al.* (2010). Breastfeeding and risk of epithelial ovarian cancer. Cancer Causes Control. 21:109.

Kampan NC, Madondo MT, McNally OM, *et al.* (2015). Paclitaxel and its evolving role in the management of ovarian cancer. Biomed Res Int. 2015:413076.

Karnezis AN, Cho KR, Gilks CB, *et al.* (2017). The disparate origins of ovarian cancers: pathogenesis and prevention strategies. Nat Rev Cancer. 17:65–74.

Kelland L. (2007). The resurgence of platinum-based cancer chemotherapy. Nat Rev Cancer. 7(8):573-84.

Ketabi Z, Bartuma K, Bernstein I, *et al.* (2011). Ovarian cancer linked to Lynch syndrome typically presents as early-onset, non-serous epithelial tumours. Gynecol Oncol. 121:462–5.

Kim A, Ueda Y, Naka T, Enomoto T. (2012). Therapeutic strategies in epithelial ovarian cancer. J Exp Clin Can Res. 31:14.

Kipps E, Tan DS, Kaye SB. (2013). Meeting the challenge of ascites in ovarian cancer: new avenues for therapy and research. Nat Rev Cancer. 13:273–282.

Komatsu M, Sumizawa T, Mutoh M, *et al.* (2000). Copper-transporting P-type adenosine triphosphatase (ATP7B) is associated with cisplatin resistance. Cancer Res. 60:1312–1316.

Konecny GE, Wang C, Hamidi H, *et al.* (2014). Prognostic and therapeutic relevance of molecular subtypes in high-grade serous ovarian cancer. J Natl Cancer Inst. 10.

Koneru M, Purdon TJ, Spriggs D, *et al.* (2015). IL-12 secreting tumor-targeted chimeric antigen receptor T cells eradicate ovarian tumours in vivo. Oncoimmunology. 4(3):e994446.

Kononen J, Bubendorf L, Kallioniemi A, *et al.* (1998). Tissue microarrays for high-throughput molecular profiling of tumour specimens. Nat Med. 4:844-847.

Koulouris CR, Penson RT. (2009). Ovarian Stromal and Germ Cell Tumours. Semin Oncol. 36(2):126-136.

Kurien BT, Scofield RH. (2009). Introduction to protein blotting. Methods Mol Biol. 536:9-22.

Kurman RJ, Carcangiu ML, Herrington CS, Young RH. (2014). WHO Classification of tumours of female reproductive organs. WHO. 4th edition. Geneva, Switzerland.

Kurman RJ, Shih Ie M. (2008). Pathogenesis of ovarian cancer: Lessons from morphology and molecular biology and their clinical implications. Int J Gynecol Pathol. 27:151–160.

Kurman RJ, Shih Ie M. (2010). The origin and pathogenesis of epithelial ovarian cancer: A proposed unifying theory. Am J Surg Pathol. 34:433–443.

Kurman RJ, Shih Ie M. (2011). Molecular pathogenesis and extraovarian origin of epithelial ovarian cancer - Shifting the paradigm. Hum Pathol. 42:918–931.

Kurman RJ, Shih Ie M. (2016). The dualistic model of ovarian carcinogenesis revisited, revised, and expanded. Am J Pathol. 186:733–747.

Lai GM, Ozols, RF, Smyth JF, *et al.* (1988). Enhanced DNA repair and resistance to cisplatin in human ovarian cancer. Biochem Pharmacol. 37:4597–4600.

Ledermann J, Harter P, Gourley C, *et al.* (2014). Olaparib maintenance therapy in patients with platinum-sensitive relapsed serous ovarian cancer: a preplanned retrospective analysis of outcomes by BRCA status in a randomised phase 2 trial. Lancet Oncol. 15(8):852–861.

Lee JM, Ledermann JA, Kohn EC. (2014). PARP inhibitors for BRCA 1/2 mutation associated and BRCA-like malignancies. Ann Oncol. 25(1):32–40.

Lengyel E. (2010). Ovarian cancer development and metastasis. Am J Pathol. 177(3):1053–1064.

Lheureux S, Gourley C, Vergote I, Oz AM. (2019). Epithelial ovarian cancer. The Lancet. 393:1240–125.

Lisio MA, Fu L, Goyeneche A, *et al.* (2019). High-Grade Serous Ovarian Cancer: Basic Sciences, Clinical and Therapeutic Standpoints. Int J Mol Sci. 20(4):952.

Luan NN, Wu QJ, Gong TT, *et al.* (2013). Breastfeeding and ovarian cancer risk: A meta-analysis of epidemiologic studies. Am. J Clin Nutr. 98:1020–1031.

Lynch HT, Casey MJ, Snyder CL, *et al.* (2009). Hereditary ovarian carcinoma: heterogeneity, molecular genetics, pathology, and management. Mol Oncol. 3:97–137.

Mamenta EL, Poma EE, Kaufmann WK, *et al.* (1994). Enhanced replicative bypass of platinum–DNA adducts in cisplatin-resistant human ovarian carcinoma cell lines. Cancer Res. 54:3500–3505.

Matulonis UA, Sood AK, Fallowfield L, *et al.* (2016). Ovarian cancer. Nat Re. Dis Primers. 2:16061.

Mavaddat N, Peock S, Frost D, *et al.* (2013). Cancer risks for BRCA1 and BRCA2 mutation carriers: Results from prospective analysis of EMBRACE. J Natl Cancer Inst. 105:812–822.

McGuire WP, Hoskins WJ, Brady MF, *et al.* (1996). Cyclophosphamide and cisplatin compared with paclitaxel and cisplatin in patients with stage III and stage IV ovarian cancer. N Engl J Med. 334:1–6.

McWhinney SR, Goldberg RM, McLeod HL. (2009). Platinum neurotoxicity pharmacogenetics. Mol Cancer Ther. 8:10-16.

Meinhold-Heerlein I, Hauptmann S. (2014). The heterogeneity of ovarian cancer. Arch Gynecol Obstet. 289(2):237–239.

Mizra MR, Monk BJ, Herrstedt J, *et al.* (2016). Niraparib maintenance therapy in platinum-sensitive, recurrent ovarian cancer. N Engl J Med. 375(22):2154-2164.

Mosmann T. (1983). Rapid colorimetric assay for cellular growth and survival: application to proliferation and cytotoxicity assays. J Immunol Methods. 65(1-2):55-63.

Muniyan S, Haridas D, Chugh S, *et al.* (2016). MUC16 contributes to the metastasis of pancreatic ductal adenocarcinoma through focal adhesion mediated signaling mechanism. Genes Cancer. 7(3-4):110–124.

Nagle CM, Dixon SC, Jensen A, *et al.* (2015). Obesity and survival among women with ovarian cancer: results from the Ovarian Cancer Association Consortium. Br J Cancer. 113(5):817–826.

Nakayama K, Kanzaki A, Ogawa K, *et al.* (2002). Copper-transporting P-type adenosine triphosphatase (ATP7B) as a cisplatin based chemoresistance marker in ovarian carcinoma: comparative analysis with expression of MDR1, MRP1, MRP2, LRP and BCRP. Int J Cancer. 101:488–495.

Naora H, Montell DJ. (2005). Ovarian cancer metastasis: Integrating insights from disparate model organisms. Nat Rev Cancer. 5:355–366.

Nieman KM, Kenny HA, Penicka CV, *et al.* (2011). Adipocytes promote ovarian cancer metastasis and provide energy for rapid tumour growth. Nat Med. 17:1498–1503.

O'Brien TJ, Beard JB, Underwood LJ, *et al.* (2001). The CA 125 gene: an extracellular superstructure dominated by repeat sequences. Tumour Biol. 22(6):348–66.

O'Brien TJ, Beard JB, Underwood LJ, Shigemasa K. (2002). The ca125 gene: A newly discovered extension of the glycosylated N-terminal domain doubles the size of this extracellular superstructure. Tumour Biol. 23:154–169.

Odunsi K. (2017). Immunotherapy in ovarian cancer. Ann Oncol. 28(8):viii1–viii7.

Olsen CM, Nagle CM, Whiteman DC, *et al.* (2013). Obesity and risk of ovarian cancer subtypes: evidence from the Ovarian Cancer Association Consortium. Endocr Relat Cancer. 20(2):251–262.

Ordonez NG. (2003). Application of mesothelin immunostaining in tumour diagnosis. Am J Surg Pathol. 1418-28.

Ozols RF, Bundy BN, Greer B, *et al.* (2003). Phase III trial of carboplatin and paclitaxel compared with cisplatin and paclitaxel in patients with optimally resected stage III ovarian cancer. J Clin Oncol. 21:3194–3200.

Pardoll DM. (2012). The blockade of immune checkpoints in cancer immunotherapy. Nat Rev Cancer. 12(4):252–264.

Pennington KP, Swisher EM. (2012). Hereditary ovarian cancer: beyond the usual suspects. Gynecol Oncol. 124:347–353.

Peres LC, Cushing-Haugen KL, Köbel M, *et al.* (2018). Invasive Epithelial Ovarian Cancer Survival by Histotype and Disease Stage. J Natl Cancer Inst. 111(1):60–68.

Perren TJ, Swart AM, Pfisterer J, *et al.* (2011). A phase 3 trial of bevacizumab in ovarian cancer. N Engl J Med. 365 (26):2484–2496.

Piccart MJ, Bertelsen K, James K, *et al.* (2000). Randomized intergroup trial of cisplatin–paclitaxel versus cisplatin–cyclophosphamide in women with advanced epithelial ovarian cancer: three-year results. J Natl Cancer Inst. 92:699–708.

Pignata S, Scambia G, Ferrandina G, *et al.* (2011). Carboplatin plus paclitaxel versus carboplatin plus pegylated liposomal doxorubicin as first-line treatment for patients with ovarian cancer: the MITO-2 randomized phase III trial. J Clin Oncol. 29:3628–3635.

Pinto R, Carvalho AS, Conze T, *et al.* (2012). Identification of new cancer biomarkers based on aberrant mucin glycoforms by in situ proximity ligation. J Cell Mol Med. 16(7):1474-84.

Pradeep S, Kim SW, Wu SY, *et al.* (2014). Hematogenous metastasis of ovarian cancer: rethinking mode of spread. Cancer Cell. 26:77–91.

Praestegaard C, Jensen A, Jensen SM, *et al.* (2017). Cigarette smoking is associated with adverse survival among women with ovarian cancer: Results from a pooled analysis of 19 studies. Int J Cancer. 140(11):2422–2435.

Prat J. (2012). Ovarian carcinomas: five distinct diseases with different origins, genetic alterations, and clinicopathological features. Virchows Arch. 460(3):237-49.

Prat J & FIGO Committee on Gynecologic Oncology. (2014). Staging classification for cancer of the ovary, fallopian tube, and peritoneum. Int J Gynecol Obstet. 124:1–5.

Raja FA, Chopra N, Ledermann JA. (2012). Optimal first-line treatment in ovarian cancer. Ann Oncol. 23(10):x118–x127.

Ramus SJ, Song H, Dicks E, *et al.* (2015). Germline mutations in the BRIP1, BARD1, PALB2 and NBN genes in women with ovarian cancer. J Natl Cancer In st. 107:djv214.

Ricardo S, Marcos-Silva L, Pereira D, *et al.* (2015). Detection of glyco-mucin profiles improves specificity of MUC16 and MUC1 biomarkers in ovarian serous tumours. Mol Oncol. 9(2):503-12.

Ricardo S, Marcos-Silva L, Valente C, *et al.* (2016). Mucins MUC16 and MUC1 are major carriers of SLe(a) and SLe(x) in borderline and malignant serous ovarian tumours. Virchows Arch. 468(6):715-22.

Ricardo S. (2011). Identifying cancer stem cells in breast tumours: searching for cancer origins. Pathology and Molecular Genetics PhD Programme – ICBAS, Porto.

Rieppi M, Vergani V, Gatto C, *et al.* (1999). Mesothelial cells induce the motility of human ovarian carcinoma cells. Int J Cancer. 80(2):303-7.

Riss TL, Moravec RA, Niles AL, *et al.* (2004). Cell Viability Assays. In Sittampalam GS, Coussens NP, Brimacombe K, *et al.* (Eds). Assay Guidance Manual [Internet]. Bethesda (MD). Eli Lilly & Company and the National Center for Advancing Translational Sciences.

Rouleau M, Patel A, Hendzel MJ, *et al.* (2010). PARP inhibition: PARP1 and beyond. Nat Rev Cancer. 10:293-301.

Rubin MA, Dunn R, Stawderman M, *et al.* (2002). Tissue microarray sampling strategy for prostate cancer biomarker analysis. Am J Surg Pathol. 26:312-319.

Rump A, Morikawa Y, Tanaka M, *et al.* (2004). Binding of ovarian cancer antigen CA125/MUC16 to mesothelin mediates cell adhesion. J Biol Chem. 279(10):9190-8.

Sayasneh A, Tsivos D, Crawford R. (2011). Endometriosis and ovarian cancer: a systematic review. ISRN Obstet Gynecol. 140310.

Schiff PB, Fant J, Horwitz SB. (1979). Promotion of microtubule assembly in vitro by Taxol. Nature. 277(5698):665–667.

Schiff PB, Horwitz SB. (1980). Taxol stabilizes microtubules in mouse fibroblast cells. Proc Natl Acad Sci USA. 77(3):1561–1565.

Schilder RJ, Hall L, Monks A, *et al.* (1990). Metallothione in gene expression and resistance to cisplatin in human ovarian cancer. Int J Cancer. 45(3):416-422.

Scholler N, Fu N, Yang Y, *et al.* (1999). Soluble member(s) of the mesothelin/ megakaryocyte potentiating factor family are detectable in sera from patients with ovarian carcinoma. Proc Natl Acad Sci USA. 96(20):11531-6.

Scholler N. (2011). Mesothelin. In Encyclopedia of Cancer. Schwab M (Ed). Springer. Berlin/Heidelberg, Germany. 2241–2245.

Servais EL, Colovos C, Rodriguez L, *et al.* (2012). Mesothelin overexpression promotes mesothelioma cell invasion and MMP-9 secretion in an orthotopic mouse model and in epithelioid pleural mesothelioma patients. Clin Cancer Res. 18:2478–2489.

Sharma P, Allison JP. (2015). The future of immune checkpoint therapy. Science. 348(6230): 56–61.

Shih I-M, Kurman R. (2004). Ovarian tumourigenesis: a proposed model based on morpholgical and molecular genetic analysis. Am J Pathol. 164:1511–1518.

Siegel RL, Miller KD, Jemal A. (2019). Cancer statistics, 2019. CA Cancer J Clin. 69(1):7-34.

Sieh W, Salvador S, McGuire V, *et al.* (2013). Tubal ligation and risk of ovarian cancer subtypes: a pooled analysis of case-control studies. Int J Epidemiol. 42(2):579–589.

Sjoquist KM, Martyn J, Edmondson RJ, Friedlander ML. (2011). The Role of Hormonal Therapy in Gynecological Cancers - Current Status and Future Directions. Int J Gynecol Cancer. 21:1328-1333.

Skehan P, Friedman SJ. (1985). A rapid naphthol yellow S method for measuring the cellular protein content of anchorage cultures. In Vitro Cell Dev Biol. 21(5):288-290.

Skehan P, Storeng R, Scudiero D, *et al.* (1990). New colorimetric cytotoxicity assay for anticancer-drug screening. J Natl Cancer Inst. 82(13):1107-1112.

Slack-Davis JK, Atkins KA, Harrer C, *et al.* (2009). Vascular cell adhesion molecule-1 is a regulator of ovarian cancer peritoneal metastasis. Cancer Res. 69(4):1469-76.

Song H, Dicks E, Ramus SJ, *et al.* (2015). Contribution of germline mutations in the RAD51B, RAD51C and RAD51D genes to ovarian cancer in the population. J Clin Oncol. 33:2901–2907.

Starobova H, Vetter I. (2017). Pathophysiology of chemotherapy-induced peripheral neuropathy. Front Mol Neurosci. 10:174.

Stewart C, Ralyea C, Lockwood S. (2019). Ovarian cancer: an integrated review. Semin Oncol Nurs. 35(2):151-156.

Streppel MM, Vincent A, Mukherjee R, *et al.* (2012). Mucin 16 (cancer antigen 125) expression in human tissues and cell lines and correlation with clinical outcome in adenocarcinomas of the pancreas, esophagus, stomach, and colon. Hum Pathol. 43:1755–1763.

Stuart GC, Kitchener H, Bacon M, *et al*. (2011). Gynecologic Cancer InterGroup (GCIG) consensus statement on clinical trials in ovarian cancer: report from the Fourth Ovarian Cancer Consensus Conference. Int J Gynecol Cancer. 21(4):750–5.

Su Y, Tatzel K, Wang X, *et al.* (2016). Mesothelin's minimal MUC16 binding moiety converts TR3 into a potent cancer therapeutic via hierarchical binding events at the plasma membrane. Oncotarget. 7(21):31534-49.

Tang Z, Feng M, Gao W, *et al.* (2013). A human single-domain antibody elicits potent antitumor activity by targeting an epitope in mesothelin close to the cancer cell surface. Mol Cancer Ther. 12(4):416-26.

Tavassoli FA, Devilee P (Eds). (2003). World Health Organization Classification of Tumours. Pathology and Genetics. Tumours of the Breast and Female Genital Organs. Lyon. IARC Press.

Testa U, Petrucci E, Pasquini L, *et al.* (2018). Ovarian Cancers: genetic abnormalities, tumour heterogeneity and progression, clonal evolution and cancer stem cells. Medicines (Basel). 5(1):16.

Theriault C, Pinard M, Comamala M, *et al.* (2011). MUC16 (CA125) regulates epithelial ovarian cancer cell growth, tumourigenesis and metastasis. Gynecol Oncol. 121(3):434-43.

Tothill RW, Tinker AV, George J, *et al.* (2008). Novel molecular subtypes of serous and endometrioid ovarian cancer linked to clinical outcome. Clin Cancer Res. 14:5198e5208.

Towbin H, Staehelin T, Gordon J. (1979). Electrophoretic transfer of proteins from polyacrylamide gels to nitrocellulose sheets: procedure and some applications. Proc Natl Acad Sci USA. 76(9):4350-4354.

Tschernichovsky R, Goodman A. (2017). Risk-reducing strategies for ovarian cancer in BRCA mutation carriers: A Balancing Act. Oncologist. 22(4):450–459.

Van den Bossche HV, Moereels H, Koymans LM. (1994). Aromatase inhibitors–mechanisms for nonsteroidal linhibitors. Breast Cancer Res Treat. 30:43–55.

Varga A, Piha-Paul SA, Ott PA, *et al.* (2019). Pembrolizumab in patients with programmed death ligand 1-positive advanced ovarian cancer: Analysis of KEYNOTE-028. Gynecol Oncol. 152(2):243-250.

Vasey PA, Jayson GC, Gordon A, *et al.* (2004). Phase III randomized trial of docetaxel–carboplatin versus paclitaxel–carboplatin as first-line chemotherapy for ovarian carcinoma. J Natl Cancer Inst. 96:1682–1691.

Verhaak RG, Tamayo P, Yang JY, *et al.* (2013). Prognostically relevant gene signatures of high-grade serous ovarian carcinoma. J Clin Investig. 123:517–525.

Vessey M, Painter R. (2006). Oral contraceptive use and cancer. Findings in a large cohort study, 1968–2004. Br J Cancer. 95:385–9.

Vichai V, Kirtikara K. (2006). Sulforhodamine B colorimetric assay for cytotoxicity screening. Nat Protoc. 1(3):1112-1116.

Wang D, Lippard SJ. (2005). Cellular processing of platinum anticancer drugs. Nat Rev Drug Discov. 4(4):307-20.

Wang K, Bodempudi V, Liu ZG, *et al.* (2012). Inhibition of Mesothelin as a Novel Strategy for Targeting Cancer Cells. Plos One. 7(4).

Wang P, Henning SM, Heber D. (2010). Limitations of MTT and MTS-Based Assays for Measurement of Antiproliferative Activity of Green Tea Polyphenols. PLoS ONE. 5(4): e10202.

Wang TH, Wang HS, Soong YK. (2000). Paclitaxel-induced cell death: where the cell cycle and apoptosis come together. Cancer. 88:2619–2628.

Watanabe T, Hashimoto T, Sugino T, *et al.* (2012). Production of IL1-beta by ovarian cancer cells induces mesothelial cell beta1-integrin expression facilitating peritoneal dissemination. J Ovarian Res. 5(1):7.

Webb PM, Jordan SJ. (2017). Epidemiology of epithelial ovarian cancer. Best Pract. Res. Clin Obstet Gynaecol. 41:3–14.

Weidle UH, Birzele F, Kollmorgen G, Rueger R. (2016). Mechanisms and targets Involved in dissemination of ovarian cancer. Cancer Genomic Proteomics. 13(6):407–423.

Wentzensen N, Poole EM, Trabert B, *et al.* (2016). Ovarian cancer risk factors by histologic subtype: An analysis from the Ovarian Cancer Cohort Consortium. J Clin Oncol. 34:2888–2898.

Winter WE, Maxwell L, Tian C, *et al.* (2007). Prognostic factors for stage III epithelial ovarian cancer: a Gynecologic Oncology Group study. J Clin Oncol. 25:3621–362.

Xiang X, Feng M, Felder M, *et al.* (2011). HN125: A Novel Immunoadhesin Targeting MUC16 with Potential for Cancer Therapy. J Cancer. 2:280-91.

Xu L, Yoneda J, Herrera C, *et al.* (2000). Inhibition of malignant ascites and growth of human ovarian carcinoma by oral administration of a potent inhibitor of the vascular endothelial growth factor receptor tyrosine kinases. Int J Oncol. 16:445–454.

Yeung TL, Leung CS, Yip KP, *et al.* (2015). Cellular and molecular processes in ovarian cancer metastasis. A Review in the Theme: Cell and Molecular Processes in Cancer Metastasis. Am J Physiol Cell Physiol. 309(7):C444–C456.

Yokoyama Y, Mizunuma H. (2013). Recurrent epithelial ovarian cancer and hormone therapy. World J Clin Cases. 1(6):187-90.

Zhang D, Yang R, Wang S, Dong Z. (2014). Paclitaxel: new uses for an old drug," Drug Des Devel Ther. 8:279–284.

Zheng C, Jia W, Tang Y, *et al.* (2012). Mesothelin regulates growth and apoptosis in pancreatic cancer cells through p53-dependent and -independent signal pathway. J Exp Clin Cancer Res. 31:84.